DISSERTATION

PHASE CHANGE MATERIAL IN FLOOR TILES FOR THERMAL ENERGY STORAGE

Submitted by

Amy Sarah Lee

Department of Mechanical Engineering

In partial fulfillment of the requirements

for the Degree of Doctor of Philosophy

Colorado State University

Fort Collins, Colorado

Spring 2005

COLORADO STATE UNIVERSITY

April 6, 2005

WE HEREBY RECOMMEND THAT THE DISSERTATION PREPARED UNDER OUR SUPERVISION BY AMY SARAH LEE ENTITLED PHASE CHANGE MATERIAL IN FLOOR TILE FOR THERMAL ENERGY STORAGE BE ACCEPTED AS FULFULING IN PART REQUIREMENTS FOR THE DEGREE OF DOCTOR OF PHILOSOPHY.

Committee on Graduate Work

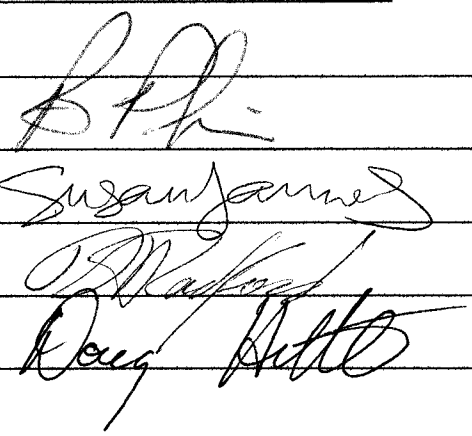

Adviser

Adviser

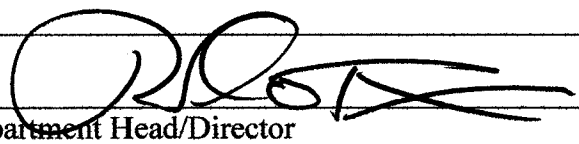

Department Head/Director

ABSTRACT OF DISSERTATION

PHASE CHANGE MATERIAL IN FLOOR TILE FOR THERMAL ENERGY STORAGE

Traditional passive solar systems have relied on sensible heat storage for energy savings. Recent research has investigated taking advantage of latent heat storage for additional energy savings. This is accomplished by the incorporation of phase change material into building materials used in traditional passive applications. Trombe walls, ceilings and floors can all be enhanced with phase change materials. Research to date has yet to produce a viable commercial product. This research introduces a new flooring material that incorporates a phase change material ready for commercial manufacture.

An agglomerate floor tile containing 20% by mass of encapsulated octadecane has been manufactured. Flexural and compressive strength of 7.4 MPa and 24.5 MPa respectively, were measured for the tile. Peak melting transition temperature was determined to be 27.2°C with a latent heat of 33.9 J/g of tile. Structural and thermal performance of the tile surpassed that of a typical ceramic tile.

Each tile was composed of quartz, resin and phase change material. Statistical modeling was performed to analyze the response of flexural and compressive strength on varying amounts of quartz, resin and phase change material. Resulting polynomials described the effect of adding phase change material into the tile. With as little as 10% by mass of phase change material, the strength was reduced to less than 50% of tile without phase change material. It was determined that the maximum phase change material content to attain structural integrity

greater than ceramic tile was 20% by mass. The importance of resin compared to quartz content was also established.

The statistical analysis used for this research was based on mixture experiments. A procedure was developed to simplify the selection of data points used in the fit of the polynomials to describe the response of flexural and compressive strengths. This procedure could be easily adapted to other four component mixture problems.

Analysis of energy savings using this floor tile containing 20% by mass of phase change material was performed as an addendum to this research. A known static simulation method, SLR (solar load ratio), was adapted to include latent heat storage. In addition a dynamic simulation was also performed using BLAST. The program had to be modified to simulate latent heat storage. Annual heating consumptions from both methods were estimated to be reduced by approximately 5%. Using this value it was concluded that if the price of $0.60 per pound of phase change material could be obtained, a five year payback could be achieved for the product.

Amy Sarah Lee
Mechanical Engineering Department
Colorado State University
Fort Collins, CO 80523
Spring 2005

ACKNOWLEDGEMENTS

After all this time I can finally say I am done. It has been a long and challenging road filled with many joys and disappointments. I started this project as a single graduate student grateful for being given the opportunity to pursue a doctoral degree. I end the project married with a beautiful young son and a huge amount of experience under my belt. I feel confident to pursue any endeavors that may come my way, which would not have been possible without the love and support of so many people.

First, I like to thank my advisor, Dr. Doug Hittle. The project would not have been possible with out his initial vision. I am grateful to my committee members for their invaluable advice that resulted in a stronger project. Thank you for use of your labs and resources to complete my research. My thanks go to Dr. Susan James, Dr. Donald Radford and Dr. Bruce Parkinson.

I addition I must thank the staff in Mechanical Engineering department, especially Susan Cavender for all her editing assistance.

I would never have had the drive to pursue this degree if it was not for the high standards set by my parents. They gave me the confidence to tackle the most challenging tasks. Other than giving birth, this project was has been the most challenging task I have faced. I look forward for many more to come.

I owe a special thanks to my husband, my best friend and confidant. Without his continual support and motivational speeches I never would have finished.

TABLE OF CONTENTS

LIST OF TABLES

LIST OF FIGURES

Chapter 1: Introduction

The use of solar energy to offset fuel consumption in commercial and residential buildings can be accomplished by implementing active or passive solar systems. Duffie and Beckman[17] give the following basic distinction of these two systems. Active solar systems include the use of collectors and storage systems that are not integrated with the building structure, while passive systems are integrated within the building structure. This dissertation is concerned with increasing the efficiency of passive solar applications by enhancing the thermal mass. Thermal storage capacity of floor tile will be increased with the addition of phase change materials.

Traditional passive design involves the addition of a sunspace to a structure. The purpose of this room is to store thermal energy and then subsequently release the energy to aid in the reduction of the heating load. Energy is gained directly from the sun through the glazing in the sunspace, with the majority entering through the south-facing windows. The south-facing wall should contain 0.19 to 0.38[17] glazing area to floor area in order to maximize energy collected.

Floors and walls traditionally make up the thermal mass of a sunspace. Typically construction materials are concrete, masonry brick or dark clay tile. Thermal storage is usually accomplished by sensible heat storage. Heat is stored as the material temperature increases due to the solar energy entering the space. As a result, the space can easily become overheated. Solutions to prevent overheating can be accomplished in several ways. The south-facing glazing area can be decreased or an overhang can be placed over the south

facing glazing to reduce the amount of direct sunlight entering the space during the summer months. Installation of fans for increased ventilation and circulation can also aid in reducing overheating. Another solution is to incorporate latent heat storage.

Heat is released during a change in phase of a material. All materials undergo phase transitions, thus have an associated latent heat. When a substance melts, vaporizes and sublimates, heat is absorbed. Heat is released when a material solidifies and condenses. During a change in phase, the temperature remains practically constant.

Since the temperature stays virtually constant during a change in phase, the temperatures of the thermal mass are lower. Lower temperatures mean less heat loss and a comfortable room temperature even during the summer months. It also results in a more consistent room temperature and reduction in overheating. Another advantage of latent heat storage is greater volumetric energy storage compared to sensible heat storage.

Phase change materials can be incorporated into building materials used in passive applications. Wood, gypsum board, lightweight concrete and floor and ceiling tile can all be enhanced with the addition of phase change materials. The ceiling, floor and walls are all large surface areas in a sunspace that are perfect candidates for latent heat storage.

1.1 Agglomerate Floor Tile

The proposed building material for incorporation of phase change materials is agglomerate floor tile. Agglomerate floor tile is composed of natural stone such as marble and quartz

chips that are bonded together with a resin to form a durable floor tile. Marbles, granites and limestone have been used in the past as floor tile and counter tops. They are aesthetically pleasing but are highly porous and easy to stain and scratch. Inconsistency in color and limitation to colors found in nature can cause design issues.

Agglomerate tile offer a less expensive solution. Tiles are uniform in color and can be manufactured in a variety of colors to suit any taste. In order to absorb the maximum amount of solar energy the tile will have to dark in color, which can easily be accomplished with agglomerate floor tiles. The material also has superior strength and durability over natural stone.

Manufactures of this type of tile are Dupont, Silestone and the Verona Marble Company. All these companies have similar products that use quartz chips and a resin to form a floor tile. Dupont acquired a Canadian based company called Granirex in 1998. The manufacturing process used by Granirex was used as a guide for the prototype tile of this research.

The manufacturing process of agglomerate floor tile is conducive for the incorporation of phase change materials. Quartz chips, a fine quartz powder and binder are combined in a mixer. It is during the mixing process that offers the opportunity to add the phase change material. The mixture is then agitated and placed under a vacuum to remove air bubbles and increase the density of the tile. Once molded into sheets it is heated to induce the cure of the binder. After the cure is complete the tiles are cut to size.

The manufacturing process used for this research included combining the ingredients in a mixer and then placing it in a four-inch square mold. A press is used to compress the mixture to ¾ inch of thickness. The mixture in the mold is then heated to induce the cure of the binder.

Chapter 2: Background

2.1 Phase Change Materials

All materials have an associated latent heat for each phase change, but only a few are appropriate for passive solar applications. They need to have a reversible transition, a high latent heat, and small changes in volume between phases and low vapor pressure. They must be chemically stable and good heat conductors. These properties also have to occur at the appropriate transition temperature. Depending on the passive application the required transition temperature will vary, for a sunspace it needs to be approximately 27°C (80°F). The transition temperature is crucial to attain the maximum heat storage during the day and maximum heat release at night.

During the heating season, the nights are longer than the daylight hours. The optimal transition temperature is one-third of the way between the lowest tolerable temperature and the highest tolerable temperature of the space.[47]

2.2 Phase Change Material Candidates

Traditional phase change materials that have been studied and used in applications are alkanes, paraffin waxes and salt hydrates. These materials undergo a reversible solid to liquid phase change at various transition temperatures. Studies have been performed for the feasibility of using solid-state phase change materials for latent heat storage. The biggest advantage the solid-state phase change materials have is no liquid phase to contain the materials change from amorphous to crystalline phases while remaining "solid." Both

paraffin wax and salt hydrates usually have to be encapsulated to contain the liquid phase, which adds to the final cost of the material.

Paraffin wax and salt hydrates have been successfully incorporated into building materials such as wallboard and concrete. A few products have been marketed commercially. Incorporation of solid-state phase change material in concrete has been accomplished in laboratory settings. Sheets of the solid-state phase change materials have also been used as flooring for a research simulation of the effect of latent heat storage in flooring.

2.2.1 Salt Hydrates

Salt hydrates are inorganic materials. Inorganic compounds have twice the volumetric latent energy storage compared to organic compounds. The organic compounds however, have the advantages of melting congruently, self-nucleation and are non-corrosive.[32] Salt hydrates will melt incongruently causing phase separation.

Naumann[46] reported that the incongruent melting behavior of Glauber salts results in two or three different solidification steps upon cooling below the melting temperature. This was observed at 20 degrees below the melting temperature. The application of nucleating agents reduced this effect to one degree.

These materials were not considered a candidate for floor tile for several reasons. If a container is required to contain the liquid phase, metal containers cannot be used because the salt hydrates are corrosive. Crystallization of the salts can also lead to tears forming in

polymer containers. They are also known to form partially hydrated or less soluble crystals due to the high rates of crystallization of the subcooled melts.[9] These less soluble crystals undergo phase transitions at much higher temperatures, thus lowering the thermal storage capabilities over time.

2.2.2 Solid-State Phase Change Materials

Materials that undergo an additional phase transition between the solid and liquid state belong to a group of solid-state phase change materials. A transition occurs from one solid state to another. This transition is associated with large latent heats of transformation. Additionally, melting temperatures are significantly above the solid-solid transition temperature so containment is not required for the liquid phase. They are also expected to be easily incorporated in building materials since there is no liquid phase to contain. There are two categories of solid-state phase change materials, layered perovskites and plastic crystals.

2.2.2.1 Layered Perovskites

Layered perovskites are chemical compounds with the general formula of:

$$(n\text{-}C_n H_{2n+1} NH_3)_2 MCL_4 \qquad (2\text{-}1)$$

Where:

M = is a divalent metal atom such as Mn, Cu, Hg or Fe.
n = $8 \leq n \leq 18$

The structure is composed of regular alteration of inorganic and hydrocarbon regions. Each inorganic layer is sandwiched between two hydrocarbon layers. The hydrocarbon regions are composed of long chain alkylammonium groups ionicly bonded to the inorganic support.[12] These linear alkyl chains are responsible for thermal behavior of the material.

At low temperatures the alkyl chains are in an ordered planar zigzag arrangement. The chains are in a disordered state at high temperatures. They exhibit "liquid-like" behavior in this state. A liquid phase is not obtained at this point because the alkyl chains are fixed on one end to the inorganic layer, thus keeping its lattice structure.[12]

One advantage is that transition temperatures are dependent on alkyl chain length so control of transition temperatures can be accomplished. Other advantages are a relatively high thermal conductivity and chemical stability at high temperatures.[11] Disadvantages are possible toxicity, lower value of enthalpy per unit cost and the total latent heat is reduced due to the inorganic regions of the molecules that are inert.[12]

2.2.2.2 Plastic Crystals

NASA studied a group of solid-state materials during the 1970's for passive temperature control of earth satellites.[10] Three materials were shown to be promising for passive applications: pentaerythritol (PE), pentaglycerine (PG) and neopentyl glycol (NPG).

These materials belong to a class of compounds called polyalcohols or polyols. Each molecule has a central carbon atom with four attached carbon atoms forming a tetrahedron. The number of hydroxyl groups attached to the four carbon atoms distinguished the three compounds from each other.[59] Pentaerythritol is the largest molecule, the smallest is neopentyl glycol. Molecular structures of these materials are presented in Figure A-1 thru Figure A-3.

The most stable form of these materials is a crystalline solid. As heat is applied the material undergoes a transition to a plastic crystal. This behavior comes from the tetrahedral molecular shape and the hydrogen resonant bonding that occurs between neighboring molecules.[9] The substance will eventually melt as the temperature is further increased and will eventually turn into a gas. It is the transition from crystalline solid to a plastic crystal that is of interest.

An advantage of these materials is the ability to custom make blends to fit specific applications. Binary and ternary mixtures can be formed by fusing various combinations of these three materials. The resulting new blends will have new thermal properties, such as transition temperatures and latent heat capacity.

2.2.2.2.1 Background on Plastic Crystals

Plastic crystals are defined as a type of mesophase. The term mesophase, shortened from mesomorphic, was introduced by Friedel in 1922.[29] He defined it as a phase with microscopic structures between solids and ordinary isotropic liquids. He stated that there were two distinct types of this phase, which he described as smectic and nematic. Earlier, the term "liquid crystal" was used to describe both these phases. Otto Lehmann coined the phrase "liquid crystal" in 1889. The actual discovery of this phase is attributed to an Austrian botanist, Friedrich Reinitzed, in 1888.[29] Friedel did not agree with the term "liquid crystal" which lead to his use of smectic and nematic to describe two types of this phase.

In 1935, Timmermans recognized a third type of mesophase, "plastic crystals". Later, Wunderlich and Grebowitz[11] further distinguished three types of mesophases referred to as liquid crystals, plastic crystals and condis. Condis is often confused with liquid crystals since they are similar in nature. All three types exhibit some degree of long-range order similar to crystals. They also show a degree of mobility other than segment vibrations, which is similar to isotropic liquids.[11] This is why the term "liquid crystal" was first used to describe this phase.

The difference between these three types of mesophases are the types of disordering they display. Liquid crystals exhibit a positional disordering. Plastic crystals show positional disordering but also display orientational disordering. The final type, condis, displays conformational disordering as well as positional and orientational disordering.[11] In positional disordering, the intermolecular distances become less uniform and the molecules can arrange themselves parallel, perpendicular or randomly. Conformational disordering is the acquisition of freedom of executing rotations about single bonds.[43]

A further distinction between liquid and plastic crystals can been seen in Figure 2-1. In this figure, the phases are given for liquid, plastic and ordinary crystals. A typical crystal on increasing temperature will transform directly into the liquid state. This is shown by Case II in Figure 2-1. Both liquefaction and isotropy occur at the same temperature. This is not true of plastic and liquid crystals. Liquid crystals first undergo liquefaction then become isotropic. The opposite is true of plastic crystals were isotropy occurs first. Case I and III

both show the behavior of liquid and plastic crystals respectively. This figure was taken from Timmermans.[59]

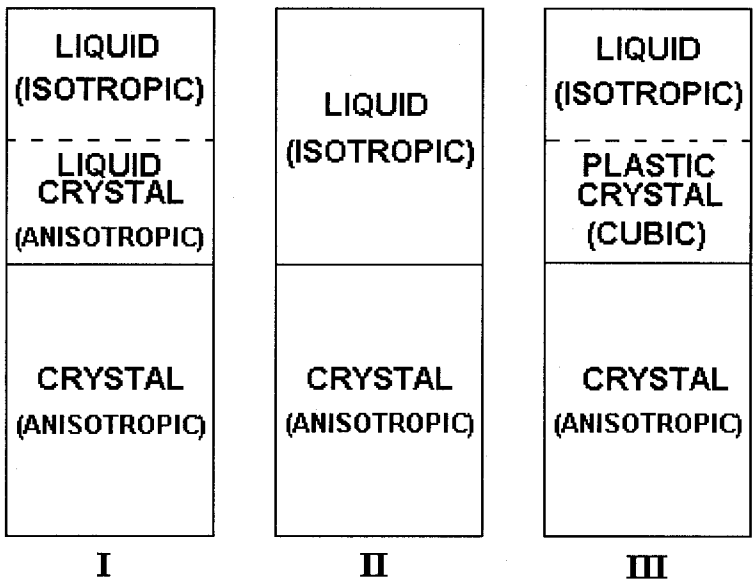

Figure 2-1. Phase of a: I. Liquid Crystal II. Typical Crystal III. Plastic Crystal

2.2.3 Paraffin Wax

Normal paraffin waxes are part of a family of saturated hydrocarbons. The structure is the type C_nH_{2n+2}. Those with carbon atoms between five and fifteen are liquids at room temperatures and are not considered. Normal or straight chain and symmetrically branched chain paraffin waxes are the most stable. Typically, paraffin waxes with odd numbers of carbon atoms are more widely used because they are more available, more economical and have higher heats of fusion.

Paraffin waxes are composed mainly of alkanes, approximately 75%.[32] Alkanes and paraffin waxes are both organic compounds. Paraffin can contain several alkanes resulting in a melting range rather than a melting point. As the molecular weight increases, the melting

point tends to increase as well. Using different mixtures of alkanes, specific transition temperatures for paraffin waxes can be attained. Paraffin waxes and alkanes at the transition temperature melt to a liquid and solidify upon cooling. They do not have the containment problems of salt hydrates. The only requirement is a flexible containment to allow for the small volume change from the melt.

The properties of normal paraffin wax are very suitable for latent heat storage. They have a large heat of fusion per unit weight, non-corrosive, nontoxic, chemically inert and stable below 500°C (932°F). On melting, they have a low volume change and a low vapor pressure. Mixing different molecular weight paraffin waxes together can easily vary melting temperature. Since they are commercially available, the cost is reasonable. Prime candidates for passive applications are tetradecane, hexadecane, octadecane and eicosane. Paraffin wax, as well as solid-state phase change materials, has a low thermal conductivity. However, the addition of additives such as graphite could increase the thermal conductivity.[9]

2.2.3.1 Outlast Technology

A Boulder, Colorado company, Outlast Technology, is incorporating encapsulated paraffin wax into fabric for outerwear using a technology originally developed for NASA. The technology involves the microencapsulation of microscopic size droplets of paraffin wax. These encapsulated particles of wax are then incorporated into fabrics and foams that are used for lining materials.

Outlast currently uses two grades of phase change materials in order to fit to different applications. One application is for cold weather/extremity wear designed to operate from 18.3°C to 29.4°C (65°F to 85°F). The other grade is used in four season applications designed to operate from 26.7°C to 37.8°C (80°F to 100°F).[41] The grades are composed of a mixture of paraffin waxes from a carbon count of 15 to 24. A mixture is used in order to cut production costs. Pure forms of paraffin waxes are significantly more expensive due to the refining processes involved. Capsules are on the order of 16.3μm +/- 8.9μm. Using this process of microencapsulation and the appropriate mixture of paraffin, a suitable candidate was found for the floor tile application.

2.3 Latent Heat Applications

Phase change materials can be incorporated into building materials to increase the thermal storage in passive applications. Wood, gypsum board, lightweight concrete and floor and ceiling tiles can be enhanced with the addition of phase change materials. Computer simulations and experimental analysis has shown the addition of latent heat storage to be a factor in reducing the annual heating costs. Several different phase change materials have been evaluated experimentally in various building materials.

2.3.1 Trombe Wall Application

Benson[10] studied the feasibility of using solid-state phase change materials in Trombe walls. A thermal network model was used and applied in thermal simulation code for residential buildings. Forward finite differencing was used with time steps of one hour or less. It was assumed there was no undercooling.

Multiple thermal nodes were used to model thermal storage in the wall. This increased the thermal conductivity of the wall and allowed thermal gradients to be measured.

The results show a wall with solid-state phase change material dispersed throughout could outperform a concrete wall that is up to four times thicker and nine times heavier. Figure 2-2 presents the solar savings fraction of two walls containing phase change material and a concrete wall without for a range of wall thickness. The figure was taken from the research performed by Benson[10].

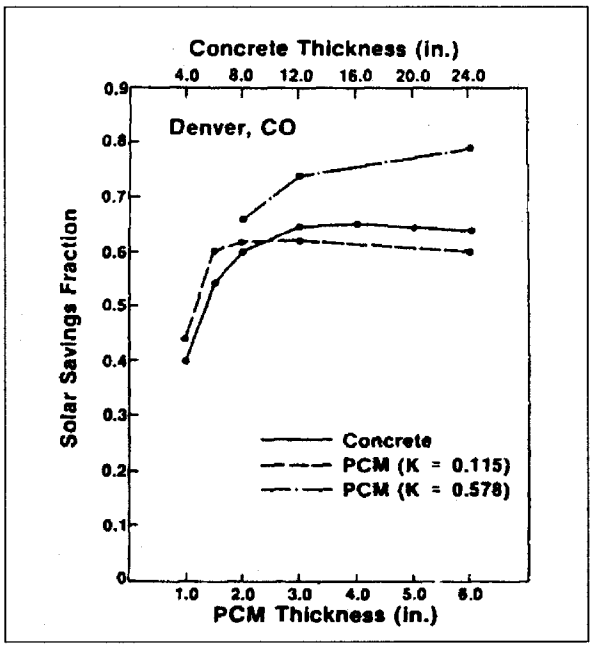

Figure 2-2. Predicted Trombe Wall Performance taken from Benson[10]

High performance of the phase change wall was dependent on thermal conductivity. A thermal conductivity of 1.0 W/m °C (0.578 Btu/ft °F hr) was shown to outperform the concrete wall at any thickness. At a lower thermal conductivity of 0.2 W/m °C (0.115 Btu/ft °F hr) the wall only outperformed concrete walls of thickness of nine inches or less. The

thermal conductivity of a mixture of 40% PG and 60% NPG has been measured to be 0.23 W/m °C (0.133 Btu/ft °F hr). It has yet to be determined if the thermal conductivity can be increased to 1.0 W/m °C with the addition of powdered graphite.

2.3.2 Ceiling Tile Application

Polymer concrete tiles containing a modified Glauber salt was developed at MIT by Johnson[36]. An experimental building was constructed using latent heat storage in ceiling tiles for thermal storage and temperature regulations.

Tiles were manufactured with a hollow core, which was filled with the phase change material. Aluminum bags, laminated with a polymer composite, were used to encase the salts. Bags prevented water seepage to the salts. The polymer concrete casing was capable of handling high foot traffic. It also had a high thermal conductivity.

Room temperatures were decreased with the addition of the tiles. On a sunny day in February a high of 86°F was recorded. Once the tiles were installed, the space never peaked higher than 74°F, the transition temperature of the salt.

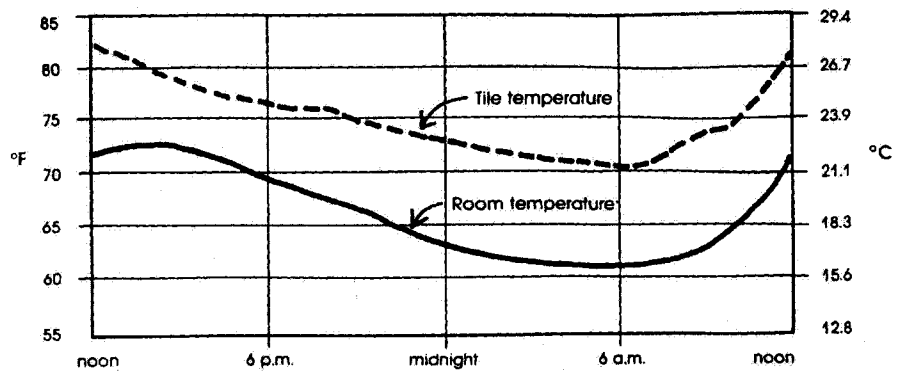

Figure 2-3. Temperature Variation of Ceiling Tiles and the Room taken from Johnson[36]

The phase change material in the ceiling tiles regulated temperature of the space. Data taken on a day in February, which was bordered by two sunny days, is presented in Figure 2-3.

Tiles were determined to store 200 Btu/ft^2(631 Wh/m^2) over a 10°F swing. After a year and half of operations the tiles did not show any signs of leaking or thermal aging. Latent heat of the salts is known to decrease over time, but was overcome in this application by packaging the salts in two adjacent layers that are thin enough to allow crystal growth by diffusion.

Later, the building was expanded to include a pavilion called the Crystal Pavilion[37]. The addition used the same polymer concrete tile, but was installed on the floor instead of the ceiling. Results showed 100% solar heating could be accomplished on most winter days, even cloudy days, as long as the outdoor air temperature remained above 7°C (44°F).

Results from the study show a promising side effect of using phase change materials in the building material. Thermal storage can be increased as well regulating the room temperature. During a phase change the temperature will remain constant, which in turn prevents the space from over heating. Over heating is a common occurrence in many passive applications that employ only sensible heat for thermal storage.

2.3.3 Floor Applications

Barrio[6] investigated the use of solid-state phase change material in a radiant floor system for thermal storage of off-peak power. A comparison was made between floors using sensible heat storage to a floor using latent heat storage. Sand was used for the sensible heat storage

floor and panels with NPG incorporated into it were used for the latent heat storage floor. Figure 2-4 shows the experimental setup.

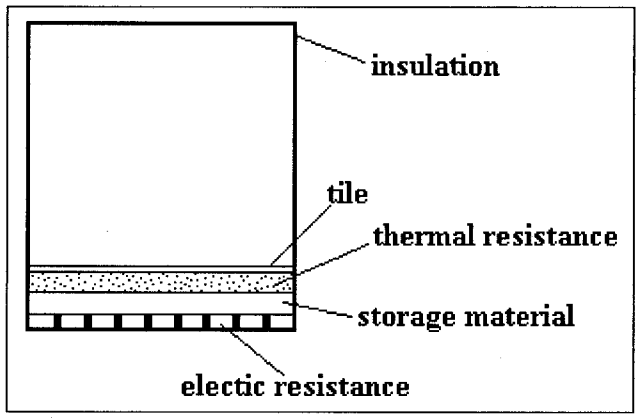

Figure 2-4. Barrio[6] Experiment Setup

The thermal storage layer was 2.5 cm thick and had an area of 1 m^2. Electrical resistance heated the floor from the bottom. Thermocouples were place at each level to monitor temperature changes.

Charging of the storage material occurred over an eight-hour period for the sand floor and for 4.7 hours for the NPG floor. The NPG floor was charged to just above the transition temperature resulting in the lower charge time and less power usage.

Several conclusions were made based on the results. First it was determined that the NPG floor regulated the temperature better. Temperatures between the floor surface and the space above was smaller, approximately 0.6°C compared to 2.6°C measured from the sand floor. At this thickness the sand floor discharged faster than the 16-hour time necessary for using off-peak electricity for charging. The sand floor also reached higher floor surface temperatures than the NPG floor.

The NPG floor was also shown to have a greater thermal inertia than the sand floor. The temperature continued to increase for 3.3 hours compared to 0.5 hours for the sand floor. In conclusion the NPG floor was shown to be more efficient, used less electrical power to charge fully and required less mass than the sand floor. A storage material thickness of 2.5 cm corresponded to 18 kg for the NPG floor and 40 kg for the sand floor. Even more sand would have to be added in order to equal the thermal performance of NPG.

Work by Yamaguchi[63] showed a possible benefit of using salt hydrates in a floor heating system. A test room was constructed that consisted of a stage with hot water panels placed on top. These panels were then superimposed with packages of the salt hydrates. An appropriate amount of packages were laid on the floor to match the expected heating load.

Off peak electricity was used to run a heat pump, which was used as the heat source for the phase change material. The pump was run for an eight our period and then shut off for sixteen hours.

Once the heat pump was turned off, the temperature of the water panel dropped rapidly until the phase change material began to freeze. At this point the temperature leveled off until all the material has solidified. This process took approximately nine hours. After which the room temperature once again started to drop until the pump was turned on again.

Problems were encountered with the heat pump set-up, which prevented the study from being performed in the cold winter months. Results were based on a day in April, and promising

results with the behavior of the phase change material were obtained. The addition of the phase change material allowed a constant room temperature to be kept for nine hours.

2.3.4 Wallboard Applications

There have been several research efforts to incorporate phase change material into gypsum board. Wall surfaces of a sunspace offer a large area for latent heat storage. One of the main obstacles is the possible decrease in the structural integrity of the gypsum board with the addition of phase change materials. Finding an inexpensive method of incorporating the phase change material is another concern.

At the University of Dayton work has been carried out by Ival O. Salyer[55], which has focused on the incorporation of phase change material into wallboard and concrete blocks. Series of linear crystalline alkyl hydrocarbons were selected as the phase change material. Several methods of incorporating the phase change material in the wallboard have been developed.

The first issue addressed was the encapsulation of the phase change material. Microencapsulation was investigated but was determined too expensive for the project. Macroencapsulation offered a less expensive method by enclosing the material in plastic or metal pouches, bottles, cans or pipes. These macrocapsules had problems with leaking, poor heat transfer and flammability, and were therefore not used.

Containment in a high-density polyethylene was another possibility. This method has a high cost associated with it and the phase change material tended to ooze out at high

concentrations. Further research showed a combination of high-density polyethylene, ethylene -vinyl acetate copolymer and silica, reduced the cost and the oozing problems.

Silica gels were used as another form of containment. Melted phase change material is easily absorbed into the hydrophilic silica forming a highly viscous fluid. Further increase in phase change material concentration results in a free flowing dry powder. The powder will phase separate if exposed to water, so care has to be taken to protect the product from humidity and exposure to water. Both these materials can be added during the manufacture of wallboard.

Another method investigated and proven to be very advantageous was imbibing of phase change material into the porous wallboard material. Molten material is allowed to infuse into the wallboard. An advantage of this process is the phase change material does not need to be encapsulated. Other advantages are short and reproducible process times and low costs. It does however result in increased weight and flammability of the board. The weight of wallboard containing 25 to 30% phase change material was still found to be within the acceptable standards.[31]

Resistance to high humidity and immersion into water was found to increase with the imbibing process. This could be an advantage in applications were humidity is a problem.

The compressive strength of the wallboard was found to increase with the addition of phase change materials in the form of pellets or a dry powder. However the adhesion of the paper to the core of the board was reduced.

Feldman[20] investigated wallboard soaked with 93-95% methyl palmitate with 7-5% methyl stearate. Phase change material was impregnated into the wallboard up to 25% of the total weight. The total capacity of the wallboard was found to be 381 kJ/kg, which was about twelve times higher that the storage capacity of wallboard without the phase change material. Physical testing showed comparable results to commercially available wallboard.

2.3.5 Concrete Block Application

The methods used to impregnate wallboard were also applied to incorporating phase change materials into concrete blocks. Concrete block used in outer walls produce a large mass available for latent heat storage. Salyer[54] investigated incorporating phase change material into concrete blocks by imbibing, pellets added during manufacture, and as inserts to the hollow portions of the blocks.

Concrete blocks were composed of Solite granules and portland cement. Heating expanded shale clay and slate in a rotary kiln produces Solite.[54] Phase change materials were incorporated by soaking the block in molten material or by adding dry powder and pellets during manufacture. It was found that the compressive strength of the imbibed specimens was higher than the control and that of specimens containing dry phase change powder and those with phase change pellets. There was no difference in the physical properties of blocks incorporated with dry powder or pellets.

One of the side effects of imbibing concrete blocks was the reduction in adhesion strength of the block to the mortar. This can be avoided by adding the phase change material to the hollow core of the cement block, instead of in the block itself. Hollow cores can be filled with inserts during manufacture or during installation. Core inserts can be made of Solite material imbibed with phase change materials, bags containing the phase change material or a solid molding composed of pellets.

Estimated thermal storage of an outer wall of dimension 9.144m x 12.192m x 3.048m (30ft x 40ft x 10ft) was 1 MBtu. This can be further increased if internal walls are also composed of concrete blocks with latent heat storage. Calculation performed by Hawes[31] found concrete blocks incorporated with phase change material to have a greater thermal storage than wallboard.

2.3.6 Additional Applications

Solomon[56] used a packed bed of encapsulated phase change materials for thermal energy storage of heat recovered from a kiln at a brick factory. Heat recovered and stored in the phase change material could then be used towards a subsequent cycle to reduce the fuel usage. Over 25 hours 525 pounds of fuel was saved.

An application applied by Yamagishi[62] used encapsulated phase change material in a heat transfer fluid slurry. Sözen[57] used latent heat storage in packed beds, using refrigerant R-12, as the transport fluid. Latent heat storage has also been investigated for use on bridge decks

to prevent overnight freezing, for warm clothing applications and for hot and cold medical therapy.

2.3.7 Summary

Past research has shown the ability of phase change material incorporated into building materials to increase thermal storage in passive solar applications. These products have not been shown to be commercially practical. Currently the only commercial application is the incorporation of phase change material in fabric. Products include socks, hiking boots and ski jackets.

There have been leakage and flammability concerns with incorporating paraffin wax into wall board. Adhesion problems to mortar were found when wax was imbibed into concrete blocks. Flooring applications have been limited to heating systems requiring electrical power to heat the phase change material above the transition temperatures. Limited physical testing has been performed to show products incorporating phase change materials will meet standards set for similar product with out phase change material.

Investigation of incorporating phase change material into agglomerate floor tile has not been performed. Floors offer a potential volume for latent heat storage. Although not as larger as walls, it is an area that received direct sunlight. Typically in a sunspace the floor is used for sensible heat storage since is it in direct contact with solar radiation entering though south facing glazing. The addition of latent heat storage can only increase the performance, but incorporation of the phase change material represents a challenge.

2.4 Goal, Hypothesis and Objectives

2.4.1 Goals

The goal of this research is to incorporate a phase change material in to an agglomerate floor tile, while maintaining structural integrity of the tile, for use in passive solar applications. A product of this nature has not been manufactured. End result of the research is the manufacture a new composite material composed of resin, quartz chips and phase change material for commercial use.

Solid-state phase change material and paraffin wax will be investigated as possible candidates for the phase change material. The paraffin wax candidate is encapsulated in a melamine-formaldehyde resin shell. This will eliminate any undesired reaction between the phase change material and the binder. An adverse reaction between the solid-state material and binder is a possibility since the material is not encapsulated.

Minimizing the overall cost of the final tile will be a major factor when bringing the final prototype tiles to the commercial market. This project will use cost as a factor, however not key, in selection of final prototype tiles. It will be left to future work to reduce the overall cost of the final prototype tiles.

2.4.2 Dissertation Hypothesis

Agglomerate floor tile containing a significant amount of phase change material, approximately 40% by mass, can be manufactured with appropriate thermal properties, and be comparable in physical strength to tile without phase change material.

2.4.3 Dissertation Objectives

1) Select a phase change material and binder to manufacture agglomerate floor tiles.
2) Develop a design of experiment to develop fitted models, which will estimate mechanical strength of tiles with varying compositions of phase change material, quartz chips and binder.
3) Execute the design of experiment and develop fitted models using statistical methods appropriate for mixture problems.
4) Using the developed fitted models to select two final prototype tiles with at least the minimum strength requirements for tiles without phase change material.
5) Perform mechanical and thermal testing of final prototype tiles.
6) Complete potential energy savings analysis to demonstrate annual heating savings when using floor tile containing phase change material in passive solar applications.

2.5 Floor Tile Standards

Quartz-based agglomerate floor tiles fall under standards for stone tiles, such as marble, granite and limestone. The Institute of America (MIA) publishes a manual for stone tile selection and testing. Many of the tests used on stone tiles are similar to tests performed on ceramic tiles. The American National Standards Institute (ANSI) together with the American

Society of Testing and Materials (ASTM) are responsible for establishing guidelines and minimum performance levels for the manufacture of ceramic tile in the United States. Majority of the guidelines focus on the safety and wear of the tiles during and after installation, such as flammability, slip and abrasion resistance

Tile companies typically will list the physical strengths of the product for comparison to other products of similar design. Tests performed by three manufacturers of an agglomerate floor tile composed of polyester resin and quartz chips are listed in Table G-1. Each test performed by the manufacturer is marked. Physical tests were selected from this list. The six tests that have been selected for this project are given in Table 2-1.

Table 2-1 Selected Physical Tests

Test
ASTM C-170 Compressive strength
ASTM C-1161 Flexural Strength
NTMA Impact Resistance
ASTM C-97 Absorption and bulk specific gravity
ASTM C-484 Thermal Shock
Morphology

Final selection of tests was made from those performed by Granirex, since they will supply tile recipe and supplies for the manufacture of prototype tiles. A majority of those tests focus on performance of the product under traffic and weather conditions. Although they are important tests for tiles entering the commercial market, they were not the main focus of this research and were disregarded. It will be left to future work to perform these tests.

Compressive strength is typically used by tile manufactures for comparison to other products. Granirex claims their product has a compressive strength greater than 172 MPa (25,000 psi),

which is superior to the standard for granite tiles at 131 MPa (19,000 psi). There is no standard for ceramic tile since they are not expected to have significant compressive strength, especially when compared to natural stone products.

Following ASTM 880 for flexural strength, the strength of Granirex tiles is documented to be 45.9 MPa (6650 psi). The standard under 4-point loading for natural stone is 8.3 MPa (1200 psi). As with compressive strength there is no standard for ceramic tile, but it is expected to lower than natural stone.

Since there is no available minimum compressive and flexural strength for ceramic tiles, a commercially available ceramic tile will be tested along with prototype tiles manufactured for this research. These calculated strengths will be used as the minimum strength prototype tile must achieve. In addition a piece of Granirex tile obtained from the company will be tested. Strengths from this tile will be used as the ideal standard for the prototype tiles to attain, although it is not expected.

A morphology analysis will be performed to describe the behavior of how the phase change material is dispersed throughout the mixture and to verify PCM capsules will not be compromised during the manufacturing process. There is a concern that capsules may rupture resulting in leakage of the paraffin wax. The wax is not expected to adhere to the binder. If large amounts of wax leak from the capsules the overall physical strength of the tile will be severely compromised. Severe leakage is expected to be visually noticeable during the manufacturing process.

2.6 Design of Experiment Overview

The tile mixture is composed of quartz chips, quartz powder, polyester resin, pigment and a phase change material (PCM). One of the final objectives of this research is to arrive at two final prototype mixtures that maximize the PCM amount and the physical strength of the tile. Determination of these final mixtures involves designing an experiment, which studies the behavior or response of the physical strength of the tile on varying amounts of PCM in the mixture.

The experiment falls under the category of a mixture problem. A mixture problem is defined as the mixing together of two or more ingredients to form a final product. Properties of the final product may or may not be better than that of the single components alone. Typically the objective is to determine if there is combination of components that will result in the "best" final product. The "best" final product for this project will not be the tile with the highest physical strength, but one that fits the required criteria. Final tiles must have at a minimum the flexural and compressive strength of ceramic tile while maximizing the PCM content.

Determination of the "best" final product will be accomplished by studying the response of flexural and compressive strength on varying component proportions. These two properties were selected because they are common physical characteristics of floor tiles and because testing can be easily performed.

Final properties of the product are assumed to depend only on the proportions of the components, not on the amount of the mixture. Simply stated, a mixture to manufacture one six-inch square tile will yield the same properties as a mixture to yield 100 six-inch square tiles.

2.6.1 Estimation of the Response

The design of experiment will establish the number of data points required to solve for the parameters of the polynomials that describe the response of flexural and compressive strength. Parameters are estimated by the method of least squares. Depending on the desired accuracy, the polynomials can be as uncomplicated as a simple quadratic or as complex as a fifth degree polynomial. Typically the accuracy of a simple quadratic is sufficient.

A statistical program, SAS (Statistical Analysis System), will be used to solve the unknown parameters of the polynomials. It will also be used to calculated simple statistics, such as t-tests and F-tests, to determine the statistical significance of the parameters and final fitted models.

2.7 Mechanical Testing Overview

2.7.1 Flexural Strength Testing

Four-point and three-point loading will be used for the flexural strength testing of prototype tiles. Models will be developed from flexural strength data obtained from a three-point bending test. The equation is given here:

$$S = \frac{3PL}{2bd^2} \qquad (2\text{-}2)$$

Where:

S	=	flexural strength (MPa)
P	=	break load (N)
L	=	outer span (mm)
b	=	specimen width (mm)
d	=	specimen thickness (mm)

The two final prototype tiles will be subjected to three-point as well as four-point bending testing. The standard formula for four-point flexure is as follows:

$$S = \frac{3PL}{4bd^2} \qquad (2\text{-}3)$$

Testing will be performed on an ATS 900 test machine. Diagrams of the setup for three-point and four-loading are given in Figure 2-5 and Figure 2-6.

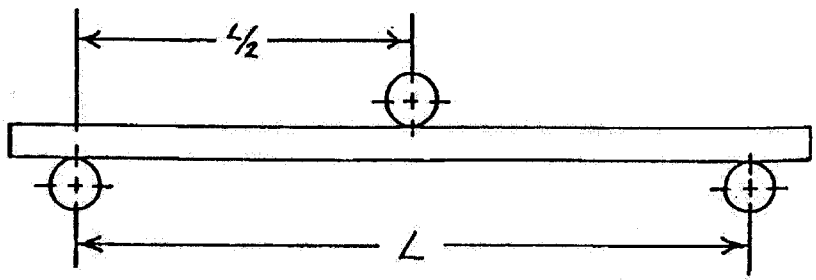

Figure 2-5. Three-point Loading Flexural Strength Testing Setup

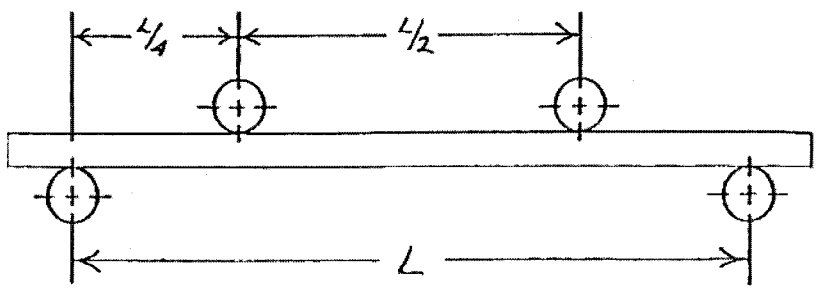

Figure 2-6. Four-point Loading Flexural Strength Testing Setup

The break load is measured at sample failure and is used to determine the maximum flexural strength. Dimensions of the samples are given in Table 2-2. Loading will be applied at a rate of 1.0 mm/min (0.039 in/min) for both three-point and four-point loading.

Table 2-2. Flexural Strength Test Sample Dimensions

b	8 mm
d	6 mm
L	80 mm

A minimum of ten samples will be tested for each prototype tile. An average will be taken to given the final flexural strength.

2.7.2 Compressive Strength Testing

Samples will be loaded between two platens to perform the compressive strength test. A diagram of the setup is given in Figure 2-7. A MTS testing machine will be used to perform all testing. Dimensions of samples may be either one inch (25.4 mm) or two inch (50.8 mm) square and the thickness of the prototype tile. Loading will be done at 0.05 in/min (1.3 mm/min).

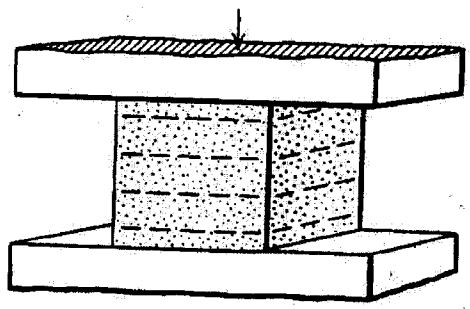

Figure 2-7. Loading of the Sample for Compressive Strength Testing

The equation to determine the compressive strength is as follows:

$$C = W/A \qquad (2\text{-}4)$$

Where:

C	=	compressive strength (psi)
W	=	total load on specimen at failure (lbf)
A	=	calculated area of bearing surface (in^2)

Failure of the specimen is assumed to be the maximum load the sample holds. Five samples will tested for each prototype tile and an average taken to give the final compressive strength.

2.7.3 Impact Strength Testing

The NTMA (National Terrazzo and Mosaic Association) impact test consists of dropping a 0.91 kg (2-pound) steel ball from 2.44 m (eight feet). Granirex claims their product passes this test were marble, granite and marble agglomerate floor tiles fail. Ceramic tile is expected to fail as well.

The apparatus for this test will be a simple PVC pipe of suitable length and diameter to allow the steel ball to pass freely. A base will be placed at the bottom opening of the pipe, where test samples will be placed. The ball will be allowed to impact the center of each sample once.

Failure will be determined visually. Any visible crack or breakage of the sample will be considered a failure. One or two samples will be tested for each prototype tile.

2.7.4 Absorption and Thermal Shock Testing

ASTM testing standards will be followed for both of these tests. A tile must have a water absorption by weight less than 0.5% to be considered "impervious". Granirex tile is considered "impervious".

2.8 Thermal Testing Overview

The main tool for thermal analysis of phase change materials is the differential scanning calorimeter (DSC). Latent heat of transformation, transition and melting temperatures, specific heat, kinetics of transformation and under cooling effects can all be determined using the DSC. It will also be used to investigate the behavior of the phase change material when incorporated into a piece of floor tile. Each of final two prototype tiles will undergo DSC testing to determine the transition temperatures and latent heat capacity.

A typical setup of a DSC unit is shown in Figure 2-8. It consists of two sample pans on heaters that are controlled by a computer. One pan is for the sample and the other is for a standard, which is usually air. When the standard is empty the pan is generally kept empty.

Heating and cooling rates are kept the same for each pan. As a result the heater under the sample pans has either to work harder or less to maintain constant rates, since it contains material that is undergoing transitions. The DSC measures the amount of energy supplied to the heater along with the temperature.

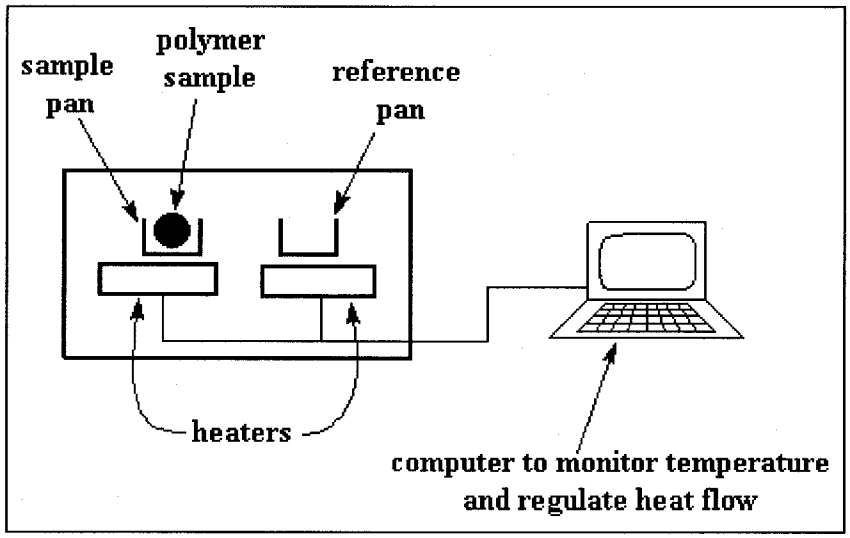

Figure 2-8. Typical DSC Setup taken from Macrogalleria[16]

Samples sizes are on the order of a few milligrams. Material will have to be scraped or chipped from full size tiles and used to fill the sample pans. Pans will be crimped shut.

Chapter 3: Tile Manufacture

3.1 Tile Mixture

During the course of this research we have collaborated with the Zodiaq Company, Thedford Mines, Quebec, Canada. They have supplied the raw materials for our research. The company was originally known as Granirex and we refer to their tile product as Granirex tile. The original recipe supplied by the company served as a basis for the prototype tile mixture. It is composed of seven ingredients, quartz chips of various sizes, quartz powder, binder and pigment. The pigment used was carbon black. Table 3-1 lists the proportions of the components. Mesh conversion to SI units are given in Table D-1.

Table 3-1. Granirex Recipe Proportions

Component	Density [g/cm^3]	Mass Fraction f	Volume Fraction x
Quartz Chips, Mesh 6 (quartz-6)	2.65	0.048	0.043
Quartz Chips, Mesh 10 (quartz-10)	2.65	0.057	0.051
Quartz Chips, Mesh 34 (quartz-34)	2.65	0.411	0.366
Quartz Chips, Mesh 84 (quartz-84)	2.65	0.124	0.111
Quartz Powder, Mesh 325 (powder)	2.65	0.229	0.204
Resin	1.35	0.121	0.212
Pigment	1.75	0.010	0.014

Binder used by Granirex was an unsaturated styrene based polyester resin (AROPOL C 324). A catalyst (LUPEROX 26P50) and a wetting agent, silane (CAS: 2530-85-0), were premixed with the resin before the other components are added. The catalyst is 2% by weight of the resin and the silane is 1% of the weight.

The following outlines the steps that were followed to fabricate the wet tile mixture. A mixture of the consistency of wet sand was the result.

1) Mix together all four sizes of quartz chips.
2) Add pigment and mix well.
3) Mix catalyst and silane with resin for 30 seconds.
4) Add the resin with the quartz and mix together for at least a minute or until fully combined.
5) Combine the quartz powder slowly into the mixture. At this point the PCM can be added along with the quartz powder.

The tile mixture was combined in a kitchen mixer. Once all components were added the mixture was mixed for another two minutes or longer when necessary to fully incorporate all the ingredients.

It was very important to ensure that the PCM was fully coated by the binder to ensure proper bonding with the other components. Adding extra wetting agent, a couple of drops from an eyedropper, as the PCM was mixed in to the mixture seemed to improve the incorporation of the material.

3.2 Full Tile Manufacture

Aluminum molds were made to produce four-inch and six-inch square tiles of varying thickness. The four-inch square mold used for a majority of the prototype tiles is shown in Figure 3-1.

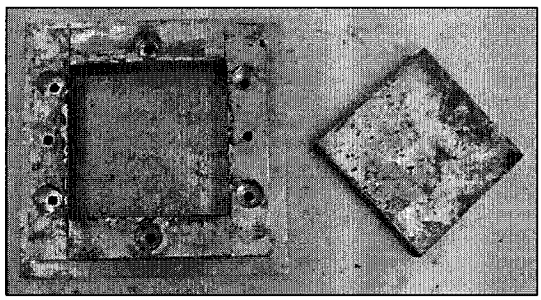

Figure 3-1. 4" Tile Mold

The mixture was added to the mold and pressed under 3,450-6,900 kPa (500-1000 psi) of pressure. Figure 3-2 shows the mold in the press.

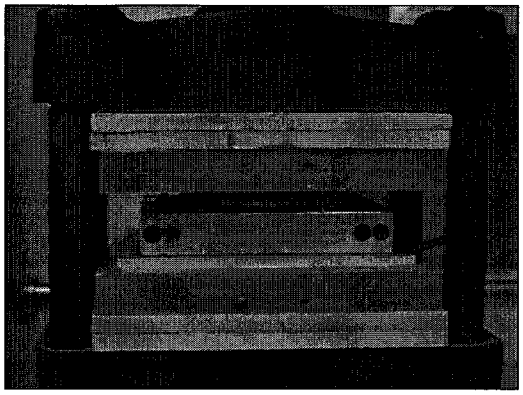

Figure 3-2. Tile Mold in the Press

While the mixture was still in the mold it was heated to approximately 100°C (212 °F) for twenty minutes. The polyester resin was required to reach a temperature of 80°C (176°F) to initiate the curing process, however with the addition of phase change material this temperature was required to be increased. After twenty minutes the tile was removed and the curing process was finished in an oven set to 100°C (212 °F) for approximately four hours. This second heating in the oven was done to ensure that entire tile reached the curing temperature and fully cured. A tile was assumed to be fully cured when there was no residual odor of styrene. The tiles were then allowed to rest for at least 24-hours to complete the curing process.

Once tiles had rested for 24-hours, tiles were cut to the appropriate sizes for testing. A wet-saw with a diamond blade was used to cut the tiles.

Top surface preparation of the tiles was achieved with a wet polishing wheel. Paper of grit varying from 40 to 600 was used to attain a honed appearance.

3.3 Sample Tile Manufacture

In addition to the manufacture of full size tiles, smaller samples were made. These samples were made to investigate different component combinations and various resins where a full size tile would a needless waste of material.

Samples were mixed by hand and pressed into two-inch diameter aluminum weighing pans. The pans were heated in an oven to initiate and complete the curing process.

3.4 Phase Change Material Preparation

Before the phase change material could be incorporated into the tile mixture, it had to be prepared to ensure proper mixing. If the material contains residue that residue may hinder the ability of the resin to bind to it. In the case with the solid-state phase change material, binary blends had to be prepared, in order to tailor the melting point temperature to a useful passive solar application temperature of 27°C (80°F).

3.4.1 Solid-State Phase Change Material

The three solid-state PCM pentaerythritol (PE), pentaglycerine (PG) and neopentyl glycol (NPG) were obtained in a solid white powder form. Binary mixtures were prepared by fusing both materials while in a molten state. Once combined it would be cooled forming a new blend. The material was first combined together in the powder format, placed in a sealed jar and heated until it was completely in a molten form. A magnetic stir rod was placed in the jar to make certain that the mixture was fully fused. The jar was placed in a mineral oil bath to ensure uniform heating. This process was executed under a hood. Once

the mixture was completely molten, it was stirred for at least five minutes to ensure proper mixing. It was then allowed to cool at room temperature. Once cooled the mixture was removed from the jar and ready for use.

3.4.2 Encapsulated Octadecane

The PCM obtained from Outlast typically contained residue and were damp. Outlast used the material suspended in water for its product. Therefore it was necessary to ensure the material was rinsed of residue and dried. The material was rinsed with water and dried using a desiccator.

Chapter 4: Experimental Investigation of Phase Change Material

4.1 Introduction

Three categories of phase change materials were discussed as potential candidates for incorporation into floor tiles: salt hydrates, solid-state phase change materials and paraffin wax. Salt hydrates were not considered due to containment problems and long-term degradation of the material. Solid-state phase change materials (SS PCM's) in the form of plastic crystals and paraffin wax were investigated in detail before a final selection was made. Based on the selection of phase change material a compatible binder was selected.

Selection of a phase change material for this project had to fit several criteria. The most important being appropriate thermal properties. It was necessary that the material have a transition temperature around 27°C (80°F), the ideal temperature for passive solar applications. In addition the heat of fusion or latent heat must be large enough to ensure adequate thermal storage. Other criteria were no adverse interaction with the binder, ease of material preparation and low costs of raw materials.

4.2 Experimental

4.2.1 Comparison of Thermal Properties

Paraffin wax and solid-state phase change materials have transition temperatures and heats of fusion suitable for passive solar applications. Thermal properties of these materials are presented in Table 4-1.

Table 4-1. Thermal Properties of Phase Change Materials

Material	Peak Transition Temperature on Heating	Heat of Fusion on Heating	Density
Solid-State Phase Change Material			
Pentaerythritol (PE)	188°C (370.4°F)	269 J/g (115 Btu/lbm)	1390 kg/m^3(86.8 lb/ft^3)
Pentaglycerine (PG)	89°C (192.2°F)	139 J/g (59.8 Btu/lbm)	1220 kg/m^3 (76.2 lb/ft^3)
Neopentyl Glycol (NPG)	48°C (118.4°F)	119 J/g (51.2 Btu/lbm)	1060 kg/m^3 (66.2 lb/ft^3)
60%NPG and 40%PG	26°C (78.8°F)	76 J/g (32.7 Btu/lbm)	1124 kg/m^3 (70.2 lb/ft^3)
Normal Paraffin			
Tetradecane C_{14}	5.5°C (41.9°F)	228 J/g (98 Btu/lbm)	825 kg/m^3 (51.5 lb/ft^3)
Hexadecane C_{16}	16.7°C (62.1°F)	237 J/g (102 Btu/lbm)	835 kg/m^3 (52.1 lb/ft^3)
Octadecane C_{18}	28.0°C (82.4°F)	244 J/g (105 Btu/lbm)	814 kg/m^3 (50.8 lb/ft^3)
Eicosane C_{20}	36.7°C (98.1°F)	244 J/g (105 Btu/lbm)	856 kg/m^3 (53.4 lb/ft^3)
Outlast			
Kenwax 18	25.9°C (78.6°F)	119.7 J/g (51.5 Btu/lbm)	765 kg/m^3 (47.8 lb/ft^3)
Kenwax 19	32.8°C (91.0°F)	134.3 J/g (57.7 Btu/lbm)	811 kg/m^3 (50.6 lb/ft^3)
C18 Octadecane	27.9°C (82.2°F)	173.9 J/g (74.6 Btu/lbm)	740 kg/m^3 (46.2 lb/ft^3)

The transition temperature of the solid-state phase change materials in the pure form is not low enough for use in passive applications. By mixing these compounds in various ratios, the transition temperature can be lowered. The ideal ratio was determined to be a mixture of 60% neopentyl glycol (NPG) and 40% pentaglycerine (PG). Both Benson[7,9] and Font[21] have presented this ratio in their research. It also has been repeated in the laboratory during early research for this project using differential scanning calorimeter (DSC) to calculate heat of fusion of the binary mixture.

Benson[9] reported the number of intermolecular hydrogen bonds largely controls the amount of energy absorbed at transition. Altering the number of hydrogen bonds can have a significant effect on the energy absorbed and the transition temperature. This can be

accomplished by mixing the pure forms of the solid-state materials with each other. The materials readily form binary mixture with each other either by dissolution in water or in their molten forms. Binary mixtures were produced by combination of the two materials in molten forms for this research.

Pure octadecane and the Outlast encapsulated octadecane are very close to the defined ideal passive temperature. Outlast uses mixtures of normal paraffin wax, Kenwax 18 and 19, for the phase change material in their products. The paraffin content of these two mixtures is listed in Table B-1 and Table B-2. By mixing normal alkanes of different molecule weights, the melting or transition temperature can be altered from that of the pure form.

One obvious effect of mixing phase change materials is that the latent heat is lowered. For example, the mixture of 60% NPG and 40% PG, as presented in Table 4-1, results in more than 50% decrease in the latent heat storage capabilities. Kenwax mixtures experience a decrease, although not as drastic. Outlast determined that the latent heat of a blend can be found from a linear equation, presented below:

$$\text{Final Blend J/g} = (\text{wt.\%}_{\text{mPCM1}} \times \text{J/g}_{\text{mPCM1}}) + (\text{wt.\%}_{\text{mPCM2}} \times \text{J/g}_{\text{mPCM2}}) + \ldots \qquad (4\text{-}1)$$

Latent heat of the encapsulated octadecane differs from the pure form because of encapsulation and a lesser grade is used. A technical grade of 95% octadecane is used. The microencapsulation shell is approximately one micron thick with the core taking 80-85% of the weight.[14]

Studies performed by Benson[9] and Font[24] did not show a linear relationship between the molar percentage of neopentyl glycol and pentaglycerine, and latent heat. The latent heat decreases from the pure form of pentaglycerine as neopentyl glycol was added until the mixture contained 60% NPG. At that mixture, the latent heat, as well as the transition temperature, began to increase to the latent heat for the pure form of neopentyl glycol. Results of analysis done by Benson and Font are presented in Figure 4-1.

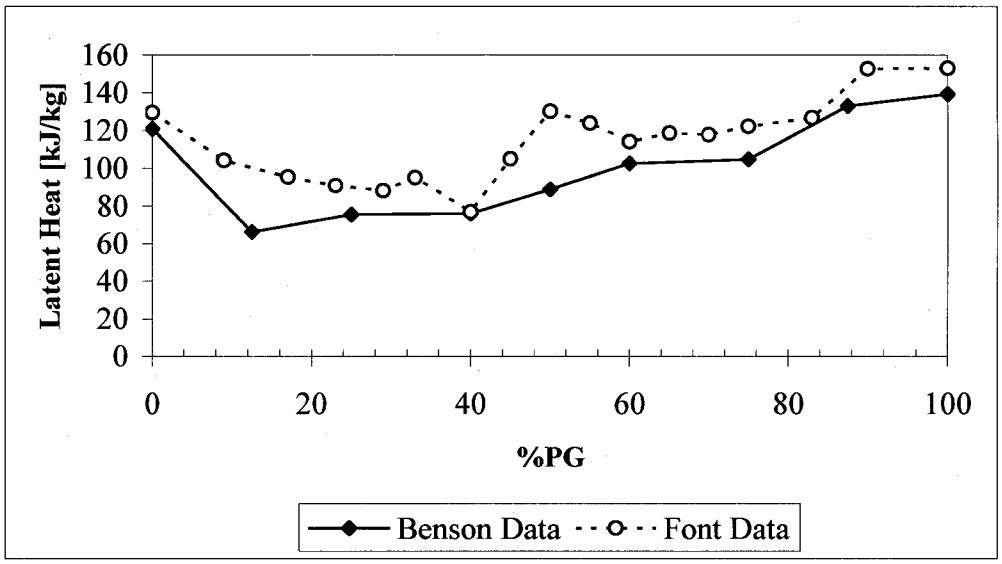

Figure 4-1. Variation of Latent Heat for Binary Mixture of Neopentyl Glycol and Pentaglycerine

Octadecane in its pure form has the highest heat of fusion with a transition temperature close to the ideal passive temperature. Its latent heat storage is more than three times greater than the NPG/PG mixture. Based on thermal storage capabilities, pure octadecane is the superior material, followed by the encapsulated octadecane. Kenwax 18 has a suitable transition temperature as well, but a significantly lower latent heat storage capability than the encapsulated octadecane, thus not a good candidate for this project. Kenwax 19 will be disregarded due to its high transition temperature.

Encapsulation of the paraffin wax for this project was necessary to ensure bonding with the resin. Pure octadecane was therefore disregarded at a potential candidate.

Solid-state phase change materials and encapsulated octadecane were both experimentally investigated as possible candidates for incorporation into the floor tile. Based on the results of the investigation encapsulated octadecane was selected.

4.2.2 Solid-State Phase Change Material

A blend of 60% NPG and 40% PG was selected to investigate as a possible candidate for incorporation. Its lack of requiring encapsulation made it an ideal candidate even though the latent heat capacity was not as high was the paraffin waxes.

4.2.2.1 Material Preparation

Pure forms of NPG and PG were required to combine to produce the necessary blend. There are two different methods that can be used. The first method involves dissolving the two components in water and then drying the compound. The second method combines the two components in their molten form.

Drying the mixture after combination in water proved to be a long and difficult process, since the materials are highly hydroscopic. It was therefore decided to combine the materials in their molten form. This involved melting the materials in a sealed container in an oil bath to

ensure uniform heating. A magnetic stir rod was used to fully mix the components. After the compound was cooled to room temperature it was ready for use.

Neither method could ensure a perfect ratio of NPG to PG each time. Inadequate mixing while in the molten form resulted in the blend containing segments of pure material. The dissolution method required several cycles to ensure a homogenous mixture.[24] In addition neopentyl glycol sublimates at approximately 50°C, which further increases the difficulty of combining the materials their molten form. A seal container was required to contain the vapor and condense it back into the mixture. This however was a small amount and was not a concern.

A differential scanning calorimeter (DSC) was used verify the blend. It was assumed if the transition peak temperature on heating was within five degrees of the reported value of 26°C (78.8°F)[7], a good mix was achieved. However since the DSC sample sizes were on the order of milligrams compared to batch sizes of a few grams, there was no guarantee that samples from the blend were a true representation of the mixture. X-ray diffraction has been used successfully by Font[24] to verify proportion of blends.

Several blends of varying ratios of NPG to PG were prepared. Peak transition temperatures were measured with a DSC and results compared to data collected by Benson[9]. Values were comparable, verifying the accuracy of the fusion method used for this research.

4.2.2.2 Interaction with Binder

The agglomerate floor tile recipe used for the basis of this research used unsaturated styrene based polyester as the binder. Adverse reaction with the binder was possible since the solid-state phase change material was not encapsulated. Test samples were made containing only solid-state phase change material and resin to determine any unwanted reaction. Sample mixture was approximately 15% resin by mass and 85% solid-state phase change material. The 60% NPG and 40% PG blend was used.

A successful cure was not obtain after heating the mixture of solid-state phase change material and resin to 80°C for 20 minutes. The curing time and temperature was increased with no change. Additional curing agent was added with no improvement. The solid-state phase change material was observed to dissolve in the resin. It was concluded the phase change material was prevented the cure process.

Polyesters use carboxylic acids and polyfunctional alcohols like neopentyl glycol, to impart flexibility, toughness and stain and chemical resistance. Neopentyl glycol is often used in the polyester synthesis for improved stain and chemical resistance.[51] Propylene glycol is typically used with the unsaturated monomer styrene. Cross-linking was mostly likely being prevented by the addition of neopentyl glycol to the mixture, affecting the ratio of polyester to curing agent.

Epoxies were then investigated as possible binders for solid-state phase change materials. An epoxy resin and curing agent produced by Shell Chemicals was the second binder tested.

EPON 828 and curing agent 3140 was combined with the phase change materials and quartz. This mixture did cure to form a piece of prototype tile. The amount of phase change material was small, but DSC runs did show a phase transition at the appropriate transition temperature.

EPON 828 is an undiluted clear difunctional bisphenolA/epichlorohydrin derived liquid epoxy resin.[19] This material is cross-linked with an appropriate curing agent to form a material with good mechanical and chemical resistance properties. The curing agent 3140 is a low viscosity reactive polyamide and high imidazoline, which is based on dimerized fatty acid and polyamines.[18]

Solid-state phase change materials have also been shown to react adversely with the epoxy resin. The solid-state materials, NPG, PG, PE and the 60/40 NPG/PG mixture all have available hydroxyl groups to react with epoxy groups. The solid-state phase change material was causing the rate of cross-linking to increase by acting like a curing agent. This resulted in a decrease in the thermal storage capability of the phase change material, since some of phase change material was being consumed during the cure.

4.2.3 Encapsulated Octadecane

This material was selected as a possible candidate because of its large latent heat and not requiring any major processing. The only processing was drying the material since it was supplied slightly damp.

4.2.3.1 Structural Integrity of Encapsulated Particles

Structural integrity was a concern for encapsulated particles. Polyesters often involve an exothermic cure, which could possibly reach temperatures high enough to degrade the encapsulation. Encapsulated particles used by Outlast were tested by thermogravimetry analysis to 300°C without any noticeable damage.

Thermal stability of melamine resin has been shown to be dependent on the curing time and on several pyrolysis steps. Mass lost during thermogravimetry analysis became smaller with increased curing times.[34] No damage is expected at the curing temperatures of the polyester.

Encapsulated wax particles of a diameter of 5 μm were subjected to the thermal cycling tests by Yamagishi.[62] Tests were performed for a temperature range to allow melting and solidification. After 5000 cycles, the particles examined under a microscope showed no damage.

Another concern was any damage that may result from the procedure to manufacture the tile. Currently, the manufacturing process for agglomerate tile using polyester as a binder is accomplished by mixing the components in a vessel that resembles a concrete mixer. The mixture is then agitated under a vacuum to remove air bubbles. It is then heated to induce the curing process. Agitation is not seen as a risk, but the batch mixing could possibly cause damage. However, the size of the encapsulated particles is significantly smaller than that of the quartz chips, so damage is expected to be minimal if at all. Quartz chips are on the order of several millimeters.

Yamagishi[62] performed tests on the structural stability of an encapsulated paraffin particle, similar to the particles used in the Outlast technology. Encapsulated wax in a brine slurry as a heat transfer fluid was the focus of the research. The slurry was circulated using a pump system. Breakage rate was found to increase with increasing circulation times. It was found that the structural stability of the particle was dependent on its diameter. Smaller particles withstood pressures of a slurry flow and pressure from volumetric expansion. Volumetric expansion was not a problem due to the flexibility of the shell.

A particle will be broken when the external pressure equals the internal pressure. The internal pressure in a spherical microencapsulated particle was defined by Yamagishi[62] to be related to the wall tension, thickness and particle diameter.

$$P = 4 \sigma t / d \qquad (4\text{-}2)$$

Where:

σ	=	tension of the microencapsulated particle
t	=	wall thickness
d	=	diameter

The particles were also subjected to agitation from a magnetic stirrer. It was found that the agitation did not damage particles from the size of 5 to 1000 μm.[62]

Research performed by Roy[53] found that the structural strength of particles of wax encapsulated with polyvinyl alcohol was dependent on the wall thickness. Particles with a wall thickness comprising 30% of the total particle volume withstood thermal cycling better than particles with a 15% wall thickness. Particles used by Yamagishi had wall material comprising 14 to 20% of the total volume. Outlast particles are 20% wall material. The

encapsulation material used by both Yamagishi and Outlast is melamine resin, which is more durable than polyvinyl alcohol.

Outlast uses the encapsulated particles in phase change fabrics for thermal comfort outdoor wear. Foams are soaked with a solution of the particles. The particles have to be durable enough for wear and washing in a machine. A concern expressed by Outlast is that high shear stress may cause damage to the particle. The tile manufacturing process is not expected to exert high shear stress on the particles.

4.2.3.2 Interaction with Binder

It was expected that paraffin wax would not react adversely with epoxies or polyesters. The material used for the encapsulation is relatively inert. Encapsulation of melamine resin was determined by Yamagishi[62] not to react with the brine solutions $CaCl_2$, NaCl, glycol or silicon oil. Outlast Technology uses melamine-formaldehyde as the encapsulation material and found it was durable and did not react adversely with other materials.

Melamine-formaldehyde resin belongs to the family of thermosets. The high cross-linking nature of the cure product results in superior hardness, strength and rigidity. High chemical and abrasion resistance are other strong attributes of the material. It is widely used in decorative laminate such as Formica. The molecular structure is given in Figure C-1. Sites can remain active if cross-linking is not complete, which may react with the tile binder. However this is not seen as a risk, as the encapsulation process is expected to cure completely.

Curing temperature of the resin was affected by the addition of the phase change material. The polyester without any additions was required to be heated to 80°C (176°F) to initiate the curing process. During the curing process the resulting reaction is exothermic. Therefore a spike in the heat flux would be visible using differential scanning calorimeter (DSC). Results of the DSC scan of the curing process of the resin by itself, resin combined with quartz and resin combined with quartz and PCM are presented in Figure 4-2.

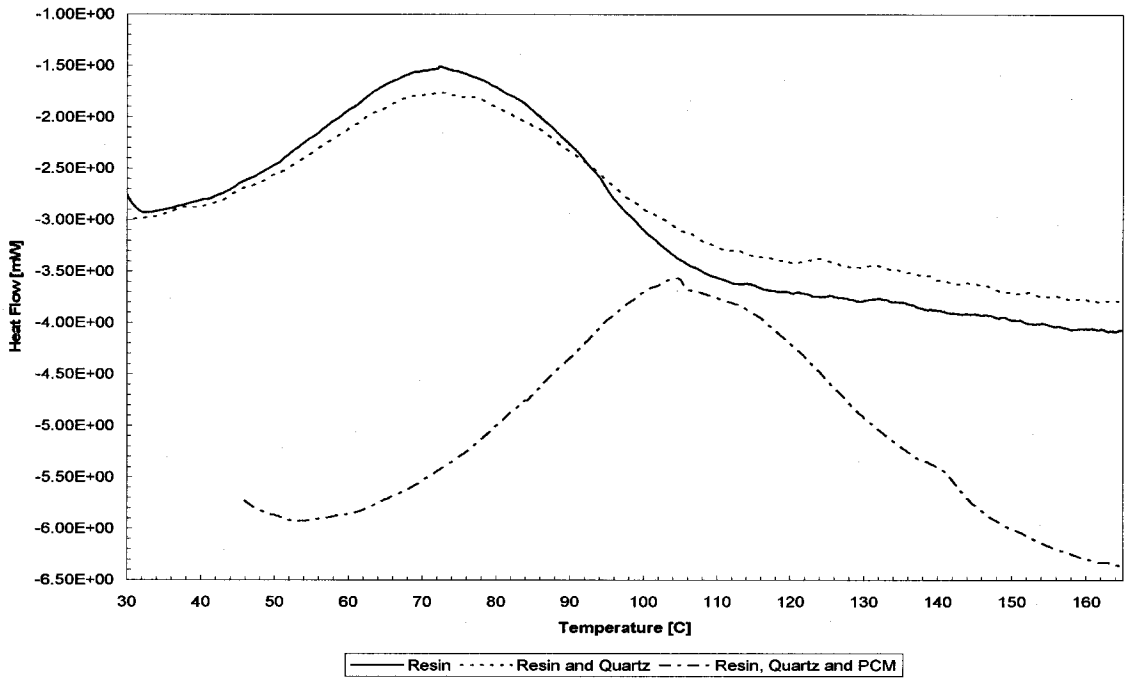

Figure 4-2. Effect of Phase Change Material in Curing Process of Polyester Resin

It was obvious the effect the phase change material had on the peak curing temperature. As expected the addition of quartz had no effect. Based on these results, tile mixtures containing phase change material were heated to 100°C (212°F) to initiate the curing process.

4.2.4 Cost Analysis of Components

Another area of concern was the final cost of the floor tile. The type of binder and phase change material used affects final costs. It was assumed that the amount of quartz rock and powder would be the same regardless of binder and phase change material used. The type of binder will depend on the phase change material selected. Solid-state phase change material requires an epoxy to be used, while polyesters can be used with encapsulated paraffin particles. Table 4-2 shows that the costs of general-purpose polyesters are half the cost of epoxies.

Table 4-2. Binder Approximate Costs

Binder	Price
Epoxy	
Basic grades	$1.30 to $1.50 / lb
SPECIALTY GRADES	$2.00 to $4.00 / lb
Shell EPI-CURe 3140	$1.65 / lb
Shell EPI-CURe 3234	$1.65 / lb
Shell Resin 828	$1.65 / lb
Polyesters	
General purpose	$0.65 to $0.70 / lb
Ashland chlorendic polyester HETRON 197-3	$1.81 / lb
Ashland isophthalic polyester AROPOL 7241	$1.44 / lb

Bulk costs of the phase change materials depend on the current commercial use of the materials. Neopentyl glycol is used in paint and resin production, which reduces the cost of the raw product. However pentaglycerine is not as widely used and will increase the final cost of the solid-state phase change mixture significantly.

Paraffin waxes are widely used in many different applications and can be obtained in many different grades. The level of processing assigns grades. A pure form of octadecane, 99%, is more expensive than the 97% form. Kenwax used by Outlast is a mixture of paraffin waxes

and does not undergo as much refinement, so the cost is even less. However a decrease in the latent heat storage accompanies the use of unrefined paraffin, as values in Table 4-1 show.

Encapsulation processing for the paraffin wax makes up most of the final costs as seen in Table 4-3. The table also shows the bulk costs of the raw phase change materials.

Table 4-3. Final and Bulk Cost of Phase Change Materials

Material	Price
Solid-State Phase Change Materials	
Eastman NPG	$0.74 / lb
Eastman NPG-90	$0.67 / lb
PG	$9 - $12 /lb
Paraffin Wax	
Outlast Kenwax 18 and Kenwax 19	$0.59/lb
Technical Grade Octadecane (~95%)	$2.71/lb
Encapsulation Final Costs	
Outlast Kenwax 18 and Kenwax 19	$8.60/lb
Technical Grade Octadecane (~95%)	$11.13/lb

The final costs of the encapsulated paraffin and solid-state material are not very different. In order to obtain the 60% NPG and 40% PG mixture, a processing step to combine the raw materials needs to be included in the final cost. This added cost is not reflected in Table 4-3. The final cost would still be expected to be on the same order of the encapsulated paraffin. It is expected that cost would be drastically reduced on a large-scale production for both materials.

An advantage paraffin wax has over the solid-state material is in the choice of binder. Encapsulated paraffin wax can be bonded with quartz chips using a polyester resin, which

significantly reduces the overall cost of the floor tile. Solid-state materials have to use an epoxy for the binder, which is twice the cost of polyesters.

4.3 Results and Discussion

4.3.1 Final Phase Change Material Selection

Encapsulated octadecane was selected as the phase change material. The material, C18 Octadecane, was supplied by Outlast. A technical grade of 95% octadecane was used because of the extremely high cost of pure grade octadecane. Pure grade alkanes require increased costs in refining, distillation and crystallization, which would not be cost effective for commercial usage.

This decision was based on the thermal properties. Octadecane has more than twice the latent heat storage of the 60%NPG/40%PG mixture. Currently, the cost of the encapsulated material is the largest drawback of the octadecane. This cost, however, is expected to decrease with large-scale production.

By selecting encapsulated octadecane, polyester was chosen as the binder. Polyester is typically less than half the cost of epoxies. The encapsulated material will not react adversely with the binder, as would be the case with the solid-state phase change material.

4.3.2 Final Binder Selection

Since encapsulated octadecane was selected for the phase change material, a polyester binder was used. The polyester resin selected was a styrene-based resin that is used by agglomerate

tile manufacturers. It required heating to 80°C to initiate the curing process. A curing agent was also used to aid the curing process.

Room temperature and UV cured resins were researched as a possible replacement. The UV cured resins typically are used for coatings and do not possess the mechanical strength required for a floor tile application. Suitable room temperature cured resins were not found.

A polyester resin that would gel at room temperature was evaluated, but it still required heating in order to reach full strength.

4.4 Conclusions

Final selection of encapsulated octadecane supplied by Outlast had several advantages over solid-state phase change materials. First, there was no processing required. The material only had to be rinsed and dried before use, while solid-state phase change materials had to be combined into a binary mixture before used. This proved to be rather time consuming and did not always result in a perfect ratio of the two materials. The encapsulation process is also extensive, but is currently being performed commercially for products produced by Outlast, so it was not considered to be a limitation.

In addition, as with solid-state phase change materials, blends of paraffin waxes can be manufactured with varying thermal properties. This allows for the possibility of custom tailoring tiles with specific transition temperatures to suit any application.

It may be possible to apply the encapsulation process to solid-state phase change materials, but the latent heats would still be less than the paraffin waxes. Solid-state phase change materials are better suited for applications were the phase change material is added to the material after processing. An example is soaking concrete blocks or wall boards in a slurry of phase change material allowing it to saturate the material.

Since the ultimate goal of this research was to manufacture a floor tile that will have the maximum thermal storage capacity, the phase change material with one of the largest latent heat capacity was chosen. In order to maximize the storage capacity the amount of phase change material has to be maximized. Therefore a tile of ¾ of an inch thickness was selected to be manufactured. Obviously a thicker tile would yield higher thermal storage, but it was felt that ¾ of an inch was a workable thickness for installation.

Chapter 5: Design of Experiment

5.1 Introduction

Prototype tiles manufactured for this research were based on a recipe supplied by a company called Granirex. The original recipe was composed of seven ingredients. Four sizes of quartz chips, a fine quartz powder, pigment and polyester resin made up the mixture. The number of components increased to eight with the addition of the phase change material (PCM). One of the final objectives of this project was to select two tile mixtures that maximize the PCM content while maintaining acceptable physical strength. It was not practical or possible to make hundreds of prototype tiles to determine the combination with the highest PCM content and necessary physical strength. Fitted models were required to be developed in order to study the behavior of varying PCM content on physical strength and the interaction of components. Based on these models, the best two tile mixtures were selected.

Polynomials were used to describe the response of physical strength on varying tile components. A minimum number of design points were needed to solve for the unknown parameters of the polynomials. Each design point represented a prototype tile made from a different combination of components. The design of experiment for this project focused on the selection of these design points and the determination of the degree of the polynomial using basic statistics. The purpose of this chapter was to outline steps followed for the design of experiment.

5.2 Experimental

5.2.1 Component Selection

The first step in designing the experiment was to determine the number of components from the tile recipe. The proportions of components for each prototype tile must add to unity.

$$\sum_{i=1}^{q} x_i = x_1 + x_2 + x_3 + \cdots + x_q = 1.0 \qquad (5\text{-}1)$$

The original tile recipe was composed of four sizes of quartz chips ranging from 6 to 84-mesh. Smaller mesh sizes corresponds to larger chips. It was determined that the larger chips, 6 and 10 mesh, were present in small amounts and mainly contribute to the aesthetic appearance of the tile. The smallest quartz chips, mesh 84, were also present in small amounts, so it was assumed not to be a major contributor to the overall strength of the tile. This left the mesh 34 quartz chips as the main contributor to the overall strength and was selected as the first component for the design. The remaining quartz chips and pigment were kept constant for all the prototype tiles.

Quartz powder, polyester resin and phase change material were the other three selected components. Quartz powder was mainly used as filler in the tile mixture. Due to the small size of the particles, mesh 350, the powder also contributed to the overall strength of the tile. Polyester resin was included since all tiles must contain a minimum amount. Since the final cost of the tile is largely affected by the percentage of resin, an upper limit would have to be placed on the resin component.

In summary, the four components of the mixture problem are:

- Polyester Resin (resin), x_1
- Quartz Chips Mesh 34 (quartz-34), x_2
- Quartz Powder (powder), x_3
- Phase Change Material (PCM), x_4

5.2.2 Determination of Experimental Space

A geometric description, simplex region, was developed to give a visual description of the design space. Using a simplex coordinate system, the components were plotted. A three-component system can be represented by a triangle, were a four-component system is represented by a tetrahedron. Samples of each simplex region are presented in Figure 5-1 and Figure 5-2.

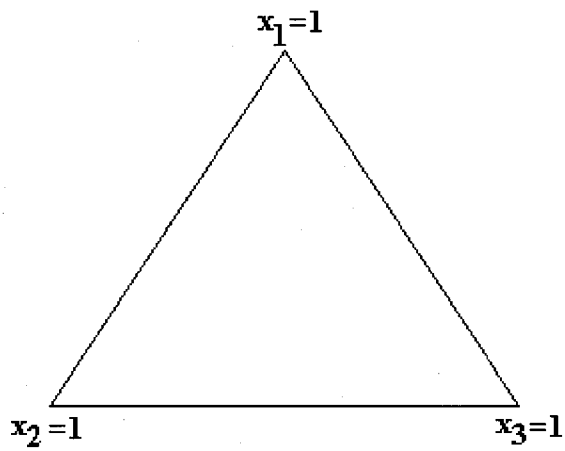

Figure 5-1. Three-component simplex region

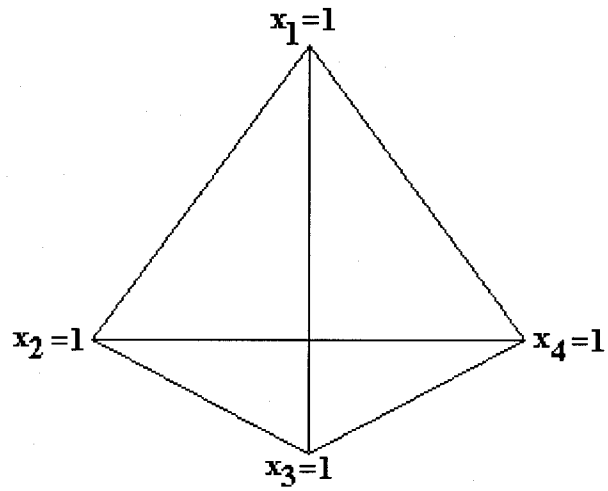

Figure 5-2. Four-Component Simplex Region

At each vertex the component is considered to be a single component mixture, 100% of the single component. When the mixture is at $x_1=1$, all other components are zero. There are cases when a mixture must contain one or all the components in some proportion. This results in a confined region within the simplex where the components may have upper or lower limits. All the components for this research design space have been assigned upper and lower limits.

5.2.2.1 Upper and Lower Limits

Limits have been placed on all four components of this design. All mixtures must contain resin in order to manufacture a tile. Upper limits based on the original commercial recipe have been placed on the quartz 34 chips and quartz powder. Phase change material is expected to replace a combination of quartz chips and powder. The limits are presented in Table 5-1.

Table 5-1. Upper and Lower Limits by Mass of Components

Component	Lower Limit	Upper Limit
Polyester Resin	0.121	0.201
Quartz Chips Mesh 34	0.0	0.411
Quartz Powder	0.0	0.229
Phase Change Material	0.0	0.411

The lower limit of the resin was based on the original recipe. It was decided to set the upper limit to approximately 20% of the tile mixture in order to keep overall cost at a minimum. Higher strength was expected with increased resin amounts up to a certain point, where the resin properties start to determine the overall strength of the composite. A study on the behavior of filler and a thermosetting resin found this to occur above a 30% resin concentration.[45] A trend of increased strength was observed in a separate experiment were flexural strength of tiles with varying resin amounts was compared, however a maximum point was not determined.

As stated earlier the proportion of all components in a mixture design must add to unity. The above limits were based on the entire recipe. This included the quartz chips of mesh 6, 10 and 84 and the pigment. These ingredients comprised of 23.9% by mass of the tile. The remaining tile is composed of the quartz 34 chips, quartz power, resin and PCM. By dividing the limits by 76.1, the proportions of the four components add to unity. The adjusted limits are presented in Table 5-2.

Table 5-2. Adjusted Upper and Lower Limits by Mass of Components

Component	Lower Limit	Upper Limit
Polyester Resin	0.159	0.264
Quartz Chips Mesh 34	0.0	0.54
Quartz Powder	0.0	0.301
Phase Change Material	0.0	0.54

5.2.2.2 Constrained Simplex Region

Using the upper and lower limits of the four components, a constrained region was developed within the simplex. Extreme vertices, edges and 2-dimensional faces define this region. The following equation was used to determine the number of these boundary points.

$$N_d = C(q,q-d-1) + \sum_{r=1}^{q-d-1} L(r)C(q-r,q-r-d-1) - \sum_{r=d+1}^{q}[L(r)+E(r)]C(r,r-d-1) \qquad (5\text{-}2)$$

Where:

N_d	=	number of d-dimensional boundaries
d	=	dimension
q	=	number of components
r	=	1,2,…,q
$C(q,r)$	=	q!/r!(q-r)!
$L(r)$	=	the number of combinations of component ranges that sum to a number that is lower than R_p
$E(r)$	=	the number of combinations of component ranges that sum to R_p
$G(r)$	=	the number of combinations of component ranges that sum to a number that is higher than R_p
R_p	=	min(R_L,R_U)
R_L	=	1 – sum of lower limits
R_U	=	sum of upper limits - 1

Results of the four-component design and the above upper and lower limits are:

N_o = number of extreme vertices = 10
N_1 = number of edges = 16
N_2 = number of faces = 8

Based on these results and the upper and lower limits the design points for each of the extreme vertices were determined. These points are listed in Table 5-3.

Table 5-3. Extreme Vertices of the Four-Component Confined Simplex Region

Extreme Vertices	x_1	x_2	x_3	x_4
1	0.159	0.54	0.301	0.0
2	0.159	0.54	0.0	0.301
3	0.159	0.301	0.0	0.54
4	0.159	0.0	0.301	0.54
5	0.264	0.435	0.301	0.0
6	0.264	0.54	0.196	0.0
7	0.264	0.54	0.0	0.196
8	0.264	0.196	0.0	0.54
9	0.264	0.0	0.196	0.54
10	0.264	0.0	0.301	0.435

Using these design points the confined region can plotted graphically. An Excel spreadsheet was developed to plot the confined region in a four-component simplex region. The spreadsheet can be easily modified for additional design points and adjustment of the limits. Using the ten design points listed above the constrained region with the extreme vertices labeled is given in Figure 5-3.

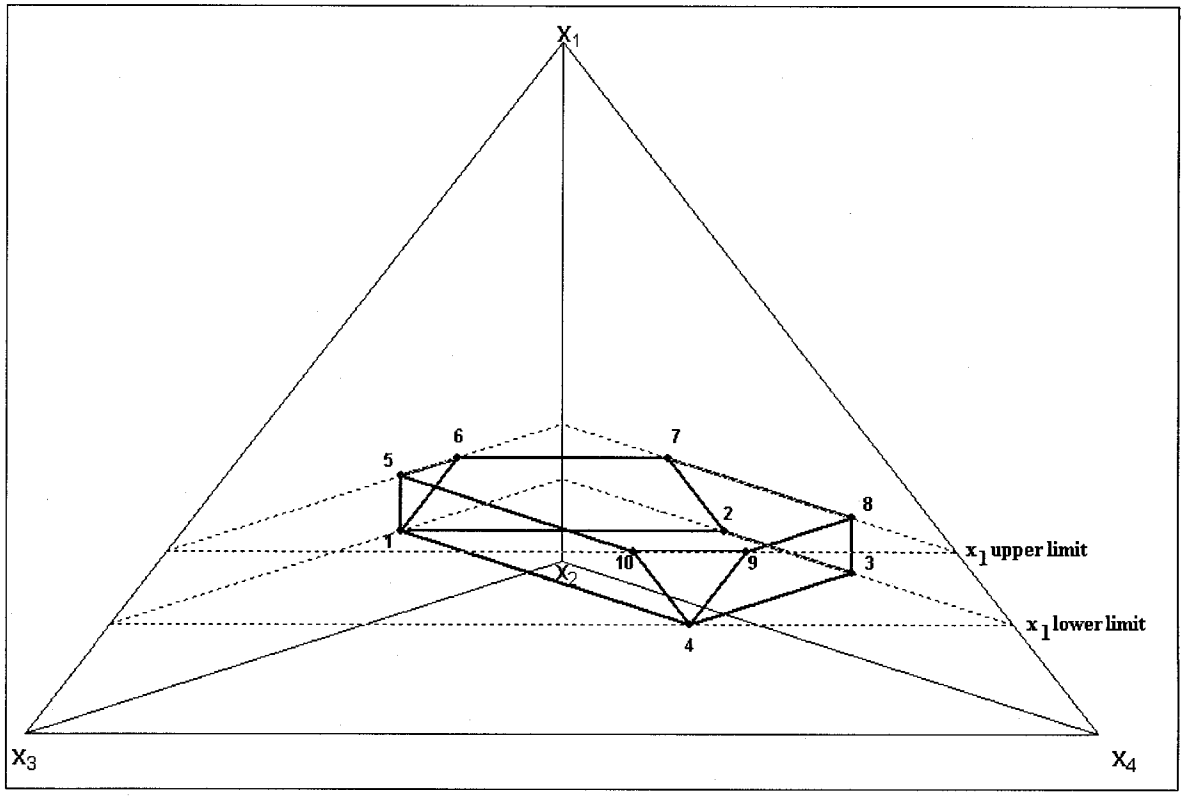

Figure 5-3. Constrained Region for the Four-Component Simplex

5.3 Results and Discussion

5.3.1 Response Surface

The purpose of the mixture experiment is to determine the response of different proportions of components on selected properties. In the case of this research flexural and compressive strength were the responses of interest. The response can be geometrically projected on the simplex region. Figure 5-4 shows an example of the response plotted on the simplex for a three-component mixture.

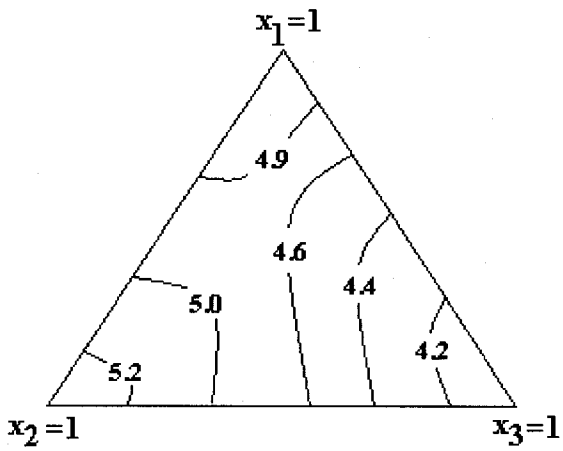

Figure 5-4. Sample Contour of Response on Three-Component Simplex Region

Projecting the contours on a four-component simplex is slightly more difficult. Typically plots of three components, while holding one constant, are created to visually describe the behavior of the response.

Contours are developed from a model based on design points within the simplex region. A function is assumed to exist to describe the behavior of the response. Typically a polynomial function is assumed. A *m*th-degree polynomial equation is given by:

$$\eta = \beta_o + \sum_{i=1}^{q} \beta_i x_i + \sum_{i \le j}^{q} \sum^{q} \beta_{ij} x_i x_j + \sum^{q} \sum_{i \le j \le k}^{q} \sum^{q} \beta_{ijk} x_i x_j x_k + \cdots \qquad (5\text{-}3)$$

Where:

q	=	number of components
β	=	constant
x	=	component proportions

A first-degree polynomial is made of the first two terms with a second-degree polynomial using the first three terms. The number of components and degree of polynomial determines the number of terms in the polynomial. A four-component design requires ten terms to solve

the second-degree polynomial, while a first-degree polynomial only requires four terms. Final derived equation is presented below. It contains both liner and quadratic terms.

$$\eta = b_1x_1 + b_2x_2 + b_3x_3 + b_4x_4 + b_{12}x_1x_2 + b_{13}x_1x_3 + b_{14}x_1x_4 + b_{23}x_2x_3 + b_{24}x_2x_4 + b_{34}x_3x_4 \quad (5\text{-}4)$$

Where:

b	=	unknown constant
x	=	component proportion

A statistical program called SAS (Statistical Analysis System) was employed to solve a second-degree polynomial for this design. At least ten design points were required to determine a model for flexural and compressive strength, since there were ten unknown parameters. Each design point is a mixture combination located within the simplex region of the design. Prototype tiles were manufactured at selected points and were subjected to flexural and compressive testing to determine the response.

5.3.2 Selection of Design Points

There are countless numbers of design points that can be selected to develop a model of the response. Design points are typically selected from three classes of points, extreme vertices, midpoints of edges and centroids of faces. Table 5-3 lists the extreme vertices and Table 5-4 lists the midpoints and Table 5-5 the centroids. The overall centroid of the constrained region has also been included in Table 5-5. The vertices, which reference Figure 5-3, of the edges and centroids have been included.

Table 5-4. Midpoints of Edges of Constrained Region

Midpoint	x_1	x_2	x_3	x_4	Edge Vertices
11	0.159	0.54	0.1505	0.1505	(1,2)
12	0.159	0.4205	0.0	0.4205	(2,3)
13	0.159	0.1505	0.1505	0.54	(3,4)
14	0.159	0.27	0.301	0.27	(4,1)
15	0.264	0.4875	0.2485	0.0	(5,6)
16	0.264	0.54	0.098	0.098	(6,7)
17	0.264	0.368	0.0	0.368	(7,8)
18	0.264	0.098	0.098	0.54	(8,9)
19	0.264	0.0	0.2485	0.4875	(9,10)
20	0.264	0.2175	0.301	0.2175	(10,5)
21	0.2115	0.4875	0.301	0.0	(1,5)
22	0.2115	0.54	0.2485	0.0	(1,6)
23	0.2115	0.54	0.0	0.2485	(2,7)
24	0.2115	0.2485	0.0	0.54	(3,8)
25	0.2115	0.0	0.2485	0.54	(4,9)
26	0.2115	0.0	0.301	0.4875	(4,10)

Table 5-5. Centroids of Faces of Constrained Region

Centroids	x_1	x_2	x_3	x_4	Centroid Vertices
27	0.2115	0.54	0.12425	0.12425	(1,2,7,6)
28	0.2115	0.39425	0.0	0.39425	(2,3,8,7)
29	0.2115	0.12425	0.12425	0.54	(3,4,9,8)
30	0.229	0.0	0.266	0.505	(4,9,10)
31	0.2115	0.24375	0.301	0.24375	(4,1,5,10)
32	0.229	0.505	0.266	0.0	(1,5,6)
33	0.159	0.34525	0.1505	0.34525	(1,2,3,4)
34	0.264	0.2851667	0.1656667	0.2851667	(5,6,7,8,9,10)
35	0.222	0.3092	0.1596	0.3092	(all)

This left thirty-five possible design points to select from. Prototype tiles could be made for each design point to develop the model. However making thirty-five tiles was not practical since it would be quite time consuming and unnecessary. As stated above, ten terms are required to solve the second-order polynomial. Selecting more than the minimum would ensure a better fit for the model.

There have been several strategies proposed for selection of design points. Snee[58] cites two possible strategies.

(i) Selection of extreme vertices and centroids. Midpoints are used when one edge is considerable longer than the other edges.

(ii) Use the Wynn[58] and/or exchange algorithms to pick the best design points from the extreme vertices, centroids and midpoints.

The first strategy was selected for this mixture problem. All extreme vertices were chosen as well as the overall centroid. A subset of the centroids and midpoints was selected based on the average distance from the vertices. Distances have been summarized in Table 5-6.

Table 5-6. Average Distances from Vertices of Midpoints and Face-Centroids

Point	Average Distance	Point	Average Distance
11	1.145	**24**	1.019
12	0.626	**25**	1.059
13	1.145	**26**	1.019
14	1.414	**27**	0.698
15	0.399	**28**	0.635
16	0.745	**29**	0.698
17	0.901	**30**	0.489
18	0.745	**31**	0.815
19	0.399	**32**	0.489
20	1.139	**33**	0.755
21	1.019	**34**	0.735
22	1.059		

Average distances from the vertices were determined from the following equation.

$$d_{ij} = \left[\sum_{m=1}^{q} (x_{im} - x_{jm})^2 / (b_m - a_m)^2 \right]^{1/2} \qquad (5\text{-}5)$$

Where:

q = number of components
b = upper limit
a = lower limit

From Table 5-6 it was noticed that point 14 had the largest average distance from the vertices. Centroids 31, 33 and 34 were selected since the average distances were the largest. A random point 36 was also selected so that another point was also within the simplex not just on the boundaries. Final design points selected are presented in Table 5-7.

Table 5-7. Final Design Points

Design Point	x_1	x_2	x_3	x_4
1	0.159	0.54	0.301	0.0
2	0.159	0.54	0.0	0.301
3	0.159	0.301	0.0	0.54
4	0.159	0.0	0.301	0.54
5	0.264	0.435	0.301	0.0
6	0.264	0.54	0.196	0.0
7	0.264	0.54	0.0	0.196
8	0.264	0.196	0.0	0.54
9	0.264	0.0	0.196	0.54
10	0.264	0.0	0.301	0.435
14	0.159	0.27	0.301	0.27
31	0.2115	0.24375	0.301	0.24375
33	0.159	0.34525	0.1505	0.34525
34	0.264	0.2851667	0.1656667	0.2851667
35	0.222	0.3092	0.1596	0.3092
36	0.2115	0.07525	0.1995	0.51375

Using the Excel spreadsheet mentioned above, the new design points were plotted on the constrained region. The new points are presented in Figure 5-5.

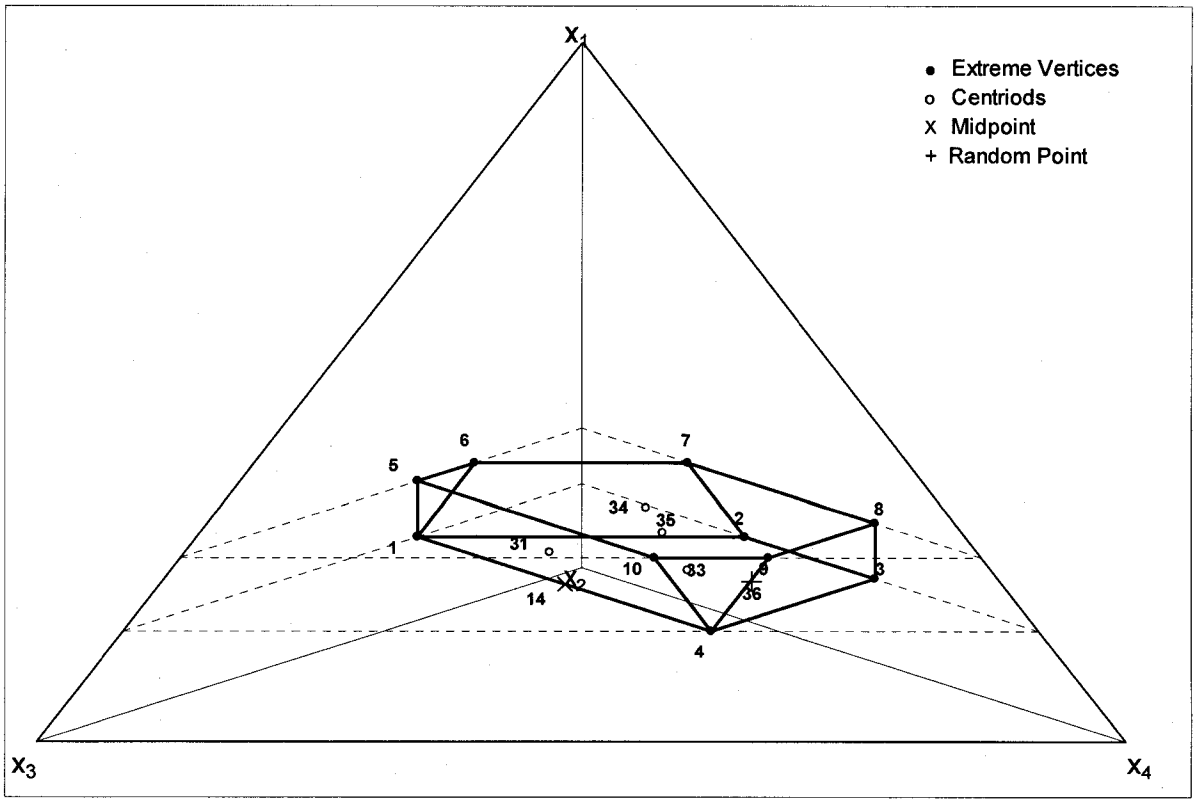

Figure 5-5. Constrained Region of Four-Component Simplex with Selected Design Points

Tests were performed on the selected design points to determine the quality of the design. It was important to determine if the selected design points would be sufficient to develop a proper model. Four popular criteria[15] for choosing a design set are:

- A-optimality – Seeks to minimize the trace of $(\mathbf{X}'\mathbf{X})^{-1}$.
- D-optimality – Seeks to maximize the determinant of $\mathbf{X}'\mathbf{X}$.
- G-optimality – Seeks to minimize the maximum predication variance, minimize $\max[d=\mathbf{x}'(\mathbf{X}'\mathbf{X})^{-1}\mathbf{x}\sigma^2]$, over a specified set of design points. Can also be found with $100*p / N*\max[v]$.
- V-optimality – seeks to minimize the average prediction variance over a specified set of design points

In matrix notation the second-degree polynomial is given by:

$$\mathbf{y} = \mathbf{X}\beta + \varepsilon \qquad (5\text{-}6)$$

Where:

$\mathbf{y}$	=	vector of observations, (N x 1)
$\mathbf{X}$	=	matrix of mixture components, (N x p)
β	=	vector of parameters, (p x 1)
ε	=	vector of random errors, (N x 1)
p	=	q(q+1)/2
N	=	number of observations or design points in model
v	=	$\mathbf{x}(\mathbf{X}'\mathbf{X})^{-1}\mathbf{x}$
σ^2	=	observation error variance

MATLAB was used to calculate the above criteria for the selected design points. The results are summarized in Table 5-8. See Appendix E for the m-file used.

Table 5-8. Criteria for Selection of Design Points

A-optimality	1.94×10^{5}
D-optimality	7.35×10^{-20}
G-optimality	72.4118
V-optimality	0.625

It was suggested by Wheeler[58] that any design with a G-optimality $\geq 50\%$ to be good. Snee[58] in addition believes the V-optimality be ≤ 1.0. When equal to unity it implies the model predictions are as precise as the measured responses. In order to determine lack of fit of the model residual degrees of freedom are necessary, meaning V-optimality < 1.0.

Several other designs with a different set of points were tested as a comparison. Changing the design points did not make a significant difference. It was therefore determined that the first set of design points selected was reasonable.

5.4 Conclusions

Once final design points were selected, prototype tiles for each of the sixteen design points of Table 5-7 were manufactured. The number of tiles produced for each point depended on the quantity required for the flexural and compressive tests. Ten samples were required for the flexural strength testing and five samples for the compressive strength testing. A four-inch square tile was divided into one two-inch square and two one-inch square compressive strength samples and six to eight flexural strength samples. Therefore at least five prototype tiles were manufactured for each design point.

The steps outlined in this chapter can be easily followed for any four-component mixture problem. Components and the upper and lower limits can be changed to suit new project objectives. A new simplex region, thus new extreme vertices, can be easily developed using the spreadsheet created for this project. Using MATLAB an optimality study can be performed using the procedures outlined in this chapter and in Appendix E to determine new design points.

Chapter 6: Response of Flexural and Compressive Strength

6.1 Introduction

In attempts to narrow the countless possible combinations of the phase change material (PCM) and the seven components of the original Granirex recipe, four components were held constant. The remaining four components were varied to produce different tile mixtures. Even with this limitation the numbers of possible mixtures were numerous. Each one has expected physical properties that may or may not meet the required standards for this project. Determining a method to eliminate unnecessary combinations was a significant part of this research. The approach selected was creating fitted models that describe the response of the physical properties of various tile compositions. Based on these fitted models a significant percentage of tile compositions could be eliminated due to low PCM content and poor strength.

Two physical properties, flexural and compressive strength, were selected to study the response to varying tile components. Prototype tiles, 4-inch square and ¾ inch thick, were manufactured for each design point. Tiles were cut to appropriate sizes to perform the physical tests. Raw data collected from the tests were fitted to polynomials. The developed polynomials were used to select two final tile mixtures that maximized the PCM content while maintaining an acceptable physical strength.

6.2 Experimental

6.2.1 Three-Point Flexural Strength Testing

At each design point several tiles were manufactured and multiple samples from each were tested. Results were averaged to determine an overall three-point flexural strength for each design point. Values along with the 95% confidence intervals are presented in Table 6-1. Adjusted proportions of the four-components for each design point can be referred to in Table 5-7.

Table 6-1. Experimental Three-Point Flexural Strength for Design Points

Design Point	Flexural Strength [MPa]	Design Point	Flexural Strength [MPa]
1	47.7 ∀ 3.7	**9**	4.1 ∀ 1.2
2	7.8 ∀ 1.0	**10**	5.5 ∀ 0.6
3	1.3 ∀ 0.3	**14**	5.3 ∀ 0.9
4	1.4 ∀ 0.3	**31**	5.9 ∀0.8
5	46.1 ∀ 6.3	**33**	3.8 ∀ 0.8
6	42.4 ∀ 3.1	**34**	6.1 ∀ 0.8
7	6.4 ∀ 2.3	**35**	6.1 ∀ 0.7
8	3.1 ∀ 1.4	**36**	2.5 ∀ 0.5

Ceramic tile, purchased at a local hardware store, and the Granirex tile were tested using the same procedure. Results are summarized in Table 6-2.

Table 6-2. Flexural Strength of Ceramic and Granirex Tiles

	Flexural Strength [MPa]
Granirex Tile	33.9 ∀ 4.7
Ceramic Tile	7.3 ∀ 1.1

These values were used as a range to compare the prototype tiles. Final prototype tiles were expected to meet the minimum strength requirements. The maximum strength was not expected to be attainable for PCM incorporated tiles, but was used as a guideline for prototypes manufactured without PCM.

The four-component simplex region, shown in Figure 5-5 developed in Chapter 5 was updated to include the flexural strength at each design point. The updated simplex can be seen in Figure 6-1. Values are reported in units of MPa. Included in the figure are the vertices for the face-centroid design points. Flexural strength values are in parentheses.

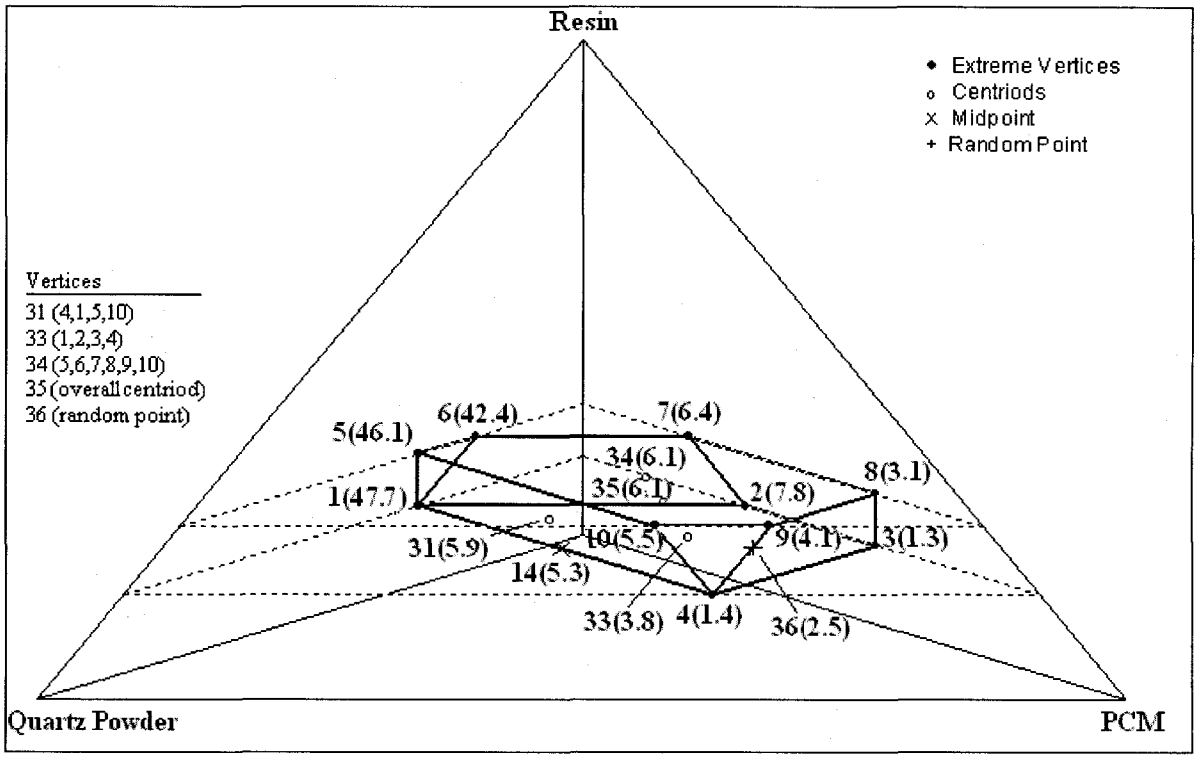

Figure 6-1. Four-Component Simplex with Flexural Strength given in MPa for the Design Points

Tiles at design points 1, 5 and 6 did not contain any PCM. All were greater in strength than the Granirex tile tested at 33.9 MPa. The strength was higher since a larger concentration of resin was used in the tiles. Granirex tiles contained 8% resin by mass, while tiles at design point 1 contained 12.1% by mass of resin. At design points 5 and 6 resin content was 20.1% by mass. Statistically the strengths at points 1 and 5 are the same with a slight decrease in

strength at point 6. Design point 6 contains less quartz powder that points 5 and 6, possible accounting for it decrease in strength.

Further emphasizing the importance of quartz powder in the mixtures was the observed decrease in strength when quartz powder was substituted with PCM. Quartz powder was primarily used as filler for the composite. Fillers can be used to reduce overall cost of the composite as well as improving physical properties. The original Granirex recipe primarily used the powder to fill in voids between the larger quartz particles. However it did impart some physical strength to the composite, since using PCM as a substitute lowered the strength of the tile. Tile mixtures at design points 2 and 7 replaced the quartz powder component with PCM. Compared to design points 1 and 6, where there is no PCM, the strength was drastically decreased.

Significant decreases in strength were observed in general as PCM was incorporated into the tile mixture. Lowest strengths were recorded for design points 3 and 4. These had the highest PCM and lowest resin content. An increase in strength was seen when resin content was increased, while maintaining the same PCM content, as design points 8 and 9 demonstrate. PCM particles are smaller than the quartz-34 and quartz powder particles, thus a higher PCM content increases the surfaces area of particles to wet. Increased resin amounts will wet the PCM particles more effectively, thus creating a stronger bond. When there is not enough resin, not all the particles will have resin between them. As a result some of the particles will mechanically lock with each other, resulting in a lower overall strength.

The lack of quartz-34 in design points 4, 9 and 10 also accounts for the poor strength as well as the high PCM content. It was expected that quartz-34 would contribute a majority of the strength to the tile, since it was the main component of the original tile recipe occupying 36.6% by volume and 41.1 % by mass.

6.2.2 Development of Fitted Model for Flexural Strength

Using the data from Table 6-1 the unknown parameters from Equation 5-4, developed in Chapter 5, were solved using the statistical program SAS (Statistical Analysis System). Since there was a large difference in magnitude of strength between tiles with PCM and those without, the raw data was first transformed to linearize the data. The log of the flexural strength was performed to create a linear relationship.[48] The effect of the linearization is evident in Figure 6-2.

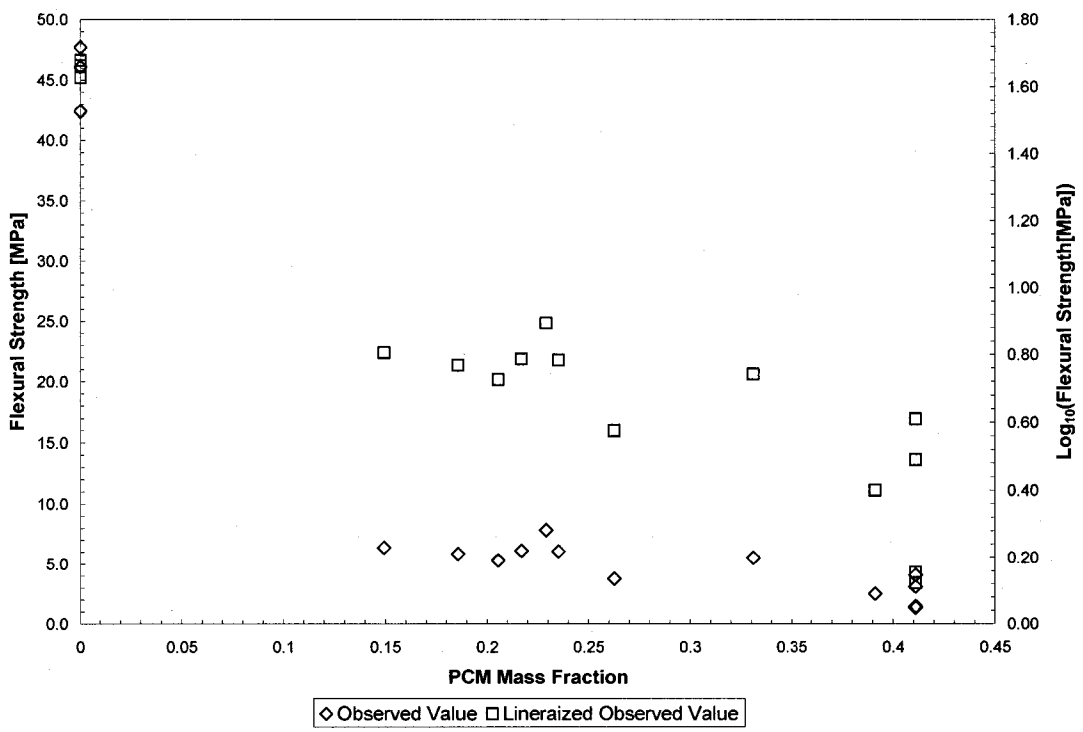

Figure 6-2. Linear Transformation of Flexural Strength Raw Data

Once the ten unknown parameters of the polynomial were determined, the number of terms was reduced. The fewer number of terms the easier it was to understand the effect of component blending. Not all components will have a direct effect on each other and therefore some terms can be ignored. Terms were determined irrelevant by two criteria, mean square error (MSE) and the coefficient of determination (R^2). The ultimate goal was to minimize the MSE and maximize R^2.

Values for R^2 and MSE were determined for each fitted model with terms ranging from ten to one. The ten-term fit had a R^2 value of 0.9961. This value decreased as the number of terms decreased. As an example a five-term fit had a R^2 value of 0.9936 compared to a two-term fit with a value of 0.9513. There was not a significant change in R^2 until the fit was reduced to two terms. Using this criteria and F-statistics to verify significance of each term, a three-term fitted model was selected with R^2 value of 0.9779 and a MSE of 0.02318.

The final fitted model is presented below. Linear terms of the original model, x_1, x_3 and x_4, were determined to be non-significant. Blending of component x_1 and x_3 and components x_2 and x_4 were the most significant. F-statistic was used to compute p-values to verify the interaction of components and significance of each of the linear terms of the fitted model.

$$y = b_1 x_2 + b_2 x_1 x_3 + b_3 x_2 x_4 \qquad (6\text{-}1)$$

Where:

y	=	log of flexural strength (MPa)
b	=	parameters
x	=	adjusted mass percentage of components

And:

$x_1 + x_2 + x_3 + x_4 = 1$

It should be noted that values obtained from this fitted model determined the flexural strength in log form. Results need to be converted to the useful unit of MPa using 10^y. Valid upper and lower limits for each component of the above model were developed in Chapter 5 and presented in Table 5-2. Limits have been repeated below in Table 6-3.

Table 6-3. Adjusted Upper and Lower Limits of Components

Component	Lower Limit	Upper Limit
x_1	0.159	0.264
x_2	0.0	0.54
x_3	0.0	0.301
x_4	0.0	0.54

The fitted model is valid for adjusted mass percentage values as explained in Chapter 5 in section 5.2.2.1. If the flexural strength for a new mixture is desired, mass percentages need to be divided by 0.761 before they are entered in the above equation. As an example, in order to determine the flexural strength of a tile mixture with 12.1% resin, 41.1% quartz-34, 11.5% quartz powder and 11.4% PCM, values of 0.159, 0.540, 0.151 and 0.150 would have to be plugged into the above equation.

Parameters, b_1, b_2 and b_3, are presented in Table 6-4. The t-statistic was used to verify the significance of each estimate. Using the standard error and the t-statistic calculated by SAS for each estimate, margin of error for a 95 percent confidence interval was calculated. These values are presented with the parameter estimates in Table 6-4.

Table 6-4. Parameter Estimates of Final Flexural Strength Fitted Model

b_1	**2.3 +/- 0.4**
b_2	**8.0 +/- 2.1**
b_3	**-2.7 +/- 1.5**

All parameters were shown to be highly statistically significant since the p-values were less than 0.01. Parameters b_1 and b_2 both had p-values less than 0.0001 and b_3 had a p-value of 0.0016. Values less than 0.01 are traditionally termed highly statistically significant where values less than 0.05 are considered statistically significant.[48] Small p-values are an indication that flexural strength is dependent of the four-components of the mixture problem.

The F-statistic and p-value were determined for the fitted model by SAS. The p-value was less than 0.0001 indicating a good fit of the model.

Blending of resin with quartz powder was determined to be the most interesting because the magnitude of the parameter b_2 was greatest. Resin and quartz powder have binary synergistic effect, meaning the binary blend strength is greater than the individual components. As expected the blending of PCM with quartz-34 reduces the strength. This was evident by the negative sign on parameter b_3. In addition as expected the quartz-34 is a significant component in providing strength to the tile, represented by the first term of the fitted model.

6.2.2.1 Comparison of Predicted Values to Experimental Data

A comparison of the experimental data collected for each of the sixteen prototype tiles to the predicted data from the fitted model is presented in Figure 6-3. Included in the figure are the resin mass fractions for each data point and a non-design point, random point RP. This point was included to further verify the fit of the model.

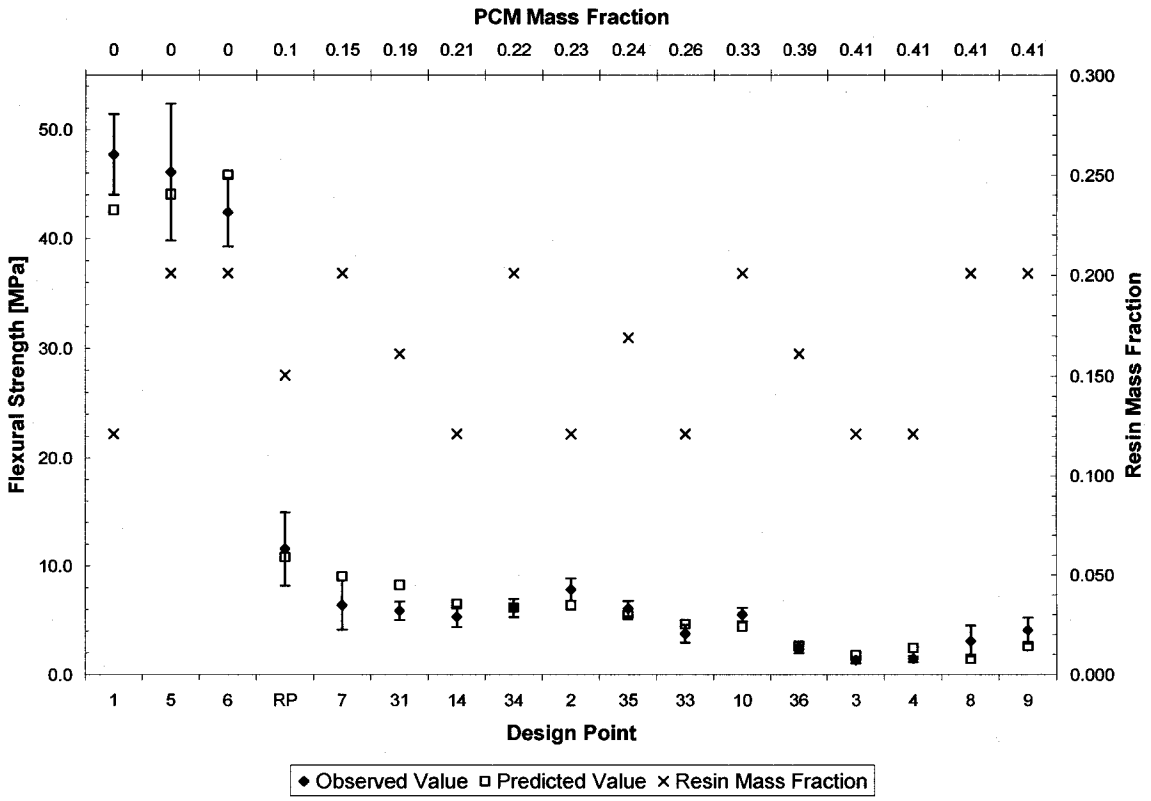

Figure 6-3. Comparison of Experimental and Predicted Values for 3-Point Flexural Strength

Experimental data matched the predicated value within expected error tolerances. The 95% confidence intervals for the predicated values are presented in Table F-1 located in Appendix F. Error intervals for the predicted and experimental data overlapped, validating the fit.

It was observed from the data in Figure 6-3 that the highest strength tiles in general corresponded to high resin content. Increased resin was expected to increase the strength when PCM was incorporated into the tile, since there would be surface area to wet.

Mass fractions of the random point RP were: resin = 0.1977, quartz-34 = 0.2244, quartz powder = 0.3756 and PCM = 0.1252. Even though the four fractions do not add to unity, the fitted still predicted the value within error tolerances, substantiating the fit of the model.

6.2.3 Compressive Strength Testing

During testing it was found that tile without any PCM did not fail when a two-inch square sample was used. When the sample was reduced to one-inch square, the samples failed. At failure, the sample typically crumbled and cracked around the edges first before completely breaking apart.

It was noticed that at the high loads, greater than 17.8 kN (4000 lbf), the encapsulation of the PCM failed, resulting in some leakage. These loads are not expected in typical use and are not a concern at this time.

The average compressive strengths for the design points along with the 95% confidence interval are presented in Table 6-5. The data for design points 4 and 33 were not reliable and were discarded from the fitted model development. Majority of the specimens tested at these points failed at very small loads. Failure was assumed to be due to flaws in the samples and therefore not a true representation of strength at these points.

Ceramic and Granirex tile samples were tested using the same procedure. These results are summarized in Table 6-6 along with the Granirex tested value for the tile.

Table 6-5. Experimental Compressive Strength for Design Points

Design Point	Compressive Strength [MPa]	Design Point	Compressive Strength [MPa]
1	183.9 ∀ 87.2	**9**	10.5 ∀ 1.8
2	17.5 ∀ 3.1	**10**	13.4 ∀ 2.3
3	7.9 ∀ 1.4	**14**	18.0 ∀ 3.1
5	141.0 ∀ 46.6	**31**	15.7 ∀ 2.7
6	137.6 ∀ 45.3	**34**	20.6 ∀ 3.6
7	29.3 ∀ 5.2	**35**	7.9 ∀ 1.4
8	11.7 ∀ 2.0	**36**	7.9 ∀ 1.4

Table 6-6. Compressive Strength of Ceramic and Granirex Tile

	Compressive Strength [MPa]
Granirex Tile	171.0 ∀ 81.1
Granirex Tile (Manufacturer Tested Value)	172.4+
Ceramic Tile	10.4 ∀ 1.8

The compressive strength data was added to the simplex region developed in Chapter 5. The updated figure is given in Figure 6-4. Values were presented in units of MPa. Included in the figure are the vertices for the face-centroid design points. Compressive strength values are in parentheses.

As expected the incorporation of PCM significantly reduced the strength of the tiles. Design points 3 having the lowest strength, corresponding to the highest PCM and lowest resin content. Increase in resin amounts to design points 8 and 9 improved the strength slightly. Addition of PCM particles to the mixture increases the wetting surface for the resin. Therefore increasing the resin would insure a continuous resin network around the PCM particles, resulting in increased strength. This behavior was also observed for the flexural strength data.

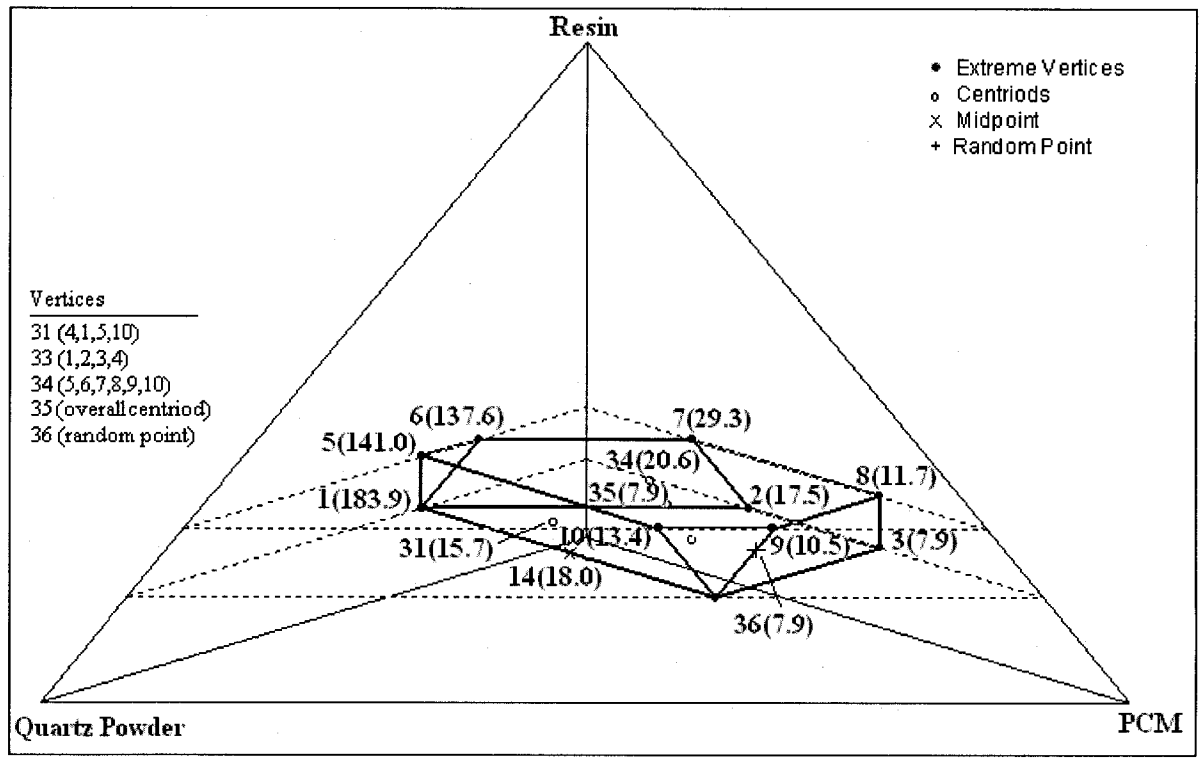

Figure 6-4. Four-Component Simplex with Compressive Strength given in MPa for the Design Points

6.2.4 Development of Fitted Model for Compressive Strength

The compressive strength fitted model was developed using the data from Table 6-1 and the statistical program SAS. As with the flexural strength fitted model, there was large difference in magnitude between tiles with PCM and those without, so the fitted model was developed using the log of the values at each data point. The effect of the linearization of the data is presented in Figure 6-5.

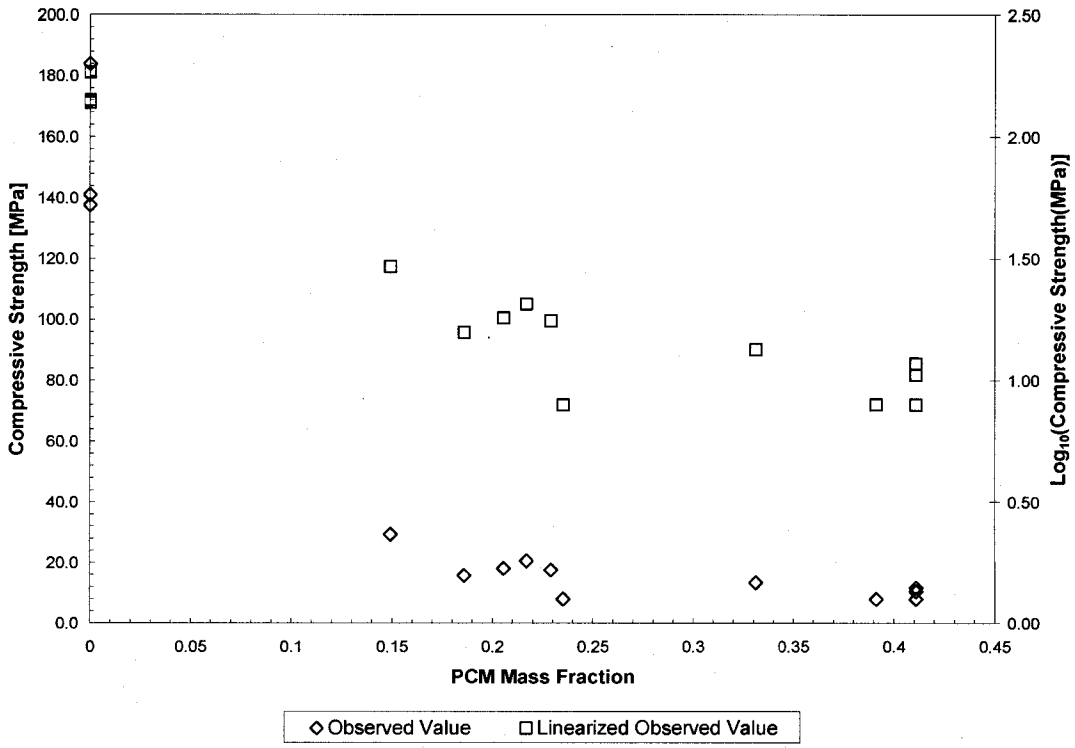

Figure 6-5. Linear Transformation of Compressive Strength Raw Data

Starting with a ten-term quadratic of Equation 5-4 developed in Chapter 5, the model was reduced to a four-term linear polynomial. F-statistics determined the quadratic terms to be non-significant and were removed from the fit. The resulting four-term fitted model had an R^2 value of 0.9971 and is presented below. It should be noted that values obtained from this fitted model give the compressive strength in log form and needs to be converted properly into the units of psi using 10^y.

$$y = b_1x_1 + b_2x_2 + b_3x_3 + b_4x_4 \qquad (6\text{-}2)$$

Where:

y	=	log of compressive strength (psi)
b	=	parameters
x	=	mass percentage of components

And:

$x_1 + x_2 + x_3 + x_4 = 1$

Valid mass percentages are presented in Table 6-3. Determination of adjusted mass percentages was explained in Chapter 5 in section 5.2.2.1. If the compressive strength for a new mixture is desired, mass percentages need to be divided by 0.761 before they are entered in the above equation. As an example, in order to determine the compressive strength of a tile mixture with 12.1% resin, 41.1% quartz-34, 11.5% quartz powder and 11.4% PCM, values of 0.159, 0.540, 0.151 and 0.150 would have to be plugged into the above equation.

The t-statistic was used to verify the significance of each estimate. Using the standard error and the t-statistic calculated by SAS for each estimate, margin of error for a 95% confidence interval was calculated. These values are presented in Table 6-7 along with the estimates.

Table 6-7. Parameter Estimates of Final Compressive Strength Fitted Model

b_1	**4.8 +/- 2.4**
b_2	**4.0 +/- 0.6**
b_3	**4.0 +/- 1.1**
b_4	**1.8 +/- 0.9**

All parameters were shown to be highly statistically significant since the p-values were less than 0.01. Parameters b_1 and b_2 both had p-values less than 0.0001. Values of 0.0001 and 0.0007 were calculated for parameters b_3 and b_4 respectively. Small p-values are an indication that compressive strength is dependent of the four-components of the mixture problem.

The F-statistic and p-value were determined for the model by SAS. The p-value was calculated to be less than 0.0001 indicating a good fit of the fitted model.

Based on the magnitudes of the parameters, the resin component has the largest effect on the compressive strength followed by the quartz powder and quartz-34 components. It is interesting that the resin component has the highest influence on the overall strength. This indicates the importance of the proper resin amount to fully wet all the components and prevent quartz particles from mechanically locking with each other.

PCM has the least influence as expected. However unlike in the flexural strength fitted model, it contributes positively to the overall compressive strength. This positive effect on compressive strength indicates PCM adds some strength to the mixture independently, although not considerable. Whereas the parameter for the linear PCM term in the flexural strength fitted model was determined to be a small negative number and did not contribute positively to strength. This term was removed from the final fit because it was found to be insignificant. It can be concluded the PCM component will hinder the strength of the tile when under tension, but will contribute slightly under compression.

Because each component contributes positively to the compressive strength, the magnitude of strength is determined by the mass percentage of each component. A mixture high in PCM content will result in a lower compressive strength, since there are less of the higher influencing components.

6.2.4.1 Comparison of Predicted Values with Experimental Data

A comparison of experimental and predicted values from the fitted model is presented in Figure 6-6. Included in the figure are the resin mass fractions for each data point and a non-

design point, random point RP. As with flexural strength this point was included to further verify the fit of the model.

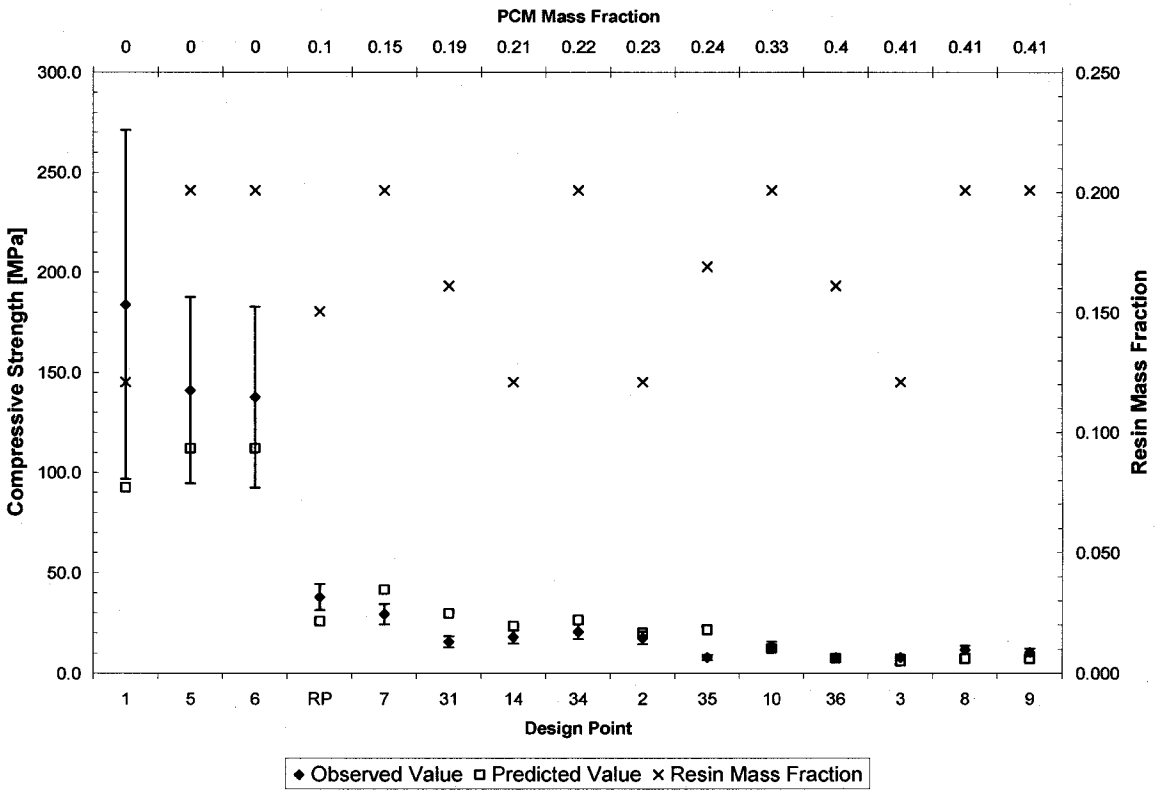

Figure 6-6. Comparison of Experimental and Predicted Values of Compressive Strength

Experimental data matched the predicated value within expected error tolerances. Upper and lower limits of the predicated values are presented in Table F-2 located in Appendix F. Predictions of the strength for tiles not containing PCM were all low. This was not seen as a concern since the main use of the fitted model was to predicted strength of tiles containing PCM.

Mass fractions of the random point RP were: resin = 0.1977, quartz-34 = 0.2244, quartz powder = 0.3756 and PCM = 0.1252. Even though the four fractions do not add to unity, the fitted still predicted the value within error tolerances.

6.2.5 Evaluation of Fitted Models

The response trace was plotted for both the flexural and compressive strength models. They are used to evaluate the effects of the mixture components without the offset of change in the other components. In a mixture problem, when one component is changed it is offset by changes in proportions of the other components, so all components add to unity. Trace plots the estimated strength values versus changes in one component from a set reference mixture. The reference mixture selected was the overall centroid of the constrained simplex region: $x_1 = 0.222$, $x_2 = 0.3092$, $x_3 = 0.1596$, $x_4 = 0.3092$. Figure 6-7 and Figure 6-8 are the resulting response traces for the flexural and compressive strength fitted models respectively.

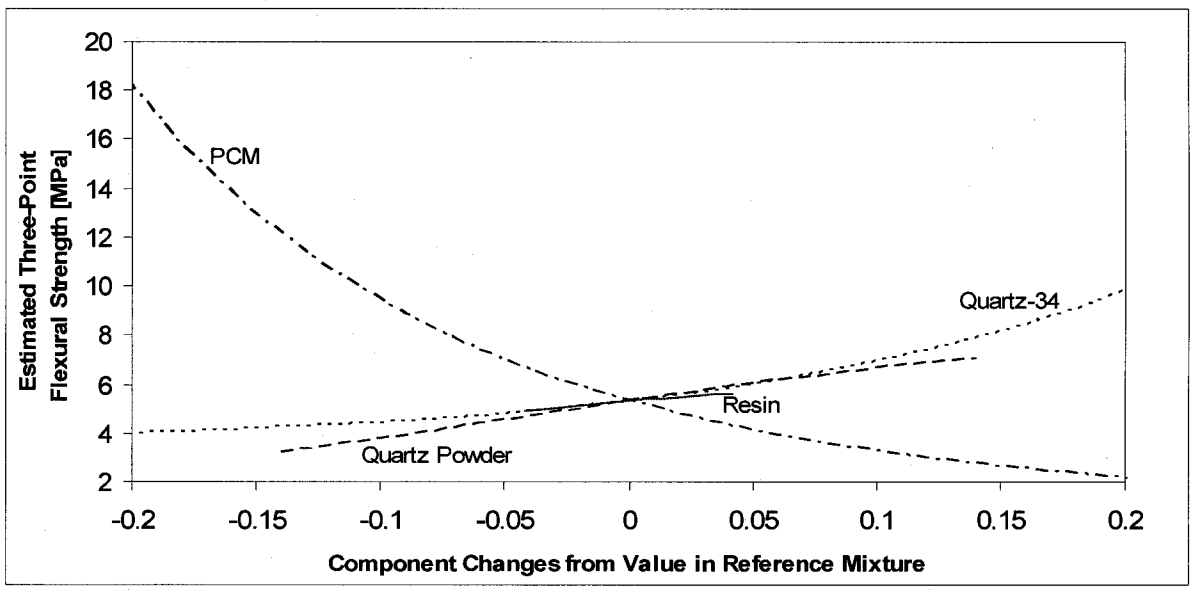

Figure 6-7. Response Trace of Three-Point Flexural Strength Model

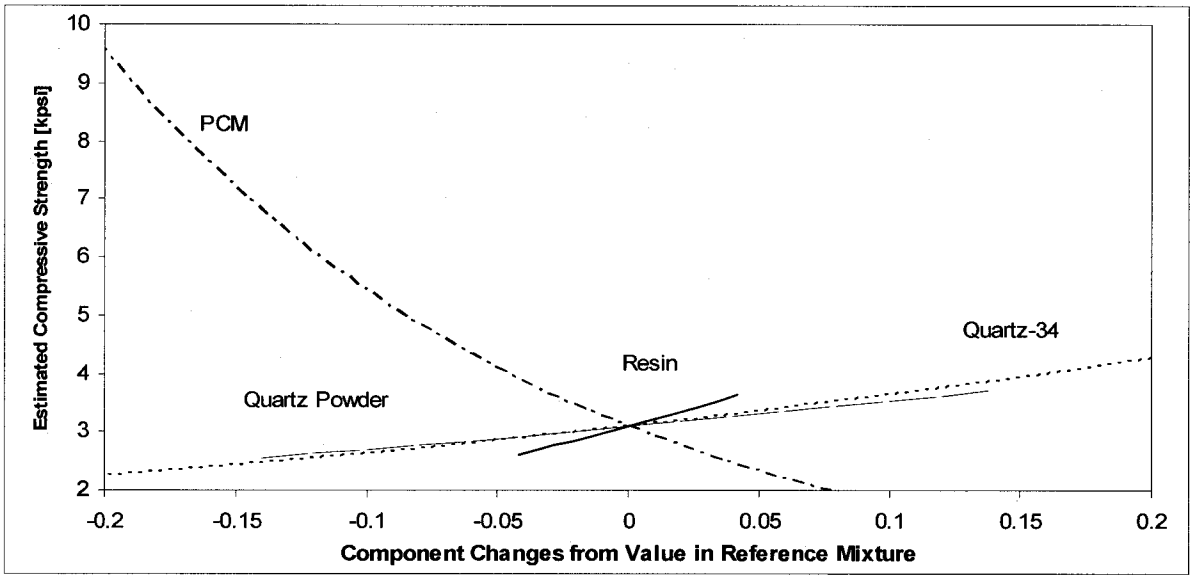

Figure 6-8. Response Trace of the Compressive Strength Model

Both response traces confirm the curvilinear effect of the quartz-34 and PCM components since both traces were curved. The compressive strength fitted model currently overlooks this behavior since contains only linear terms.

The negative effect PCM has on the tile mixture is evident in both traces as expected. A significant drop in strength is evident in both traces.

Increases in resin, quartz-34 and quartz-powder all result in a higher strength tile mixtures. It is interesting to note that increase in resin has a larger effect on compressive strength compared to flexural strength.

It is evident that the compressive strength fitted model is limited by not accounting for binary interactions. Statistical analysis showed the binary terms to be insignificant. The fit of the model was not improved with the inclusion binary terms. The lack of reliable data at design

points 4 and 33 may have hindered the fitted model development more than originally assumed.

Statistical analysis was repeated using only the compressive strength data from prototype tiles containing PCM. Results did not improve the fit of the original fitted model, therefore the original fitted model was kept.

6.3 Results and Discussion

Due to the concerns with the fitted model for compressive strength, the flexural strength fitted model was used as the main criteria for the selection of two final prototype tiles. In addition the majority of the prototype tiles tested had compressive strength greater than ceramic tile unlike flexural strength. It was obvious flexural strength was going to be the limiting factor. Therefore it will be left as future work to reanalyze the compressive strength data at data points 4 and 33 and rework the statistical analysis to develop a more accurate fit. The current fitted model is sufficient to predict within reason the compressive strength for tiles containing PCM, which is the main focus of this research.

6.3.1 Final Prototype Selection

Selection of two final prototype tiles was based on flexural strength and the amount of PCM incorporated into the tile. It was desired to have a tile with flexural strength comparable if not greater than a typical ceramic tile.

The two final prototype tiles were chosen based on two requirements. One would have a flexural strength approximately one and half times greater than ceramic tile. The second would have flexural strength near to the ceramic tile and therefore a higher PCM content. Both final prototypes were required to have compressive strength at least equivalent to the ceramic tile.

6.3.1.1 Selection of Final Prototype Tile 1

It was established that the physical strength of tiles decreased as the amount of PCM incorporated increased. Using the developed fitted model for flexural strength, Equation 6-1, plots were generated to investigate the behavior of increasing PCM amounts on strength. It was desired to find a mixture with a flexural strength approximately one-half times greater than that of the tested ceramic tile with maximum PCM content. A value of 11.55 MPa was selected.

Two dimensional plots were preferred since they were easier to interpret than a three dimensional plot. This required one component to be held constant for each graph. Resin was chosen for this analysis. Two plots were created, Figure 6-9 and Figure 6-10. Resin was held constant at the lower limit in Figure 6-9 and at the upper limit in Figure 6-10. Included on both plots is a line indicating the 11.55 MPa flexural strength level. Both figures use the true mass percentage of the components, not the adjusted amounts used in the development of the fitted models. (See Table 5-1 and Table 5-2)

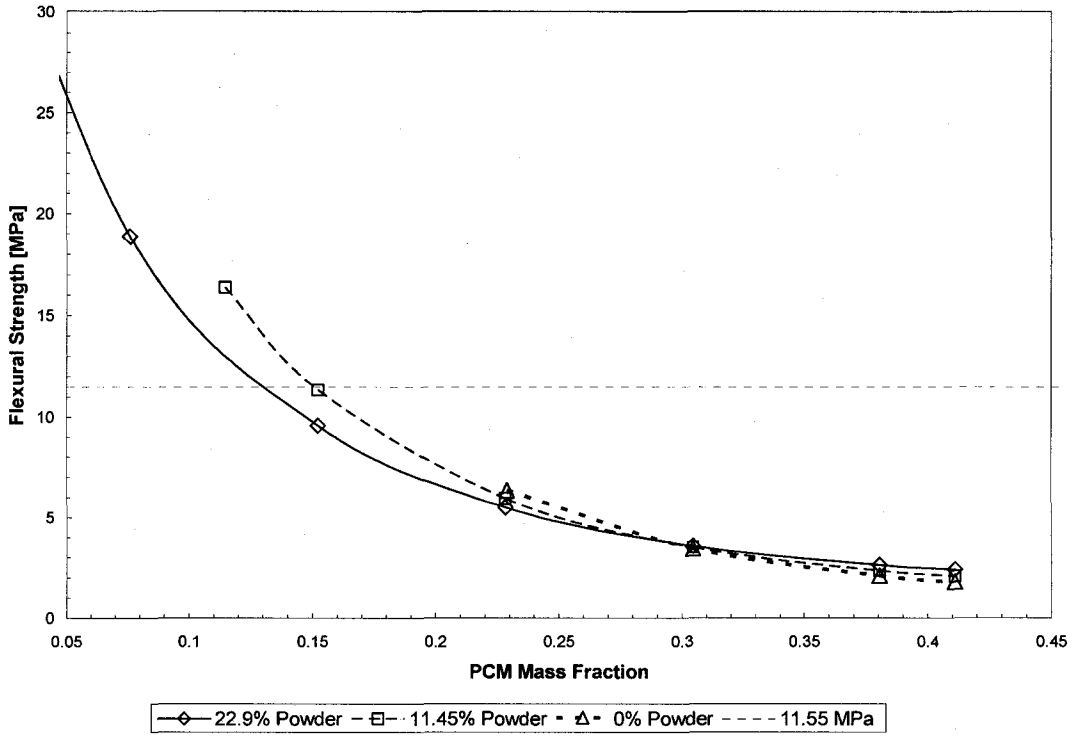

Figure 6-9. Dependence of Flexural Strength on PCM and Quartz Powder Content on Flexural Strength with a Constant Resin Mass Fraction of 0.121

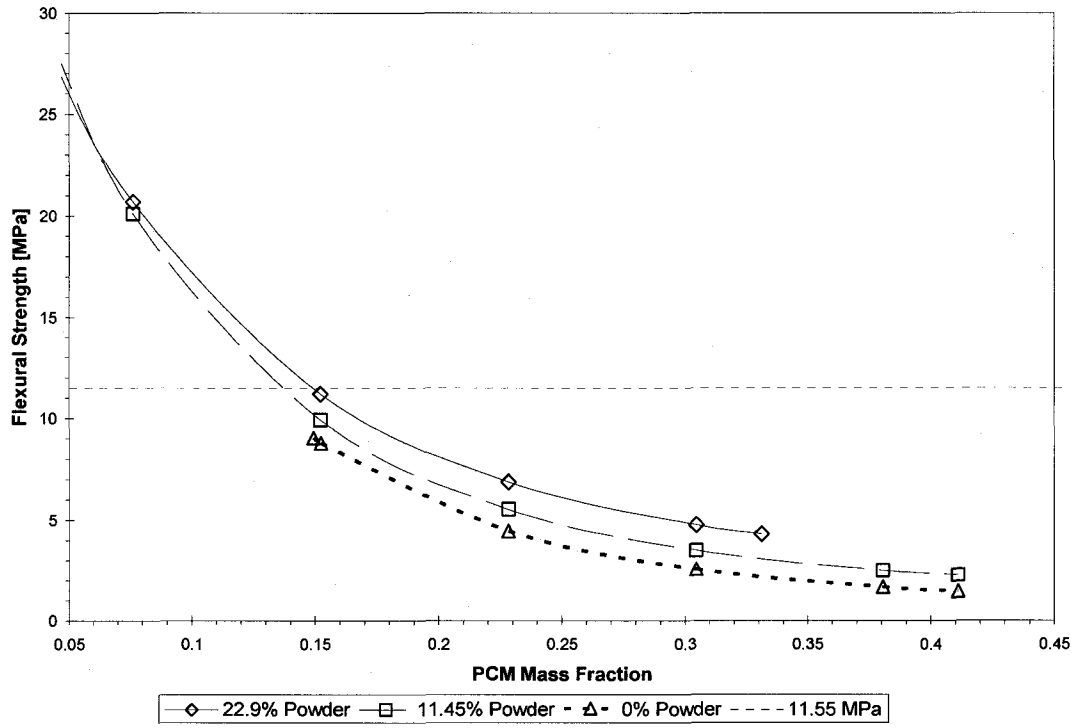

Figure 6-10. Dependence of Flexural Strength on PCM and Quartz Powder Content with a Constant Resin Mass Fraction of 0.201

Figure 6-9 and Figure 6-10 show the flexural strength decreasing rapidly with the addition of PCM in the tile mixture. Strength decreased by half with less than 10% by mass of PCM regardless of the resin content. Analysis was not carried out for PCM mass fractions greater than 0.40 since mass fractions of other components would be beyond the upper limits set for the fitted model.

Increases in PCM content in Figure 6-9 and Figure 6-10 corresponds to a decrease in the amount of quartz-34 since the powder and resin components are held constant. The higher the powder content, the lower the quartz-34 amount.

Figure 6-10 suggests that by increasing the quartz powder content beyond the upper limit set by this research, flexural strength could be improved for tiles containing higher resin. At lower resin percentages and high PCM amounts, an increase may also be possible with higher quartz powder content. Increases in quartz powder are accompanied by a decrease in quartz-34, so it is unsure if any possible increase in strength would be notable.

The minimum acceptable flexural strength of 11.55 MPa was achieved with approximately the same PCM content for both resin amounts. At the lower resin limit, a maximum PCM mass fraction of 0.157 was obtained with a quartz powder mass fraction of 0.0716. A maximum PCM mass fraction of 0.149 was achieved with the upper resin content and maximum quartz powder amount of 0.229. Mass and volume fractions for the four variable components are given in Table 6-8.

Table 6-8. Corresponding Component Mass and Volume Fractions for a Flexural Strength of 11.55 MPa

	Low Resin		High Resin	
	f	x	f	x
Resin (x_1)	0.121	0.131	0.203	0.216
Quartz 34 (x_2)	0.411	0.277	0.180	0.119
Quartz Powder (x_3)	0.072	0.049	0.229	0.151
PCM (x_4)	0.157	0.38	0.149	0.352

Based on the results presented in Table 6-8, a low resin tile mixture has a slightly higher PCM content for a flexural strength of 11.55 MPa compared to the high resin mixture. In addition reduction in resin content means lower overall cost. Thus the low resin tile mixture was selected for the first final prototype, Tile 1.

6.3.1.2 Selection of Final Prototype Tile 2

The first final prototype tile selected, Tile 1, had a PCM mass fraction of 0.157. It was desired to increase PCM content further without drastically compromising the physical strength. Investigating the behavior of the flexural strength fitted model, it was determined that a slightly higher PCM content can be achieved by increasing the resin content. A PCM mass fraction of 0.20 was chosen and an analysis of flexural strength on varying resin content was performed. Selection of this PCM content was based on the fact that it was approximately the maximum amount allowed to maintain a flexural strength equivalent to ceramic tile. Analysis is presented in Figure 6-11. As with Figure 6-9 and Figure 6-10, the upper and lower limits of the four components are followed and true mass percentages are used. (See Table 5-1 and Table 5-2)

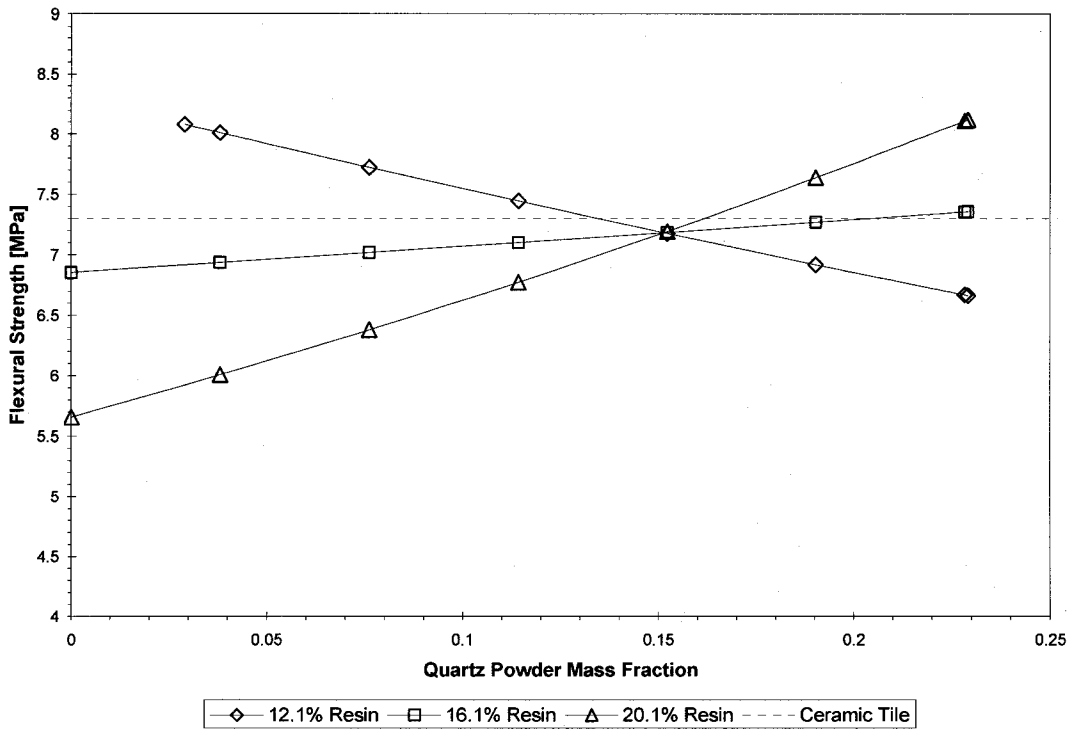

Figure 6-11. Dependence of Resin and Quartz Powder Content on Flexural Strength for a PCM Mass Fraction of 0.20

Figure 6-11 clearly shows a relationship between quartz powder and resin on overall strength for tile mixtures with 20% by mass of PCM. Strength decreases for the lower resin limit as the quartz powder amounts increase. The opposite is true for the upper resin limit. As the quartz-powder content approaches zero for the lower resin content, strength may be increased. The same can be said of increasing the quartz powder for high resin content mixtures. Strengths cannot be accurately estimated from fitted models because of the current upper and lower limits of the components. The upper limit for quartz-34 and quartz powder would have to be increased beyond the upper limits valid for the fit.

Based on the results of Figure 6-11 the highest flexural strength, 8.1 MPa, is obtained with the upper resin and quartz powder limits.

6.3.1.3 Final Prototype Tile Composition

The mass and volume fractions of the components of the two final prototype tiles are presented in Table 6-9.

Table 6-9. Final Prototype Tile Composition by Mass and Volume Percentage

	Tile 1		Tile 2	
Components	**f**	**x**	**f**	**x**
Resin	0.121	0.131	0.201	0.196
Quartz-34	0.411	0.277	0.131	0.08
Quartz Powder	0.072	0.048	0.229	0.139
PCM	0.157	0.38	0.200	0.436
Quartz-6	0.048	0.032	0.048	0.029
Quartz-10	0.057	0.039	0.057	0.035
Quartz-84	0.124	0.084	0.124	0.076
Pigment	0.01	0.009	0.01	0.009

Using the final models, the predicated flexural and compressive strength was determined for each prototype tile. The values for a 95% confidence interval are given in Table 6-10 and Table 6-11. Both final tiles have a predicted compressive strength significantly greater than the tested ceramic tile of 1500 psi.

Table 6-10. Predicated Flexural Strength for Final Prototype Tiles

Final Prototype	Predicated Flexural Strength [MPa]
Tile 1	11.5 ∀ 1.5
Tile 2	8.1 ∀ 1.4

Table 6-11. Predicated Compressive Strength for Final Prototype Tiles

Final Prototype	Predicated Compressive Strength [MPa]
Tile 1	32.5 ∀ 2.0
Tile 2	29.6 ∀ 2.2

6.3.2 Physical Testing of Final Prototype Tiles

Results of the physical tests are presented in Table 6-12 for the final two prototypes, ceramic and Granirex tiles. Tests were selected from a group of mechanical tests performed by Granirex on their products. Final tests were listed in Table 2-1 in Chapter 2. Ceramic tile was bought at a local hardware store. Granirex tile was taken from samples provided from the company.

Table 6-12. Final Physical Testing Results

Name of Test	ASTM	Tile 1	Tile 2	Granirex	Ceramic
Flexural Strength 3-point [MPa]	C-1161	9.9 ∀ 1.5	9.5 ∀ 1.4	33.9 ∀ 4.7	7.3 ∀ 1.1
Flexural Strength 4-point [MPa]	C-1161	9.0 ∀ 1.3	7.4 ∀ 0.9	23.6 ∀ 1.6	6.3 ∀ 1.0
Compressive Strength [MPa]	C-170	17.5 ∀ 2.4	24.5 ∀ 4.6	171.0 ∀ 81.1	10.4 ∀ 1.8
NTMA Impact Strength	-	Fails	Fails	Fails	Fails
Water Absorption % by Weight	C-97	3.3% ∀ 2.6%	5.2% ∀ 1.7%	0.4% ∀ 0.1%	21.8% ∀ 2.6%
Thermal Shock	C-484	Passes	Passes	Passes	Passes

The 3-point flexural strength and compressive strength were within range of the predicated values in Table 6-10 and Table 6-11. Standard 4-point flexural strength for natural stone tile is 8.3 MPa (1200 psi). Tile 1 meets this requirement while Tile 2 falls below the standard.

Results show that the compressive strength of Tile 1 was lower than Tile 2. It was expected to be slightly stronger than Tile 2 as presented in Table 6-11. In addition the strength for Tile

2 was higher than predicted, but was within the upper and lower limits. This further confirms that by choosing a simple linear model more complex behavior was overlooked.

Final values in Table 6-12 were obtained by averaging the results from several different tile samples manufactured at different times. Consequently the compressive strength behavior cannot be overlooked as manufacturing mistake, such as a measuring error, or an existing flaw in the sample. As mentioned earlier increases in quartz powder content increases the number of quartz particles per volume of tile. This would result in a higher compressive strength due to the higher concentration of quartz particles in Tile 2 when compared to Tile 1.

Using the same logic, Tile 2 should also have a higher flexural strength, but this was not the case. During three-point and four-point bending tests, the sample is under both compressive and tensile stresses. Thus it can be assumed that the tensile stresses are not improved with the increase in resin and quartz powder amounts, like compressive stress. In addition Tile 2 contains more PCM, which reduces the overall tensile strength. However under compressive loads, it not as much as a hindrance until the PCM capsules burst.

Compressive strengths are within the expected error tolerances and are greater than the tested ceramic tile. Both however are significantly below the test requirement for granite of 19,000 psi. This is acceptable since the incorporation of PCM was expected to significantly reduce the physical strength of the tile. Tiles are expected to have strength comparable to ceramic tile rather than natural or engineered stone tile.

All tiles failed the impact test. Granirex claims their product passed the test. Both Granirex and prototype tiles passed when the ball was dropped from a height of three feet. The ceramic tile failed at all heights tested. This test was found to be inconclusive. A more detailed impact test such as the Charpy or Izod test should be performed. Impact energy absorbed by the material is determined from these tests. These results than can then be used for comparison.

It is anticipated that the prototype tiles containing the PCM would be able to absorb more energy. PCM capsules are considerably smaller than the quartz powder. Resulting in more surface area for the resin to bond, thus more interface area to absorb the impact energy.

Water absorption for the final prototypes was higher than the Granirex tile, but performed much better than the ceramic tile. This value could be reduced by subjecting the tile mixture to a vacuum before curing in order to reduce air bubbles. Current values do not allow for the best moisture absorption rating "impervious", which requires absorption below 0.5%.

6.3.2.1 Morphology Results

Morphology analysis was performed on a JEOL JSM-6500F Scanning EM (SEM) at Colorado State University Electron Microscopy Center. Analysis was performed on the fractured surface of both final prototype tiles. Fracture surface was the result of a 3-point flexural strength test. Images are presented in Figure 6-12 through Figure 6-15 with a quartz chip, PCM particles and interesting features noted.

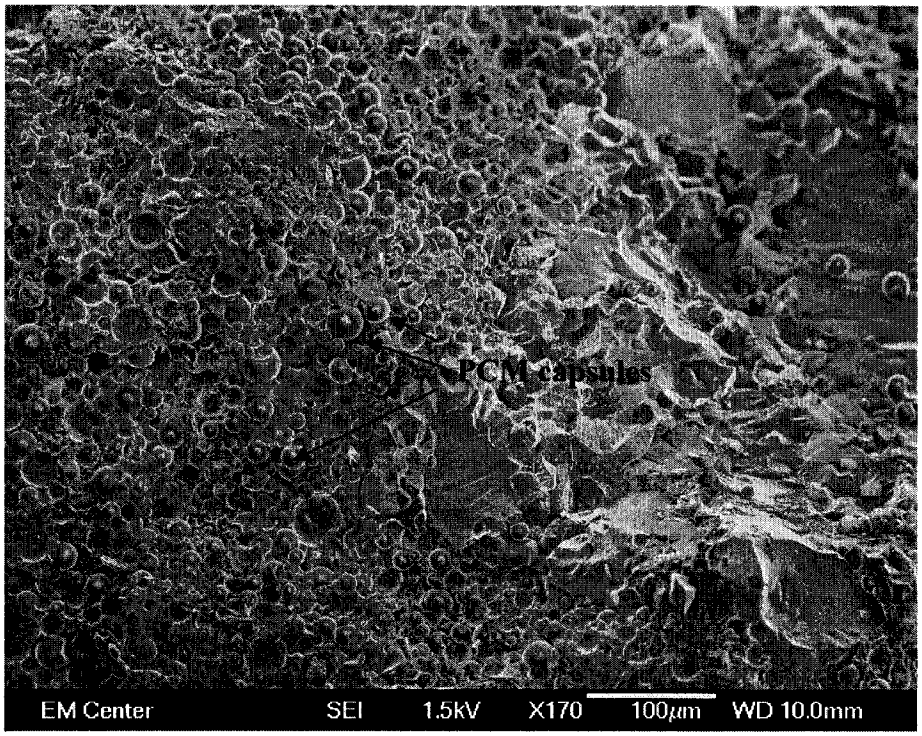

Figure 6-12. SEM Analysis at 170X Resolution for Tile 1

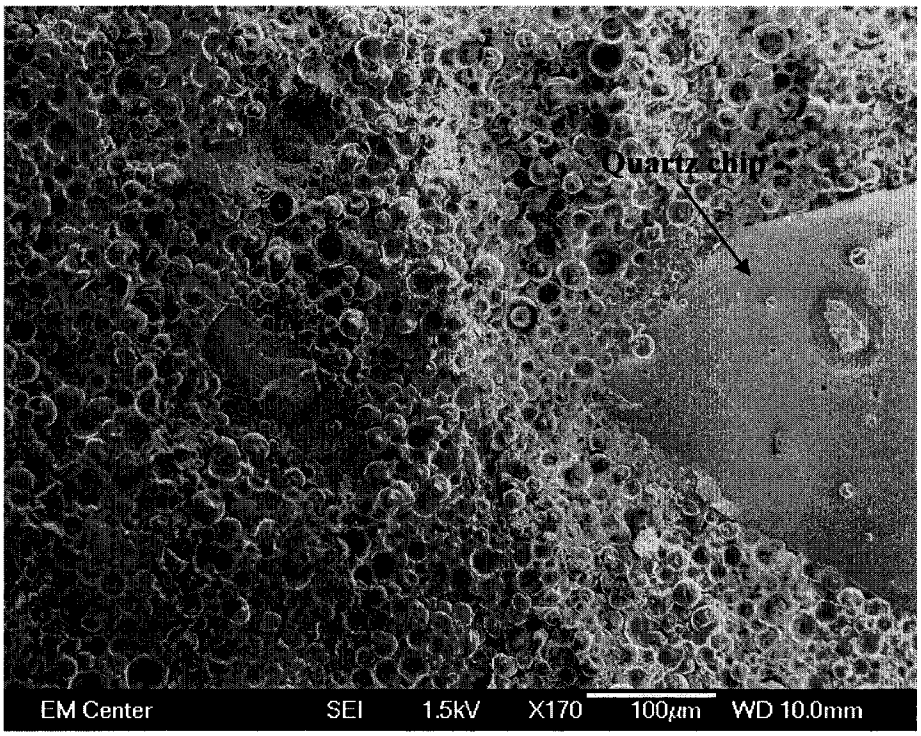

Figure 6-13. SEM Analysis at 170x Resolution for Tile 2

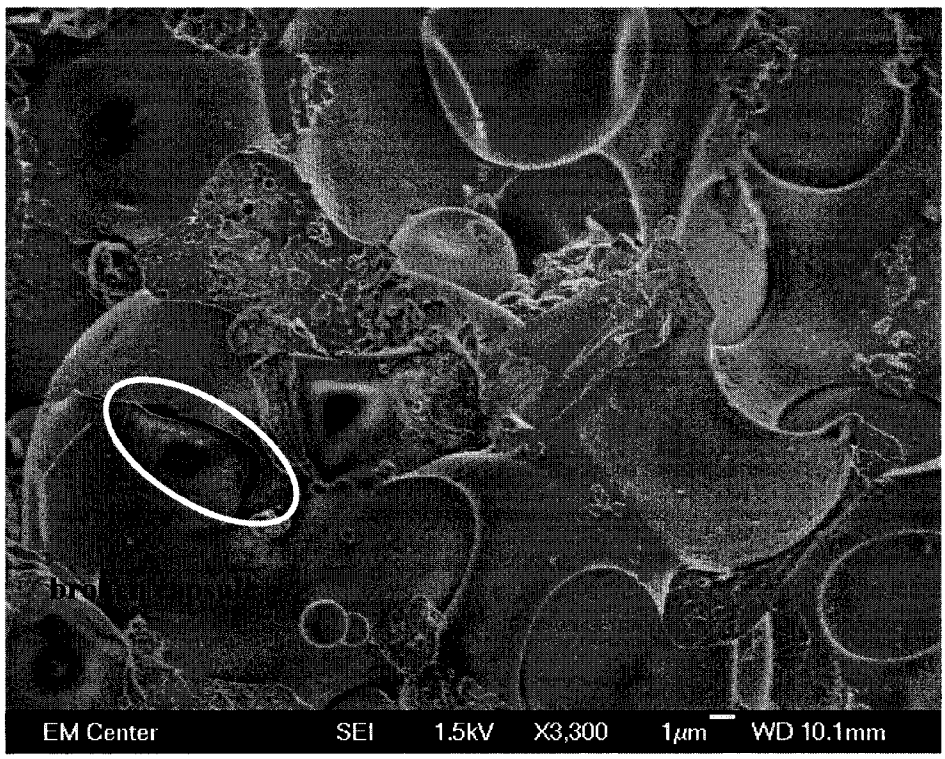

Figure 6-14. SEM Analysis at 3300X Resolution for Tile 1

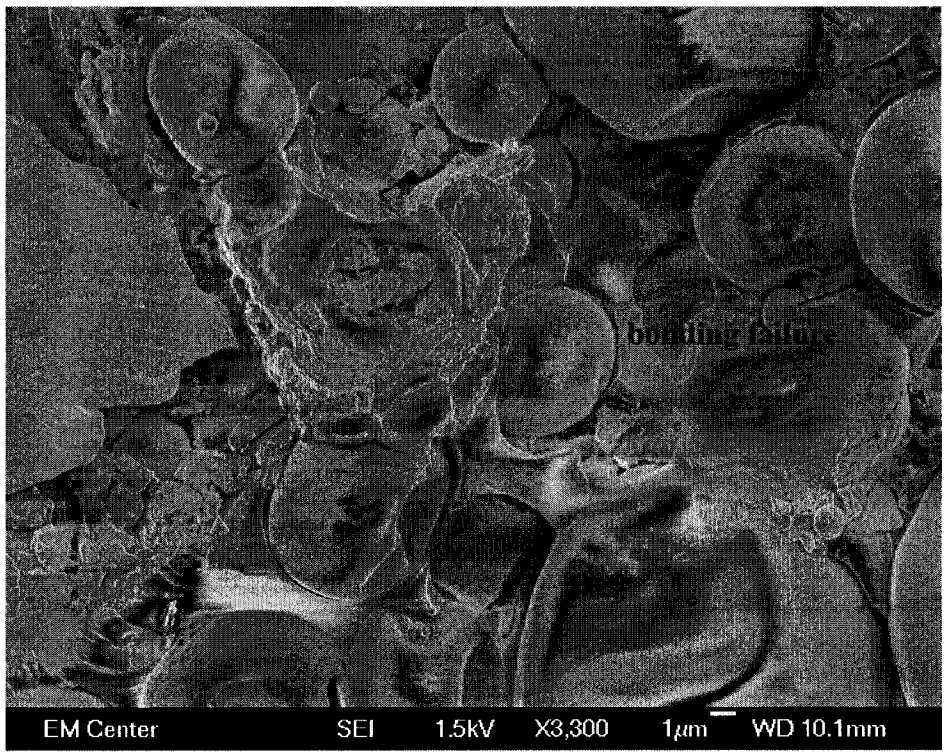

Figure 6-15. SEM Analysis at 3300X Resolution for Tile 2

Based on Figure 6-12 and Figure 6-13 the PCM is being dispersed through the mixture evenly. The large volume occupied by the PCM is evident in the images. Concerns of not using a vacuum to remove air bubbles were somewhat alleviated since large amount of air pockets were not evident in the images.

It is also interesting to note the non-spherical shape of the PCM capsules. This is due to the small air pocket in each capsule to account for the volumetric changes between phases.

Figure 6-14 shows a broken capsule, indicated by the white circle. It was assumed that this occurred during the failure and not in the course of manufacture. Since large amounts of melted wax were not observed during the tile curing process, it was assumed no massive capsule breakage occurred during the manufacturing process.

There is evidence of bonding failure between PCM capsules and matrix in Figure 6-14 and Figure 6-15. This was most likely occurred during failure testing since this is a view of the fractured surface. However a small proportion can be assumed to be due to inadequate wetting of the resin, due to poor mixing or not enough resin in the mixture. Placing tiles in a vacuum before curing may aid in improving the bonding.

6.4 Conclusions

Two final prototype tiles were developed and were found to have physical strength comparable to typical ceramic tile. Tile 1 contained 15.7% by mass of PCM and a 4-point flexural strength of 9.9 MPa. A four-point flexural strength of 7.2 MPa was achieved with

Tile 2 containing with 20% by mass of PCM. Both were stronger than a typical ceramic tile tested at 6.3 MPa. There is no requirement for ceramic tile, but the requirement for natural stone tile is 8.3 MPa.

Compressive strength for the final two tiles was twice the tested strength of the ceramic tile. Agglomerate floor tile produced by Granirex tested well above the PCM incorporated tiles as expected

It was obvious that the incorporation of PCM into agglomerate floor tile significantly reduced the overall strength of the tiles. Flexural strength was compromised by half with as little as 10% PCM by mass. There was no overwhelming combination of resin and quartz content that resulted in a significant increase in strength, unless the PCM component was significantly reduced. It was noted that a larger amount of quartz powder was required to achieve appropriate strength as the PCM content increased.

The mixture for Tile 1 has the most promise since the flexural strength was greater than the requirement for natural stone tile. In addition the resin content is lower than Tile 2, so the overall cost would be less.

Further improvement in strength could be accomplished by subjecting the mixture to a vacuum to remove all air bubbles. However it is not expected to make a dramatic difference, since morphology results did not show evidence of large amounts of air pockets. Nonetheless it should be considered for future testing.

Investigating polyester resins with a superior strength than resins used for this research could improve overall strength. The cost of a higher strength resin would be greater resulting in an overall increase in cost, so it may not be worth the increase in strength. Three different polyester resins of slightly varying strengths were investigated during the course of this research and none showed any significant increase in strength.

Tile 1 has the advantage of slightly higher flexural strength and lower resin content, while Tile 2 has a higher PCM content. The importance of maximizing the latent heat storage of the tile makes Tile 2 the best selection.

Higher resin content will allow for incorporation of larger amounts of PCM and possible higher compressive strengths. It is also possible by increasing the quartz powder content beyond the upper limit set by this research, flexural strength could be improved for tiles containing higher resin. However for tiles with low resin content and mid-range PCM content around 20% by mass, the flexural strength could be increased by removing quartz powder completely and increasing the quartz-34 component appropriately.

Investigation into adjusting the upper limits of quartz powder and quartz-34 and developing prototype tiles is recommended as future work. Testing results of the prototypes would verify if new models should be developed reflecting the new upper limits.

Neglecting the natural stone standard may be acceptable since ceramic tile does not have an equivalent standard. Standards for breaking strength for ceramic tiles are available, so it would be worth the effort to perform this test on the two final prototype tiles.

The response of three-point flexural and compressive strengths has been investigated. Using the same design points developed in Chapter 5, models could be developed for other physical properties such as four-point flexural and breaking strengths. Prototype tiles would have to be manufactured at each design point and subjected to testing. Resulting data would then be entered into SAS and fitted models determined using the same statistical analysis used to develop the flexural and compressive strength fitted models.

Chapter 7 : Thermal Analysis

7.1 Introduction

Physical strength is an important property of agglomerate floor tiles incorporating a phase change material (PCM). However, thermal performance of the tile is just as important as the physical strength. Each tile was required the following thermal properties: to have a peak transition temperature of approximately 27°C (80°F) and a high latent heat capacity.

7.2 Experimental

Thermal testing was performed on each of the prototype tiles corresponding to the sixteen design points of the fitted model development. Peak transition temperatures and latent heat were measured for all. The prototype tiles selected by physical strength testing, Tile 1 and Tile 2, were also subjected to thermal testing.

7.2.1 Verification of Transition Temperature

Verification of peak transition temperatures and latent heat capacity was performed with a Seiko differential scanning calorimeter (DSC). Since samples needed to weigh only a few milligrams, material was easily scraped and chipped from a fully cured tile. Several samples were taken from each prototype tile. Testing involved heating then cooling the samples at a rate of 5°C/min.

The average peak transition temperature was determined for each prototype tile for heating and cooling runs. Figure 7-1 plots the transition temperatures for heating and cooling for

varying PCM content. Included in the figure are the transition temperatures for a pure PCM sample.

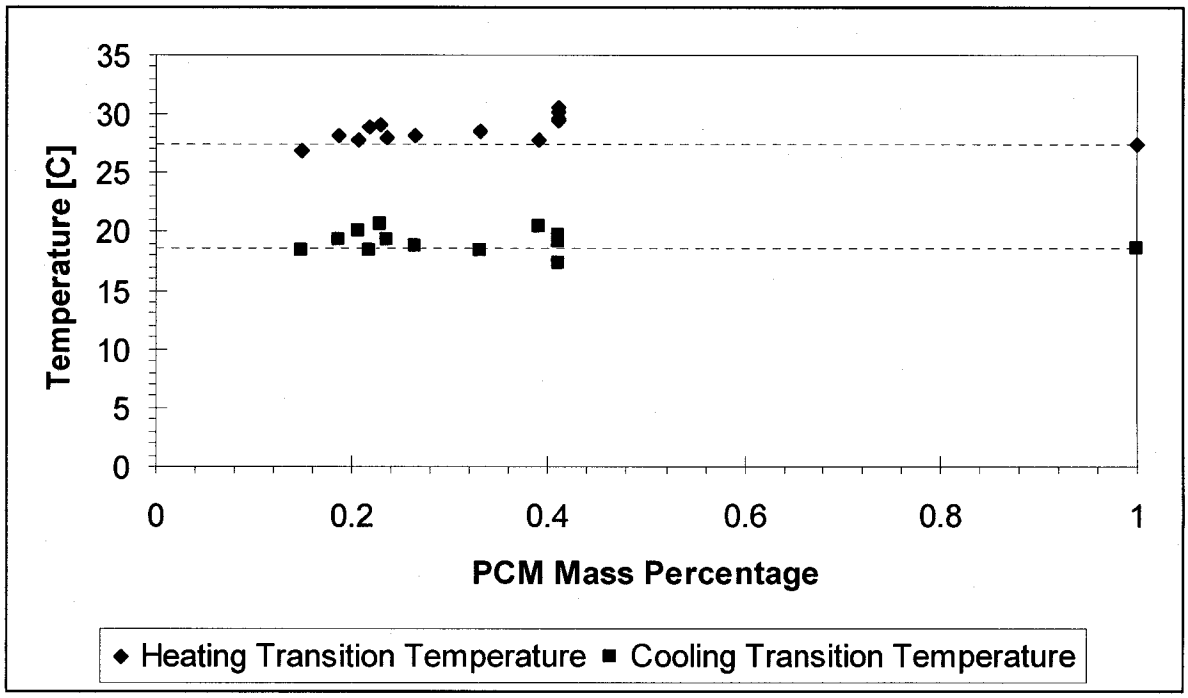

Figure 7-1. Transition Temperature for Varying PCM Content

Transition temperatures for tiles containing varying amounts of PCM did not vary significantly from the pure PCM temperatures for either cooling or heating. The average transition temperatures were calculated and tabulated in Table 7-1.

Table 7-1. Comparison of Measured Average Transition Temperatures to Pure PCM

	Heating [°C]	Cooling [°C]
Pure PCM Transition Temperatures	27.5	18.5
Average Transition Temperatures of Prototype Tiles	28.9	19.2

7.2.2 Verification of Latent Heat Capacity

Latent heat was calculated for each design point and compared to the pure PCM value. Each sample contained PCM along with the other tile components, so the latent heat measured was

for the tile as a whole not just pure PCM. In order to make a comparison to the pure PCM sample an adjustment had to be made. The following formula was used.

$$h_{PCM} = \frac{h_{sample} m_{sample}}{m_{PCM}} \quad (7\text{-}1)$$

Where:

h_{PCM}	=	estimated latent heat for the PCM componet of each tile [mJ]
h_{sample}	=	measured latent heat of tile sample [mJ]
m_{sample}	=	mass of DSC sample [mg]
m_{PCM}	=	estimated mass of PCM in sample [mg]

Obviously the accuracy of this estimation was dependent on each sample containing the same composition as a full tile. This would have been impossible to accomplish as the tile composition was not uniform throughout. By taking the average over several samples and then over all design points of the mixture design, this error would be minimized. The resulting average measured latent heat on cooling of –148 J/g was comparable to the measured value on cooling of pure PCM, –151 J/g.

7.2.3 Thermal Testing of Final Prototype Tiles

Final measurement of transition temperature and latent heat capacity was performed with a Seiko differential scanning calorimeter (DSC). Samples were taken from cured tiles and sealed in aluminum sample pans. Test conditions consisted of cooling the sample to -40°C, isothermally holding for one minute and then heating to 55°C, isothermally holding for one minute and cooling to –40°C at a rate of 5°C/min. This was performed four times for each tile and an average was taken of the data. Sample DSC traces for each of the final prototype tiles and for a pure sample of encapsulated octadecane are presented in Figure 7-2, Figure 7-3 and Figure 7-4.

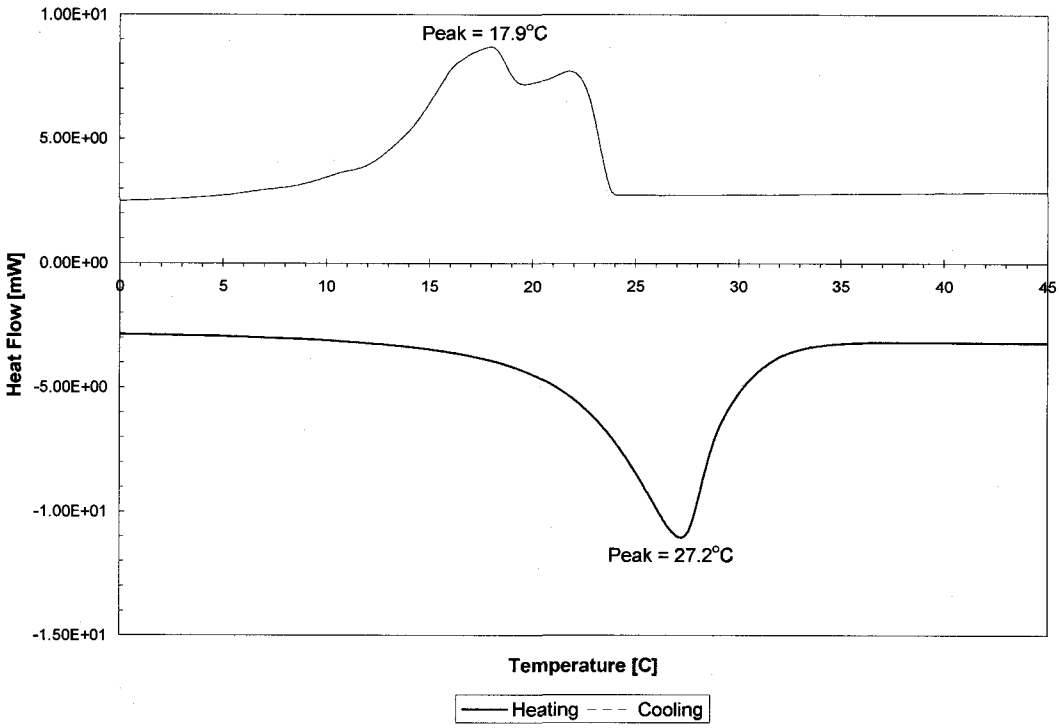

Figure 7-2. DSC Trace for Final Prototype Tile 1

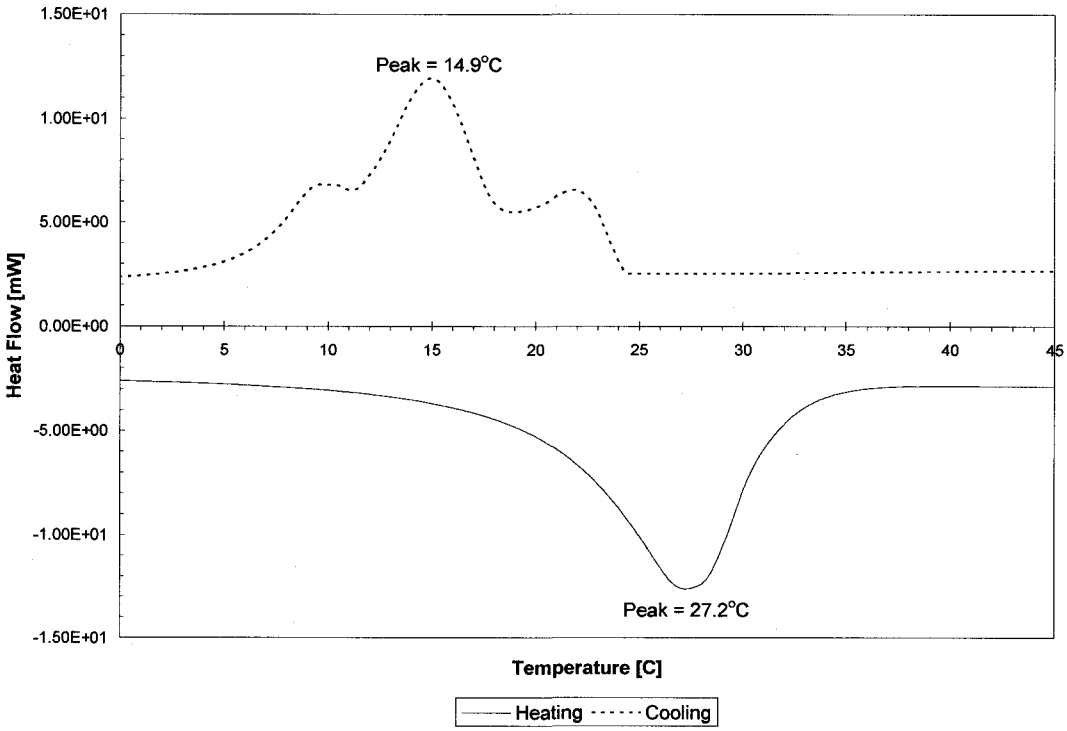

Figure 7-3. DSC Trace for Final Prototype Tile 2

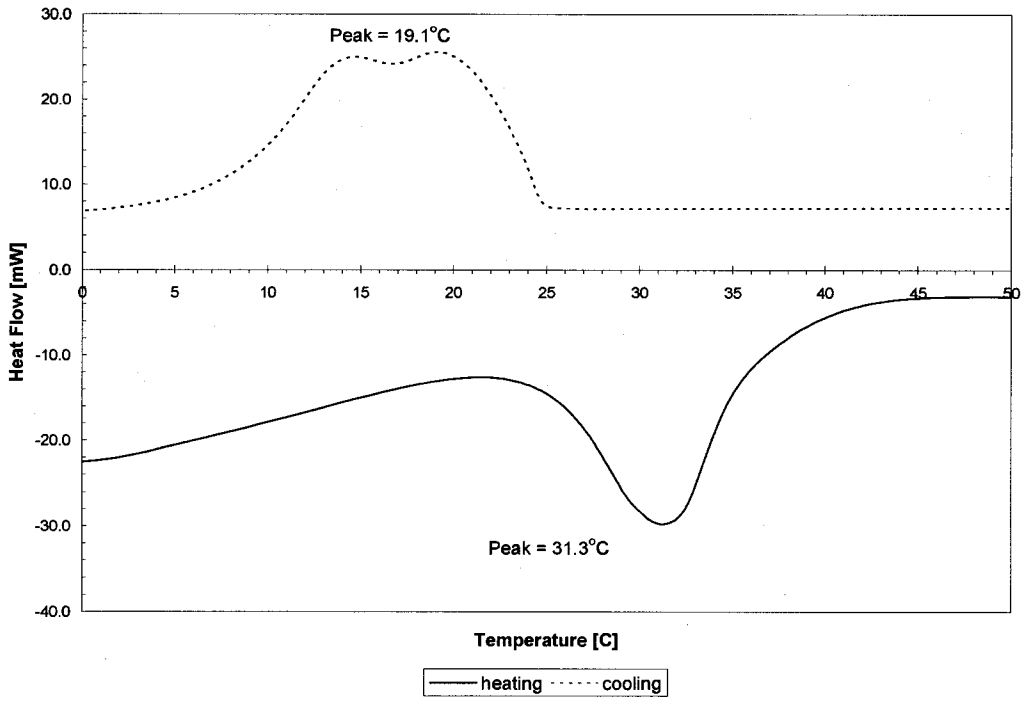

Figure 7-4. DSC Trace for Encapsulated Octadecane

7.3 Results and Discussion

Peak transition temperatures of the prototype tiles were shown in Figure 7-1 not to vary with PCM content as expected. Testing of the final prototype tiles further verified this fact. Peak transition temperatures for the two final prototype tiles are presented in Table 7-2.

Table 7-2. Peak Transition Temperatures of Final Tiles

	Tile 1	Tile 2
Peak Transition Temperature on Heating [5°C/min]	27.2°C	27.2°C
Peak Transition Temperature on Cooling [5°C/min]	16.7°C	14.9°C

A significant difference was observed between the peak transition temperatures on heating and cooling. Data in Figure 7-1 and the final prototype results show this behavior. This difference is due to under-cooling effects. Under-cooling is the behavior of a material not to

solidify at the same temperature at which it melted. At a slower heating and cooling rate, this difference was minimized. Both Tiles 1 and 2 were subjected to a cooling rate of 0.1°C/min (6°C/hour) minimizing the under-cooling effects. Results are summarized in Table 7-3.

Table 7-3. Peak Cooling Transition Temperature of Slow Cooling Rate

	Tile 1	Tile 2
Peak Transition Temperature on Cooling [0.1°C/min]	24.6°C	17.5°C

DSC traces showing the effect of reducing the cooling rate for Tile 1 and 2 are presented in Figure 7-5 and Figure 7-6. Hystorisis was greater for the data collected during the 0.1°C/min run because data was sampled at smaller time intervals.

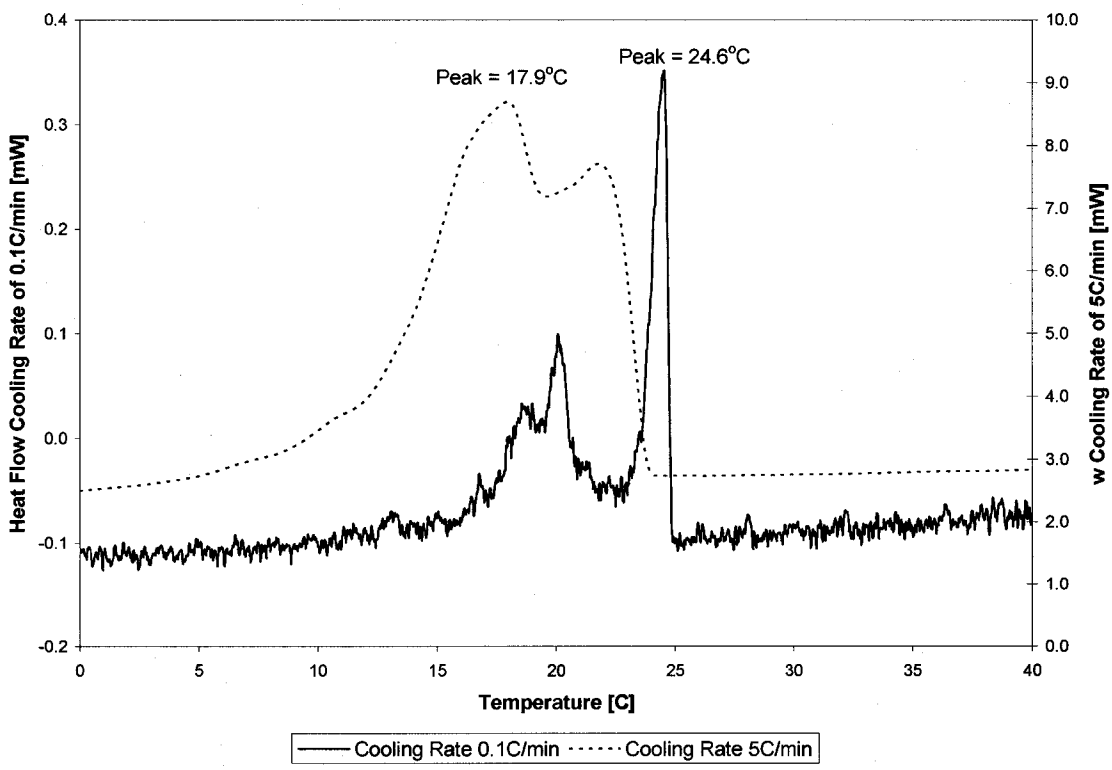

Figure 7-5. Comparison of Reduced Cooling Rates for Tile 1

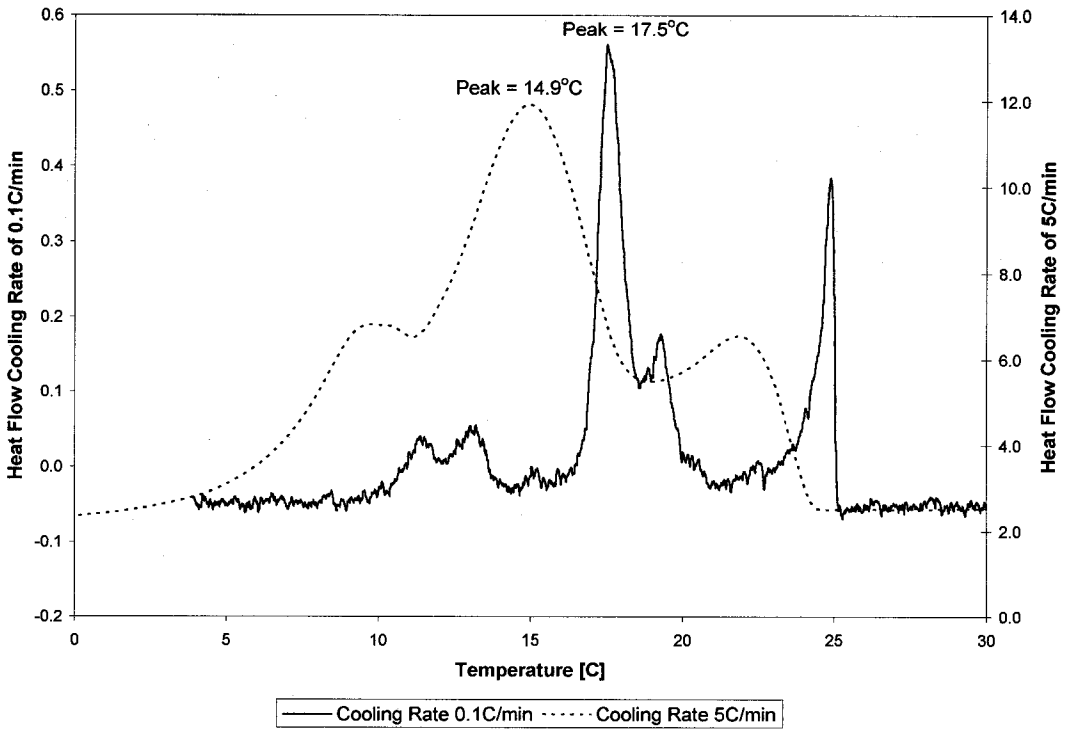

Figure 7-6. Comparison of Reduced Cooling Rates for Tile 1

The peak cooling transition temperatures at a cooling rate of 0.1°C/min were increased. This cooling rate is closer to expected rates in an actual sunspace. In fact the actual rate would be more on the order of half that rate, which would result in an even higher transition temperature. Therefore it can be concluded that under-cooling effects will not be a concern when the tile is installed in a sunspace.

A difference in the DSC trace between the final tiles was evident from Figure 7-2, Figure 7-3, Figure 7-5 and Figure 7-6. The trace for Tile 1 was similar to the pure encapsulated octadecane sample of Figure 7-4. Three peaks were noticeable in the trace for Tile 2. This was an indication that a different impurity was present in Tile 2. The trace was more similar to an encapsulated wax blend of 50% by mass of octadecane and 50% by mass of eicosane.

It was determined that a second batch of encapsulated wax received from Outlast was not the same as earlier batches. Both the encapsulated octadecane and 50/50 octadecane/eicosane blend had approximately the same peak transition temperature and latent heat capacity, so it was not considered to be a problem. The 50/50 blend of octadecane and eicosane has a reported melting transition temperature of 27.1°C and latent heat of 145 J/g.[30] The physical strength was not affected by the blend of wax used since encapsulation of particles was identical.

Latent heat values were determined from the DSC traces for each the final two tiles. Results are given in Table 7-4.

Table 7-4. Latent Heat Capacity of Final Tiles

	Tile 1	Tile 2
Latent Heat on Heating [5°C/min]	19 J/g	34 J/g
Latent Heat on Cooling [5°C/min]	-19 J/g	-34 J/g

Latent heat values measured were for the tile as a whole, not just the PCM content, resulting in values appreciably different than pure PCM. When the formula presented in Equation 7-1 is used, the values are close to the measured PCM value of -151 J/g. Calculated values are presented in Table 7-5.

Table 7-5. Adjusted Latent Heat Capacity of File Tiles

	Tile 1	Tile 2
Latent Heat on Heating [5°C/min]	122 J/g	169 J/g
Latent Heat on Cooling [5°C/min]	-123 J/g	-168 J/g

7.4 Conclusions

The manufacturing process did not adversely affect any of the thermal properties for microencapsulated PCM tiles as was the case for solid-state PCM tiles. Thermal properties of both prototype tiles were within the expected range for the PCM. Transition temperature was determined to be approximately 27°C. Under-cooling effects were noticed when a fast cooling rate of 5°C/min was used, but were insignificant when slower more realistic cooling rates were employed, approximately 0.1°C/min (6°C/hour). This rate is expected to be at least half that amount in a typical sunspace.

After manufactured it was found that Tile 1 and Tile 2 incorporated different blends of the encapsulated wax. Tile 1 used the 95% technical grade octadecane, while Tile 2 incorporated a 50/50 octadecane/eicosane blend. Since the thermal and physical properties of the two blends were similar it was not seen as concern.

Chapter 8 : Potential Energy Savings Analysis

8.1 Introduction

A final objective of this project was to perform a potential energy analysis to demonstrate possible annual heating savings using floor tile with a phase change material (PCM) incorporated. Part of the analysis involved verifying that there would significant thermal energy in a typical sunspace to allow the PCM to undergo a phase change.

Two simulations were performed, a static and dynamic. It was determined in Chapter 6 that a maximum of 20% PCM by mass could be incorporated into floor tile while maintaining the minimum required physical strength. Both simulations assumed a floor containing 20% PCM by mass and one with 100% PCM. A floor with 100% PCM gave the maximum possible savings and was used to show the potential of incorporating larger amounts of PCM.

8.2 Experimental

8.2.1 Expected Solar Gain

Phase change enhanced floor tile is to be used in a sunspace as additional thermal storage. Proving that there would be enough solar gain during the heating season to fully transition the PCM to the liquid phase needed to be determined. A typical sunspace was assumed and basic calculations were performed to determine the monthly solar gain. These value were then compared the energy requirement to melt the PCM in the tile.

The sunspace was assumed to have the appropriate amount of south facing glazing for the maximum solar gain during the winter months. Assuming Denver, Colorado as the location, the monthly-absorbed radiation was determined from the following equation.

$$\overline{S} = \overline{H}_b \overline{R}_b (\overline{\tau\alpha})_b + \overline{H}_d (\overline{\tau\alpha})_d \left(\frac{1+\cos\beta}{2} \right) + \overline{H}\rho_g (\overline{\tau\alpha})_g \left(\frac{1-\cos\beta}{2} \right) \quad (8\text{-}1)$$

Where:

$\overline{H}_b$	=	monthly average daily beam radiation on a horizontal surface
$\overline{H}_d$	=	monthly average daily diffuse radiation on a horizontal surface
$\overline{H}$	=	monthly average daily radiation on a horizontal surface
$(\overline{\tau\alpha})$	=	average transmittance-absorptance for beam (b), diffuse (d) and ground (g)
$\overline{R}_b$	=	monthly average ratio of beam radiation on a tilted plane to that on the plane of measurement (usually horizontal)
ρ_g	=	ground reflectance
β	=	collector slope

The "collector slope" of the south facing is 90°. Ground reflectance was assumed to be 0.3 for each month. Monthly average daily radiation was obtained from weather data for Denver. Remaining values were calculated using equations from Duffie and Beckman.[17] Results are presented in Table 8-1.

Total monthly radiation incident on the windows of the sunspace, $\overline{H}_T$, was also calculated and presented in Table 8-1. The percentage of the total radiation absorbed into the sunspace is presented in the last column of Table 8-1. Calculations were done assuming there was no overhang above the south facing glazing to shade during the summer. As a result, the absorbed radiation during the summer months is higher than a typical sunspace with

appropriate shading. Based on the results for the heating months, September through April, the average percentage of solar radiation that will be absorbed into the sunspace is 70%.

Table 8-1. Estimated Monthly Absorbed Solar Radiation per Area of South Glazing

Month	$\overline{H}$ [MJ/m^2]	$\overline{H}_d$ [MJ/m^2]	$\overline{H}_b$ [MJ/m^2]	$\overline{H}_T$ [MJ/m^2]	$\overline{S}$ [MJ/m^2]	$(\overline{\tau\alpha})$
Jan	9.54	2.72	6.82	18.59	14.27	0.77
Feb	12.79	3.64	9.15	18.35	13.45	0.73
Mar	17.37	4.80	12.57	17.01	11.96	0.70
Apr	21.33	6.07	15.26	13.63	8.81	0.65
May	24.24	7.10	17.14	11.49	7.10	0.62
Jun	26.68	7.16	19.52	10.94	6.57	0.60
Jul	25.8	7.13	18.67	11.27	6.72	0.60
Aug	23.21	6.42	16.79	12.93	8.14	0.63
Sep	19.6	5.10	14.50	16.25	11.01	0.68
Oct	14.77	3.84	10.93	19.02	13.80	0.73
Nov	10.03	2.94	7.09	17.89	13.43	0.75
Dec	8.3	2.50	5.80	17.39	13.50	0.78

In order to verify that there will be enough radiation absorbed to fully charge the floor tile, the results from Table 8-1 were multiplied by a typical glazing area for a sunspace and given in Table 8-3. Using the latent heat capacity of 174 J/g for encapsulated octadecane and the area of a typical sunspace floor, the potential energy storage of a floor containing 100% PCM was calculated in Table 8-2. Two common floor thicknesses are used. A floor area of 32.2 m^2 (346.5 ft^2) and a glazing area of 32.7 m^2 (352 ft^2) were chosen.

Table 8-2. Potential Energy Storage for a Floor Composed of 100% Encapsulated Octadecane of an Area of 32.2 m^2 (346.5 ft^2)

Daily Energy Storage [MJ] ½" Floor Tile	Daily Energy Storage [MJ] ¾" Floor Tile
52.7	79.0

Table 8-3. Absorbed Average Daily Radiation through South Glazing of Area 32.7 m^2(352 ft^2)

Month	Absorbed Solar Radiation [MJ]
Jan	466.7
Feb	439.9
Mar	391.1
Apr	288.2
May	232.1
Jun	215.0
Jul	219.8
Aug	266.2
Sep	360.1
Oct	451.2
Nov	439.1
Dec	441.4

Based on the results from Table 8-2 and Table 8-3 there is enough absorbed energy per day during heating season to fully charge the floor tiles containing phase change material at either tile thickness.

8.2.2 Solar Load Ratio Calculation

It was determined that there is enough absorbed solar radiation daily to fully charge phase change materials in floor tile. The next step was to establish the potential savings that can be achieved with the addition of phase change materials to floor tiles. An empirical method for estimating the monthly solar and auxiliary energy requirements for passive systems, called the solar load ratio (SLR), was used for a rough estimate. The solar load ratio is a widely used method since it can be performed either with hand analysis or simple spreadsheets. Calculations are simplified by the use of reference designs. Annual results have been reported by Duffie and Beckman[17] to be within 3-4% of more detailed simulations.

The monthly SLR is a dimensionless parameter defined as:

$$SLR = \frac{\text{solar energy absorbed per month}}{\text{building heating load per month}} \qquad (8\text{-}2)$$

A parameter correlated to the SLR is the solar savings fraction (SSF). It is defined as the following.

$$SSF = \frac{\text{solar saving}}{\text{net reference load}} \qquad (8\text{-}3)$$

The net reference load is the heat loss from the non-solar parts of a building. This includes walls, floors, ceilings and the roof of everything but the sunspace. Solar savings is the difference between the net reference load and the auxiliary heat required by the building.

$$\text{Net reference load} = (NLC)\,(DD) \qquad (8\text{-}4)$$

$$\text{Solar Savings} = \text{Net Reference Load} - \text{Auxiliary Heating Load} \qquad (8\text{-}5)$$

Where:

NLC	=	net load coefficient
DD	=	monthly degree day

The net load coefficient is found by summation of the load coefficient of each building element. Load coefficient is the overall heat transfer coefficient, times the area of the element. The following definition of NLC was used for this analysis.

$$NLC = 24\,[\,(UA)_{wall} + (UA)_{roof} + (UA)_{glazing} + (UA)_{perimeter} + (UA)_{infiltration}\,] \qquad (8\text{-}6)$$

Where:

$(UA)_{wall}$	=	(A_{wall}/R_{wall})
$(UA)_{roof}$	=	(A_{roof}/R_{roof})
$(UA)_{glazing}$	=	$(1.1 \times (A_{glazing}/\text{Number of glazing}))$
$(UA)_{infiltration}$	=	(0.018)(ACH)(ADR)(Volume of building)
R	=	Resistance of element
ACH	=	Air changes per hour
ADR	=	Air density ratio

Glazing losses were only considered for the east, west and north facing windows. ADR is dependent on the elevation of the site, and for a building in Denver, Colorado the value is 0.83. ACH is determined from the design criteria and chosen to be 0.28. Resistance values can be found from ASHRAE.[1]

Table 8-4. Coefficients used for NLC Calculation

Building Element	(UA) [W / K]
Walls	30.7
Roof	24.8
E,W,N Windows	2.9
Floor Perimeter	22.3
Infiltration	27.4

From the solar savings fraction the auxiliary heat required and the solar savings for the building can be calculated by the following equations.

$$\text{Auxiliary heat} = (\text{NLC})\,(\text{DD})\,(1\text{-SSF}) \qquad (8\text{-}7)$$

$$\text{Solar savings} = (\text{NLC})\,(\text{DD})\,(\text{SSF}) \qquad (8\text{-}8)$$

Parameters to determine the above variables have been defined for several reference designs. In the early eighties, Los Alamos National Laboratories developed reference designs representing direct gain, Trombe walls and sunspace passive systems. A reference design that simulates a passive system with an attached sunspace was chosen for this analysis. Balcomb[4] gives parameters for several different reference designs. A summary of the major dimensions of the building is given in Table 8-5.

Table 8-5. Dimensions of Passive Reference Design

Parameter	DIMENSION
Total Volume of Building	350 m^3 (12400 ft^3)
Projected area of solar gain	25 m^2 (270 ft^2)
Sunspace floor area	32.3 m^2 (346.5 ft^2)
South Facing Glazing Area	32.7 m^2 (352 ft^2)

The building's heating load was determined by calculating the expected heat loss through the walls, roof, windows, perimeter and due to infiltration. Standard values for insulation and infiltration were used, as defined by ASHRAE.[1] Sunspace losses are not considered in this calculation. Losses from the sunspace are considered in the correlation for the specific reference design. Balcomb[4] has reported these values for the reference designs.

Calculations were performed in a spreadsheet. Solar savings were first calculated for the reference design without any phase change storage. Latent heat storage was included in the calculation by assuming the heat gained would reduce the heat losses from the building. Encapsulated octadecane was used as the PCM for the latent heat storage. The solar savings fractions (SSF) for a sunspace with and without latent heat storage are presented in Table 8-6. Calculations included the fact that the encapsulation shell takes up 15-20% by mass of the PCM. A thickness of ¾ an inch was assumed for the PCM flooring.

Table 8-6. Solar Savings Fraction (SSF) for Sunspace with and without PCM Flooring

	Solar Savings Fraction (SSF)	**%**
Sunspace without PCM Flooring	0.589	-
Sunspace with 100% PCM Flooring	0.672 – 0.676	20.2 – 21.3
Sunspace with 20% PCM Flooring	0.609-0.610	4.8 – 5.1

The above results include values for a floor composed entirely of PCM and a floor containing 20% PCM. A floor containing 100% PCM was not realistic since structural integrity of the tile must be maintained. It was assumed that a floor containing 20% PCM would maintain structural integrity. Based on these results this floor would meet approximately 61% of the annual heating requirement. The SSF calculated were within the expected range of 0.4- 0.7 for reasonable SLR designs[39].

Included in Table 8-6 is the percent decrease in annual heating energy consumption for flooring containing PCM compared to one without. The range is due to the 15-20% by mass the encapsulation shell occupies in the PCM. A floor containing 20% PCM can be expected to reduce the annual heating energy consumption by approximately 5%.

8.2.3 Dynamic Simulation

The solar load ratio calculation provided a good estimate of possible savings by the addition of phase change materials in passive applications. However it does not fully show the effect of latent heat storage in the floor. It is also a static calculation, where a dynamic simulation would fully represent the latent heat storage in the floor.

An hourly energy analysis program, the Building Loads Analysis and System Thermodynamics (BLAST) program, was used for a dynamic simulation. The program has the ability of simulating heat transfer and thermodynamics in buildings to characterize the possible energy savings of using phase change floor tile. BLAST does not explicitly simulate phase change in building materials such as walls and floor; however, specifying layers of high thermal capacitance can simulate phase change materials.

A 2,400 square foot home, assumed to be built to a modern standard was simulated using climate data for Denver, Colorado. Annual heating energy consumption was calculated for the house with and without phase change floor tile in the sunroom. A sunroom of 32 m^2

($350ft^2$) and a seasonal furnace efficiency of 80 percent were assumed. Results are summarized in Table 8-7.

Table 8-7. Fuel Consumption for a House With and Without PCM Tile

	Annual Furnace Energy Consumption	Energy Savings	%
Sunspace without PCM Flooring	148,000 MJ (140,250 kBtu)	-	
Sunspace with 100% PCM Flooring	104,100 MJ (98,660 kBtu)	43,900 MJ (41,590 kBtu)	29.7
Sunspace with 20% PCM Flooring	141,583 MJ (133,833 kBtu)	6,417 MJ (6,082 kBtu)	4.3

As with the SLR method, values were calculated for flooring assuming 100% PCM and 20% PCM content. The percent decrease in annual heating energy consumption for flooring containing PCM compared to one without was also included.

8.3 Results and Discussion

Mass of the encapsulation shell was not taken in account for the BLAST simulation, which would account for higher potential savings. In addition the BLAST model used latent heat properties of pure octadecane, where from Chapter 4 in Table 4-1 the encapsulated octadecane has a lower latent heat.

8.3.1 Potential Cost Savings

Average natural gas prices at the end of last year's heating season were about $8 per 1000 cubic feet and the heating value of natural gas is about 1000 Btu per cubic foot.[1] Using these

figures, the annual heating bill can be estimated from the BLAST simulation. Results are presented in Table 8-8.

Table 8-8. Potential Annual Fuel Costs and Savings

	Annual Fuel Cost	Cost Savings
Sunspace without PCM Flooring	$1,122	-
Sunspace with 100% PCM Flooring	$789	$333
Sunspace with 20% PCM Flooring	$1071	$51

Based on the cost savings, it is evident that it is necessary to incorporate the maximum amount of PCM into the floor tile to attain large savings. In addition a larger sunroom would increase the total storage and therefore increase the savings.

Obviously as the amount of PCM is increased the manufacturing cost of the tile increases in addition. The most expensive component of the floor tile is the PCM material. Currently the bulk cost is approximately $11/lbm. Large-scale production would likely decrease this cost to perhaps half or even less. The PCM cost per square foot has been calculated and presented in Table 8-9 for tiles with 100% and 20% PCM content.

Table 8-9. PCM Cost Per Square Foot for a ¾-inch Floor Tile

Mass Percentage of PCM	Cost Per Square Foot Assuming $11/lbm of PCM [$/ft^2]	Cost Per Square Foot Assuming $5.5/lbm of PCM [$/ft^2]
100%	31.8	15.9
20%	13.8	6.9

A comparison of estimated costs shows the 20% PCM tile costing more than half the price. However the payback for the 20% PCM tile was estimated to be 95 years compared to 34

years for the 100% PCM tile. Estimated payback times are not realistic for either tile. A realistic payback period is five years. The cost per pound of PCM has been calculated for a ¾-inch tile to achieve a 5-year payback and presented in Table 8-10.

Table 8-10. Cost Per Pound of PCM to Attain a 5-Year Payback for a ¾-inch Floor Tile

Mass Percentage of PCM	Cost Per Pound of PCM [$/lbm]
100%	1.70
20%	0.60

It is unsure how realistic is to expect bulk cost of the PCM to be reduced to the amounts stated in Table 8-10. Obviously in order for commercial manufacture of the tile to be cost effective the bulk cost must be significantly reduced.

8.4 Conclusions

The static and dynamic simulations demonstrated maximum annual heating savings with the incorporation of PCM into flooring for a typical sunspace. Both methods are adequate in estimating possible solar gains when using phase change materials. The simulation program BLAST has the advantages of performing calculations dynamically over a year and a user friendly interface to input data. The SLR method was calculated with a spreadsheet, which makes varying designs more difficult. The one weakness with BLAST was that it did not explicitly simulate the behavior of phase change material. Thermal capacitance had to be increased to mimic the behavior of phase change material in the flooring.

If more accurate calculations are required, the behavior of phase change materials will have to be modeled precisely. There are other programs available that use finite difference and

finite elements methods to model phase change material. One program, SUNREL, developed by the National Renewable Energy Laboratory (NREL), was investigated during this project, but did not produce any useful results. Programming the capability to model phase change behavior into BLAST would be ideal. A comprehensive review of modeling phase change material has been performed by Jason Barbour[5] for his research at Colorado State University.

Chapter 9 : Summary and Recommendations

Past researchers have attempted to place paraffin and solid-state phase change materials (PCM) into building products such as wallboard and concrete. Among the hurdles they faced was how to place sufficient PCM in the building product or system to produce significant energy savings without unduly degrading the physical properties of the material. For example, researchers at Oak Ridge National Laboratory and in Japan tried to impregnate drywall with paraffin wax. Problems encountered included oozing, lack of structural integrity (crumbling), odor, out gassing, fire retarding, and finishing issues. Researchers at the National Renewable Energy Laboratory explored this issue using solid-state phase change material, a neopentyl glycol blend, in concrete. The proposal was to dissolve the PCM in water used to make the concrete. They found that so little material could be incorporated in the final concrete slab that it would not provide significant energy savings.

At about the same time, another NASA sponsored research program lead to the development of microencapsulated phase change material for use in satellites. The paraffin material that was encapsulated had a solid to liquid transition temperature of about 28°C or 82°F. Very recently, the microencapsulated PCM has been used in fabrics to reduce skin temperature fluctuations. Companies such as Columbia, Eddie Bauer, and Wigwam sell garments containing phase change fabrics.

The combination of these two technologies, phase change material in building products and microencapsulated PCM, allowed for a solution to most of the problems mentioned above. This research presented the possibility of including phase change component in agglomerate

floor tile. It was determined that PCM could be incorporated into the product without degrading the tile's structural integrity. As a result the latent heat storage capacity of the tile was increased, which led to a reduction in annual heating energy consumption when applied in passive solar home design simulations.

A floor tile containing 20% by mass of PCM was manufactured for this project and selected as one of two final prototype tiles. Three-point flexural and compressive strength of this tile were 9.3 MPa and 4613 psi respectively. They were both greater than the minimum standard set for this project, 7.3 MPa and 1500 psi.

Annual savings from the BLAST simulation were calculated to be 4.3% of the annual heating requirements for a floor composed of 20% PCM by mass. However compared to the annual savings of 29.7% of a tile floor composed of 100% PCM, it was not a significant savings.

It is believed that structural integrity can be sacrificed to an extent, by increasing the PCM amount, in order to achieve improved thermal storage. The maximum PCM content that has been modeled for this research was 41.1% by mass. Tile manufacture with this PCM content had flexural strength significantly lower than the minimum requirement of 7.3 MPa. However if the breaking strength for a tile with high PCM amounts are above the ceramic tile standard, this may become a viable option.

Breaking strength tests are recommended to be performed on both of the final two prototype tiles. If it is greater than the ceramic tile standard, it may be possible to increase the PCM

content. A model for breaking strength should be developed in order to determine if a tile with 41.1% by mass of PCM or even higher is practical. Tiles have been made with 41.1% by mass of PCM, but it has yet to be agreed on if the poor physical strengths are acceptable.

Adjusting the upper limits of the four components of the mixture problem may also result in increased strength. Three-point flexural strength of tiles containing high resin content could be improved by increasing the quartz powder beyond the upper limit set by this project. Tiles with low resin content and PCM content in the order of 20% by mass may be able to improve flexural strength by increasing the quartz-34 component beyond the upper limit.

In another effort to increase PCM content a new tile design that consisted of two layers has been suggested. The bottom layer is 25 mm (1 inch) of binder and phase change material only. The top 9.5 mm (3/8 inch) is traditional quartz/binder tile. This combination results in energy saving of 28.9%, which very close to the maximum energy savings of a 100% PCM tile floor. Several concerns would have to be addressed before this could be considered a viable option. First, bonding of the two layers may not be simple. There could be surface preparation and contact issues. In addition it is a concern that the tile strength would be dependent on the strength of the bond between the layers. Secondly, the structural integrity of the layer containing resin and PCM is expected to be very low due to the high PCM content. Therefore the overall strength, especially flexural strength, may not meet ceramic or natural stone tile standards.

Finally, a full scale demonstration of the energy savings potential of phase change floor tile is required to convince potential manufacturers and customers of the value of the tile. Equivalent sunspaces need to be developed. One should contain the PCM tiles and the other typical floor tile. Analysis should include monitoring room temperatures during typical winter conditions to verify potential energy savings.

It has been proven that a microencapsulated paraffin wax can be incorporated into an agglomerate floor tile without significant changes in the manufacturing process. Structural strength was severely compromised with the addition of PCM, but was comparable to ceramic tile. Using the current manufacturing process, the maximum PCM content by mass was determined to be approximately 20%. This content does not lead to significant energy saving when used in passive solar home design simulations. PCM content needs to approach 100% to make this a viable product for passive solar applications. This may not be possible without severely degrading the structural integrity of the flooring. However if the bulk cost of the encapsulated octadecane could be significantly reduced to under a dollar a pound, the 20% PCM floor tile becomes feasible for commercialization. Another possible option would be to use the tile perhaps as a wall covering or in the ceiling were the physical demands are not as essential.

List of Abbreviations

ANSI – American National Standards Institute
ASTM – American Society of Testing and Materials
BLAST – Building Loads Analysis and System Thermodynamics, simulation program
DOE-2 – building simulation program developed by the Department of Energy
DSC - differential scanning calorimeter
EPON – epoxy manufactured by Shell Chemicals
f – mass fraction or percentage
IBLAST – recent update to BLAST
MIA – Institute of America (responsible for tile stone tile standards)
MATLAB – tool for performing numerical computations with matrices and vectors
MSE – mean square error
MTS – supplier of mechanical testing and simulation equipment
NPG - neopentyl glycol
PCM – phase change material
PE - pentaerythritol
PG - pentaglycerine
Quartz-6 – quartz chips of mesh 6
Quartz-10 – quartz chips of mesh 10
Quartz-34 – quartz chips of mesh 34
Quartz-84 – quartz chips of mesh 84
R^2 – coefficient of determination
SAS – Statistical Analysis System, statistical computational program
SEM – scanning electron microscopy
SLR - solar load ratio
SSF - solar savings fraction
x – volume fraction or percentage

References and Bibliography

1. 1993 ASHRAE Handbook of Fundamentals, Atlanta, American Society of Heating, Refrigeration and Air-Conditioning Engineers, Inc, 1993

2. Arndt, P.E. , Dunn, J.G., Swillix, R.L., "Organic Compounds as Candidate Phase Change Materials in Thermal Energy Storage", Thermochimica Acta, Vol. 79, pp. 55-68, 1984

3. Askeland, D. R., The Science and Engineering of Materials, PWS Publishing Company, Boston, 1994

4. Balcomb, D., Passive Solar Heating Analysis, American Society of Heating, Refrigerating and Air-Conditioning Engineers, Atlanta, 1984

5. Barbour, Jason, Modeling Phase Change Materials with Conduction Transfer Functions for Passive Solar Applications, Master of Science, Colorado State University, Fall 2002

6. Barrio, M., Font, J., Muntasell, J., Tamarit, J., "Floor Radiant System with Heat Storage by a Solid-State Phase Transition Material", Solar Energy Materials and Solar Cells, Vol. 27, pp. 127-133, 1992

7. Benson, D.K., Chandra, D., "Solid-State Phase Change Materials for Thermal Energy Storage", Electrochemical Society Extended Abstracts, Vol. 85-2, 1985

8. Benson, D.K., Christensen, C.B., Burrows, R.W., Sinton, Y.D., "New Phase-Change Thermal Energy Storage Materials for Buildings", Enerstock 85, III International Conference on Energy Storage for Building Heating and Cooling, 1985

9. Benson, D.K., Webb, J.D, Burrows, R.W, McFadden, J.D., Christensen, C., "Material Research for Passive Solar Systems: Solid State Phase Change Materials", SERI Report TR-255-828, 1985

10. Benson, D.K., Webb, J.D, Burrows, R.W, McFadden, J.D., Christensen, C., "Material Research for Passive Systems: Solid State Phase Change Material and Polymer Photodegradation", Passive and Hybrid Solar Energy Update, 1982

11. Brostow, W., "An Introduction to Liquid Crystallinity" in Liquid Crystal Polymers: From Structures to Applications, (Eds. A.A. Collyer), Elsevier Applied Science, London, 1992

12. Busico, V. Carfagna, C., Salerno, V., Vacatello, M., "The Layer Perovskites as Thermal Energy Storage System", Solar Energy, Vol. 24, pp. 575-579, 1980

13. Chandra, D., Jorgensen, G., "The Structure and Lattice Parameters of Pentaerythritol Above and Below its Phase Transition Temperature", Advances in X-ray Analysis, Vol. 28, 1985

14. Colvin, D.P., Mulligan, J.C., Bryant, Y.G., "Enhanced Heat Transport in Environmental Systems Using Microencapsulated Phase Change Materials", Report 921224

15. Cornell, John A., Experiments with Mixtures, John Wiley & Sons, New York, 1990

16. "Differential Scanning Calorimetry", Macrogalleria, University of Southern Mississippi Department of Polymer Science, 01 Jan. 1999, <http://www.psrc.usm.edu/macrog>

17. Duffie, John A., Beckman, William A., Solar Engineering Of Thermal Processes, John Wiley and Sons, New York, 1991

18. "EPI-CURE 3140", Shell Chemicals - Online Literature, 1 Oct. 1999, <http://www.resins-versatics.com/rsins>

19. "Epon Resin 828", Shell Chemicals - Online Literature, 1 Oct. 1999, <http://www.resins-versatics.com/rsins>

20. Feldman, D., Banu, D., Hawes, D.W., "Development and application of organica phase change mixtures in thermal storage gypsum wallboard", Solar Energy Materials and Solar Cells, Vol. 36, pp. 147-157, 1995

21. Font, J., Muntasell, J., Cardoner, F., "Preliminary Study of a Heat Storage Unit Using a Solid-Solid Transition", Solar Energy Materials and Solar Cells, Vol. 33, pp. 169-176, 1994

22. Font, J., Lopez, D., Muntasell, J., "Low Temperature Invariant in Pentaerythritol/Neopentyl Glycol Binary System", Material Research Bulletin, Vol. 24, pp. 1251-1259, 1989

23. Font, J., Muntasell, J., Navarro, J., Tamarit, J., "Melanges Pentaglycerine/Neopentyl Glycol : Formation d'une Solution Solide", Thermochimica Acta, Vol. 136, pp. 55-71, 1988

24. Font, J., Muntasell, J., Navarro, J., Tamarit, J., "Calorimetric Study of the Mixtures PE/NPG and PG/NPG", Solar Energy Materials, Vol. 15, pp. 299-310, 1987

25. Font, J., Muntasell, J., Navarro, J., Tamarit, J., "Time and Temperature Dependence of the Exchanged Energy on Solid-Solid Transitions of Pentaglycerine/Neopentyl Glycol Mixtures", Solar Energy Materials, Vol. 15, pp. 403-412, 1987

26. "Granirex", Mar. 2005, <http://www.granirex.com/>

27. Granirex Tile Manufacture Video, Granirex Inc., 2001

28. Garas, Victor Y., Vipulanandan, C., "Review of Polyester Polymer Concrete Properties", Center for Innovative Grouting Materials and Technology (CIGMAT), Department of Civil and Environmental Engineering, University of Houston, Texas

29. Gray, G.W., Windsor, P.A., Liquid Crystals and Plastic Crystals Vol I, Haslted Press, New York, 1974

30. Hartman, Mark, "Blends of Microencapsulated K18 and K19 with Microencapsulated Tech. Grade Octadecane (C_{18} 95%) and Tech. Grade Eicosane (C_{20} 95%), Research and Development Report, OUTLAST Technologies, 2000

31. Hawes, D.W., Feldman, D., Banu, D., "Latent heat storage in building materials", Energy and Buildings, Vol. 20, pp. 77-86, 1993

32. Himran, S., Suwone, A., Mansoori, G., "Characterization of Alkanes and Paraffin Waxes for Application as Phase Change Enery Storage Medium", Energy Sources, Vol. 16, pp. 117-128, 1994

33. Hinkelmann, K., Kempthorne, O., Design and Analysis of Experiments: Volume I Introducion to Experimental Design, John Wiley & Sons, New York, 1994

34. Hirata, Toshimi, "Melamine Resin (Pyrolysis)" in Encyclopedia of Polymer Science and Engineering Volume 7, John Wiley and Sons, New York 1987

35. Hull, D., Clyne, T.W., An Introduction to Composite Materials, (Eds. D.R. Clarke, S. Suresh, I.M. Ward), University Press, Cambridge, 1996

36. Johnson, Timothy E., "MIT Solar Building N0. 5: The Third year Performance", Passive Solar Journal, Vol. 1, No. 3, 1982

37. Johnson, Timothy E., "The MIT Crystal Pavilion", Progress in Passive Solar Energy Systems, pp. 255-260, 1982

38. Kedl, R.J., "Conventional Wallboard with Latent Heat Storage for Passive Solar Applications", Proceedings of the InterSociety Energy Conversion Engineering Conference, Aug 12-17, Vol. 4, pp 222-225, 1990

39. Kreider, Jan F., Rabl, Ari, Heating and Cooling of Buildings, McGraw-Hill Inc., New York, 1994

40. Lee, H., Neville, K., Handbook of Epoxy Resins, McGraw Hill, New York, 1967

41. Magill, Monte, "An Overview of the Outlast Temperature Regulation Technology", 23 Jun. 2000, <http://www.outlast.com>

42. Morton, D.H, Polymer Processing, Chapman and Hall, London, 1989

43. Moscicki, J.K., "Dielectric Relaxation in Macromolecular Liquid Crystals" in Liquid Crystal Polymers: From Structures to Applications, (Eds. A.A. Collyer), Elsevier Applied Science, London, 1992

44. Mulligan, J.C., Colvin, D.P., Bryant, Y.G., "Microcapsulated Phase Change Material Suspensions for Heat Transfer in Spacecraft Thermal Systems", Journal of Spacecraft and Rockets, Vol. 33, No. 2, 1996

45. Nagy, Eleonora E., "Fills for White Marble: Properties of Seven Fillers and Two Thermosetting Resins", Journal of the American Institute for Conservation, Vol. 37, No. 1, pp 69-87, 1998

46. Naumann, R., Emons, H., "Results of Thermal Analysis for Investigation of Salt Hydrates as Latent Heat-Storage Materials", Journal of Thermal Analysis", Vol. 35, pp. 1009-1031, 1989

47. Neeper, D.A., "Potential Benefits of Distributed PCM Thermal Storage", Prepared by Advanced Engineering Technology Group at Los Alamos National Laboratory

48. Oehlert, Gary W., A First Course in Design and Analysis of Experiments, W.H. Freeman and Company, New York, 2000

49. Ott, R. Lyman, An Introduction to Statistical Methods and Data Analysis, Wadsworth, Belmont, 1993

50. "Outlast", Mar. 2005, < http://www.outlast.com/flash.cfm>

51. "Polymer Resins: Polyesters", University of Southern Mississippi, Polymer Science Department, 2003, <http://www.pslc.ws/macrog/coatings/polymers/PESTERS.htm >

52. Potter, W.G., Uses of Epoxy Resins, Newnes-Butterworths, London, 1975

53. Roy, Sanjay, Sengupta, S., "An Evaluation of Phase Change Microcapsules for use in Enhanced Heat Transfer Fluids", International Communications in Heat and Mass Transfer, Vol. 18, pp. 495-507, 1991

54. Salyer, Ival O., Sircar, Anil K., Kumar, Alok, "Advanced Phase Change Materials Technology: Evaluation in Lightweight Solite Hollow-Core Building Blocks", Proceedings of the InterSociety Energy Conversion Engineering Conference, Jul 30 – Aug 4, Vol. 2, pp. 217-224, 1995

55. Salyer, I.O., Sircar, A.K., "A review of phase change materials research for thermal energy storage in heating and cooling applications at the University of Dayton from 1982 to 1996", International Journal of Global Energy Issues, Vol. 9, No. 3, pp. 183-198, 1997

56. Solomon, A.D., "Latent Heat Thermal Energy Storage and Waste Heat Reuse in a Single Periodic Kiln", Proceedings of the InterSociety Energy Conversion Engineering Conference, Aug 12-17, Vol. 4, pp 226-229, 1990

57. Sözen, M., Vafai, K., Kennedy, L., "Thermal Charging and Discharging of Sensible and Latent Heat Storage Packed Beds", Journal of Thermophysics and Heat Transfer", Vol.5, No.4, 1991

58. Snee, Ronald D., Experimental Designs for Quadratic Models in Contrained Mixture Spaces, Technometrics, Vol. 17, No. 2, May 1975

59. Timmermans, J., "Plastic Crystals: A Historical Review", Journal of Physics, Chemistry and Solids, Vol. 18, No. 1, pp. 1-18, 1961

60. Thorncroft, G.E., Gunnerson, F.S., "Performance Evaluation of a Solid State Phase Change Material for Thermal Storage Applications", Intersociety Energy Conversion Engineering Conference, 1988

61. Tomlinson, John J., Heberie, David D., "Analysis of Wallboard Containing a Phase Change Material", Proceedings of the InterSociety Energy Conversion Engineering Conference, Aug 12-17, Vol. 4, pp 230-235, 1990

62. Yamagishi, Y., Sugero, T., Ishige, T., Pyateriko, A., "An Evaluation of Microcapsulated PCM for Use in Cold Energy Transportation Medium", Proceedings of the 31st Intersociety Energy Conversion Engineering Conference, Washington D.C, Aug 11-16, Vol. 3, 1996

63. Yamagushi, M., Sayama, S., "Heat Storage-Type Floor Heating System with Heat Pump Driven by Nighttime Electric Power", Heat Transfer-Japanese research, Vol. 26, No. 2, pp. 122-130, 1997

Appendix A : Molcular Structure of Solid-State Phase Change Material

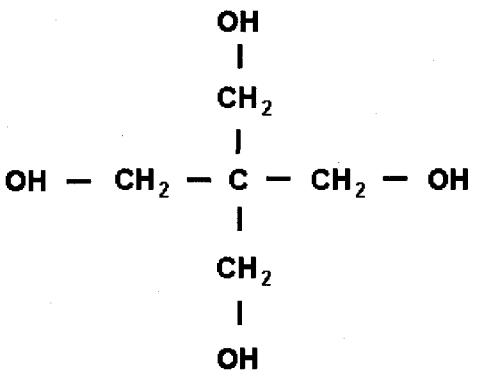

Figure A-1. Molecular Structure of Pentaerythritol, $C - (CH_2OH)_4$

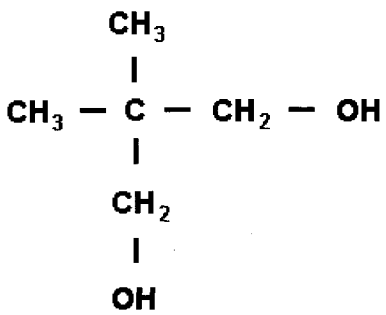

Figure A-2. Molecular Structure of Pentaglycerine, $(CH_3) - C - (CH_2OH)_3$

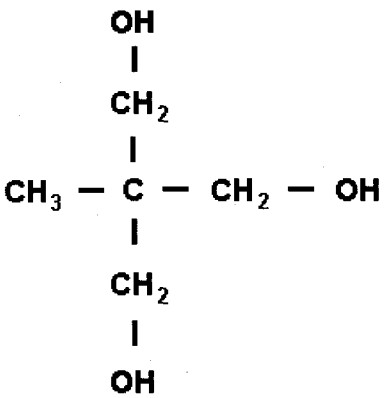

Figure A-3. Molecular Structure of Neopentyl Glycol, $(CH_3)_2 - C - (CH_2OH)_2$

Appendix B : Kenwax

Table B-1. Kenwax 18 Paraffin Content

Normal Paraffin Content	%
C-15	0.83
C-16	6.83
C-17	19.31
C-18	28.66
C-19	27.22
C-20	11.88
C-21	2.78
C-22	0.44
C-23	0.08
C-24	0.08

Table B-2. Kenwax 19 Paraffin Content

Normal Paraffin Wax	%
C-15	0.083
C-16	0.633
C-17	6.169
C-18	19.052
C-19	26.522
C-20	22.942
C-21	14.442
C-22	4.656
C-23	0.903
C-24	0.137

Appendix C : Melamine-Formaldehyde

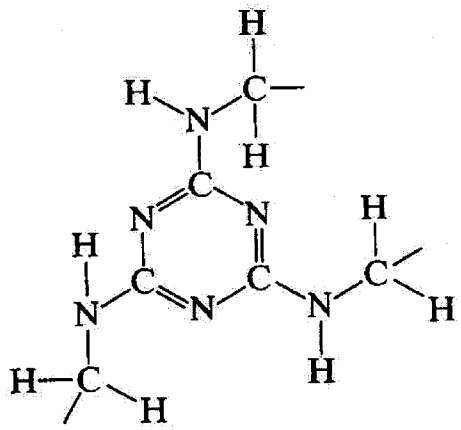

Figure C-1. Molecular Structure of Melamine-Formaldehyde

Appendix D : Mesh Conversion Chart

Table D-1. Mesh Conversion Table

US MESH	microns (µm)	pouces (inches)
4	4760	0,187
5	4000	0,157
6	3360	0,132
7	2830	0,111
8	2380	0,0937
10	2000	0,0787
12	1680	0,0661
14	1410	0,0555
16	1190	0,0469
18	1000	0,0394
20	840	0,0331
25	710	0,0280
30	590	0,0232
35	500	0,0197
40	420	0,0165
45	350	0,0138
50	297	0,0117
60	250	0,0098
70	210	0,0083
80	177	0,0070
100	149	0,0059
120	125	0,0049
140	105	0,0041
170	88	0,0035
200	74	0,0029
230	62	0,0024
270	53	0,0021
325	44	0,0017
400	37	0,0015
500	31	0,0012

Taken from http://www.granuloshop.com/Conversion.htm.

Appendix E : Design Criteria MATLAB m-file

Used for calculation of criteria for design point selection.

```
A = [0.159   0.540  0.301  0.000  0.086  0.048  0.000  0.163  0.000  0.000
0.159  0.540  0.000  0.301  0.086  0.000  0.048  0.000  0.163  0.000
0.159  0.301  0.000  0.540  0.048  0.000  0.086  0.000  0.163  0.000
0.159  0.000  0.301  0.540  0.000  0.048  0.086  0.000  0.000  0.163
0.264  0.435  0.301  0.000  0.115  0.079  0.000  0.131  0.000  0.000
0.264  0.540  0.196  0.000  0.143  0.052  0.000  0.106  0.000  0.000
0.264  0.540  0.000  0.196  0.143  0.000  0.052  0.000  0.106  0.000
0.264  0.196  0.000  0.540  0.052  0.000  0.143  0.000  0.106  0.000
0.264  0.000  0.196  0.540  0.000  0.052  0.143  0.000  0.000  0.106
0.264  0.000  0.301  0.435  0.000  0.079  0.115  0.000  0.000  0.131
0.159  0.270  0.301  0.270  0.043  0.048  0.043  0.081  0.073  0.081
0.212  0.244  0.301  0.244  0.052  0.064  0.052  0.073  0.059  0.073
0.159  0.345  0.151  0.345  0.055  0.024  0.055  0.052  0.119  0.052
0.264  0.285  0.166  0.285  0.075  0.044  0.075  0.047  0.081  0.047
0.222  0.309  0.160  0.309  0.069  0.035  0.069  0.049  0.096  0.049
0.2115 0.07525 0.1995 0.51375 0.016 0.042 0.109  0.015  0.039  0.102]

AT = A'

A1 = A(1,:)
A2 = A(2,:)
A3 = A(3,:)
A4 = A(4,:)
A5 = A(5,:)
A6 = A(6,:)
A7 = A(7,:)
A8 = A(8,:)
A9 = A(9,:)
A10 = A(10,:)
A11 = A(11,:)
A12 = A(12,:)
A13 = A(13,:)
A14 = A(14,:)
A15 = A(15,:)
A16 = A(16,:)

A1T = A1'
A2T = A2'
A3T = A3'
A4T = A4'
A5T = A5'
A6T = A6'
```

```
A7T = A7'
A8T = A8'
A9T = A9'
A10T = A10'
A11T = A11'
A12T = A12'
A13T = A13'
A14T = A14'
A15T = A15'
A16T = A16'

v1 = A1 * (AT*A)^-1 * A1T
v2 = A2 * (AT*A)^-1 * A2T
v3 = A3 * (AT*A)^-1 * A3T
v4 = A4 * (AT*A)^-1 * A4T
v5 = A5 * (AT*A)^-1 * A5T
v6 = A6 * (AT*A)^-1 * A6T
v7 = A7 * (AT*A)^-1 * A7T
v8 = A8 * (AT*A)^-1 * A8T
v9 = A9 * (AT*A)^-1 * A9T
v10 = A10 * (AT*A)^-1 * A10T
v11 = A11 * (AT*A)^-1 * A11T
v12 = A12 * (AT*A)^-1 * A12T
v13 = A13 * (AT*A)^-1 * A13T
v14 = A14 * (AT*A)^-1 * A14T
v15 = A15 * (AT*A)^-1 * A15T
v16 = A16 * (AT*A)^-1 * A16T

v = [v1 v2 v3 v4 v5 v6 v7 v8 v9 v10 v11 v12 v13 v14 v15 v16]

q = 4
p = q*(q+1)/2
n = 16

max_v = max(v)
G_eff = (100 * p) / (n*max_v)
V_eff = mean(v)
A_eff = trace(inv(AT*A))
D_eff = det(AT*A)
```

Appendix F : Upper and lower limits for predicted values of models

Table F-1. Upper and Lower Limits for Flexural Strength Model Predicated Values for 95% Confidence Level

Design Point	Predicated Value	Lower Limit	Upper Limit
1	40.25	25.97	62.39
2	6.06	4.06	9.05
3	1.75	1.18	2.59
4	2.42	1.89	3.11
5	41.78	28.32	61.65
6	43.25	27.96	66.90
7	8.62	5.97	12.43
8	1.44	1.11	1.86
9	2.60	1.99	3.41
10	4.34	2.87	6.57
14	6.28	4.98	7.91
31	7.97	6.00	10.59
33	4.48	3.43	5.85
34	5.97	4.77	7.51
35	5.31	4.21	6.71
36	2.54	2.02	3.19

Table F-2. Upper and Lower Limits for Compressive Strength Model Predicated Values for 95% Confidence Level

Design Point	Predicated Value	Lower Limit	Upper Limit
1	12878.91	6148.936	26971.18
2	2840.65	1387.075	5818.352
3	858.01	413.6185	1779.508
5	15769.29	8247.076	30150.88
6	15748.23	8214.857	30192.56
7	5885.29	2866.157	12086.48
8	1050.58	546.6382	2019.296
9	1053.20	570.5583	1944.017
10	1784.47	931.7513	3418.22
14	3330.57	1746.626	6350.384
31	1085.60	2646.062	6675.749
34	4203.29	2484.277	5730.599
35	3773.20	2259.436	4211.143
36	3084.76	643.2799	1831.893

Appendix G : Agglomerate Tile Physical Tests

Table G-1. Physical Tests Performed on Agglomerate Floor Tile by Various Manufacturers

Test	Granirex	Quartzstone	Verona Marble Co. Quartzo 88
ASTM C-615 Granite Dimension Stone	X		
ASTM C-97 Absorption and bulk specific gravity	X	x	x
ASTM C-170 Compressive strength	X	x	
ASTM C-648 Breaking Strength	X	x	
ASTM C-880 Flexural Strength	X		
ASTM C-484 Thermal Shock	X	x	X
ASTM C-531 Thermal Coefficient of Expansion	X		
ASTM C-1026 Frost Resistance	X	x	X
ASTM C-501 Relative Resistance to Wear	X	x	
ASTM C-241 Abrasion Resistance	X	x	X
ASTM C-1028 Coefficient of Friction	X	x	X
ASTM D-2299 Stain Resistance	X		
ASTM C-672 Resistance to De-Icing Chemicals	X	x	X
ASTM G-23 Ultra Violet Performance	X		
ASTM E-84 Flame Spread	X		X
ASTM E-662 Smoke Density	X		X
ASTM C-99 Modulus of Rupture			X
ASTM C-307 Tensile Strength			X
ASTM D-695 Compression Strength			X
ASTM D-1042 Dimensional Stability			
ASTM D-2583 Indentation Hardness			
ASTM D-2047 Coefficient of Friction			
ASTM D-54384 Stain Resistance			X
ASTM C-291 Wear Resistance/Hardness			X
Impact Resistance	X	x	
Mohs Hardness	X		
ANSI A-137.1 Ceramic Standard	X		
NES 713-1985 Mean Toxicity Index			